THE EFFECT OF EXOGENOUS COENZYME Q_{10} ON ITS DISTRIBUTION AND ITS ROLE AS PROTECTIVE AGENT AGAINST DNA DAMAGE

F.J. Fourie
B. Pharm.

Dissertation submitted in partial fulfillment of the requirements for the degree Magister Scientiae in the Department of Pharmaceutical Chemistry at the Potchefstroomse Universiteit vir Christelike Hoër Onderwys.

Supervisor **Prof. J.J. Bergh**
Co-supervisor **Dr. S. van Dyk**
Vice-supervisor **Prof. D.W. Oliver**

Potchefstroomse Universiteit vir Christelike Hoër Onderwys
2003

INDEX

ACKNOWLEDGEMENTS

I would like to express my sincerest gratitude to the following people, whose assistance, support and encouragement, did not go unnoticed nor unappreciated.

- First and foremost, my patient God.
- My Father, Mother and brother for their love and support.
- Maralien for all her love, advice, help and support.
- Prof. J.J. Bergh and Dr. S. van Dyk for going out of their way to always provide an answer to my questions and for giving me inappreciable advice.
- Dr. J.L. du Preez for his time and assistance with the ubiquinone analysis on the HPLC.
- Prof. L.J Mienie and Prof. C.J. Van der Schyf for their ideas and enthusiasm.
- My colleague Michael Fazakaz for his work on the SCGE technique.
- Mr. J.J. Bester, Ms. Antoinette Fick and Dr. Douw G. van der Nest (Experimental Animal Centre, Potchefstroomse Universiteit vir Christelike Hoër Onderwys) for their assistance with the mice experiments.
- Ms. Anriëtte Pretorius at the library for all her help and kindness.
- The Institute for Industrial Pharmacy for the use of their equipment and chemicals.
- Everyone at Pharmaceutical Chemistry for his or her encouragement and friendship.
- The MRC and NRF for their financial support during my study.

ABBREVIATIONS

α	alpha
β	beta
π	Pie orbital
Ⓟ	High energy phosphate
8-OHdG	8-hydroxydeoxyguanosine
γ	gamma
ANT	Adenine nucleotide translocase
ADP	Adenosine diphosphate
AIF	Apoptosis inducing factor
ATP	Adenosine triphosphate
AO	acridine orange
AUC	Area under curve
Ca^{2+}	Calcium
Cl^-	Chloride
CNS	Central nervous system
CO_2	Carbon dioxide
CoA	Coenzyme A
Cyt c	Cytochrome c
C	concentration
CoQ_{10}	Coenzyme Q_{10}
dATP	Deoxyadenosine triphosphate
DNA	Deoxyribonucleic acid
DMSO	dimethylsulfate
EC	Electrochemical
ECA	Ethyl cyanoacetate
ED	Electrochemical detection
EDTA	Ethylenediaminetetraacetate
e.g.	for instance
eNOS	Vascular endothelial cells NOS

ER	Endoplasmic reticulum
et al.	et ali (and others)
etc.	et cetera (and others)
ETF	Electron transfer flavoprotein
ETF-QO	Electron transfer flavoprotein-ubiquinone oxidoreductase
F_0	Coupling factor zero
F_1	Coupling factor one
F_6	Coupling factor six
FAD	Flavin adenine dinucleotide
FMN	Flavin mononucleotide
GC	Gas chromatography
H^+	Hydrogen ion
H_2O	Water
H_2O_2	Hydrogen peroxide
HBA	Hydrobenzoic acid
HMG-CoA	3-Hydroxy-3-methylglutaryl-CoA
$HO^\bullet$	Hydroxyl radical
HP	Haloperidol
HPLC	High-pressure-liquid-chromatography
HSLC	High-speed-liquid-chromatography
HMPA	High melting point agarose
h	Hour
K^+	Potassium
LDL	Low-density lipoprotein
$Lipid^\bullet$	Carbon centered lipid radical
Lipid-H	Lipid
$Lipid\text{-}O_2H$	Lipid hydroperoxide
LMPA	Low melting point agarose
LOD	Limit of detection
LOQ	Limit of quantification

$L(OO)^{\bullet}$	Peroxyl radicals
LC	liquid chromatography
MADD	multiple acyl-CoA dehydrogenation disorders
MAO-B	Monoamine oxidase B
mol	mole (6×10^{23} molecules)
MPP^+	1-methyl-4-phenylpyridinium ion
MPPP	1-methyl-4-propionoxypiperdine
MPTP	1-methyl-4-phenyl-1,2,3,6-tetrahydropyridine
min	minutes
MS	mass spectrometry
Mab	monoclonal antibody
NAD	Nicotinamide adenine dinucleotide
NADP	Nicotinamide adenine dinucleotide phosphate
NMDA	*N*-methyl-D-aspartate
NO	Nitric oxide
NOS	Nitric oxide synthases
O_2	Oxygen
$O_2^{\bullet -}$	Superoxide anion radical
ODS	Octadecylsilane
OH^-	Hydroxyl ion
$ONOO^-$	Peroxynitrite
PD	Parkinson's disease
PDA	Photodiode array detector
P_i	Inorganic phosphate
PB	Peanut butter
PP	pyrophosphate
$Q^{\bullet -}$	Semi-quinone radical
$Q_{10}H_2$	Ubiquinol
Q_{10}	Ubiquinone

rad	radicals
$RO^{\bullet}$	Alkoxyl radical
ROS	Reactive oxygen species
RNA	Ribo nucleic acid
SN	Substantia nigra
SOD	Superoxide dismutase
suppl.	Supplement
SO	sweet oil
SCGE	Single cell gel electrophoresis (comet assay)
TD	Tardive dyskinesia
$TO^{\bullet}$	α-Tocopherol radical
TM	Tail moment
TQ_{10}	Total coenzyme Q_{10}
Ubiquinol-10	Reduced Q_{10} ($Q_{10}H_2$)
Ubiquinone	Ubiquinone-10 (coenzyme Q_{10}), Q_{10}
UV	Ultra violet

ABSTRACT

Coenzyme Q_{10} (Q_{10}) acts as an important *in vivo* anti-oxidant and has been widely advocated to be a beneficial dietary adjuvant because elevated concentrations of Q_{10} should effect a higher energy production and anti-oxidant capacity, leading to lower DNA damage and cell death. It remains controversial however, whether oral administration of Q_{10} can significantly enhance its tissue levels and/or can modulate the level of oxidative stress (DNA damage) *in vivo.*

We investigated whether oral administration of coenzyme Q_{10} (Q_{10}) in mice could increase the levels of its reduced form, $Q_{10}H_2$, in blood and in tissue (brain, liver and heart) and determined the relationship between $Q_{10}H_2$ concentrations in the blood and various tissues. These concentrations were correlated with cell DNA damage found in blood and in brain, liver and heart tissue.

We also investigated if oral administration of Q_{10} could attenuate the neurotoxicity of 1-methyl-4-phenyl-1,2,3,6-tetrahydropyridine (MPTP) in old mice, using damage to cell DNA as the parameter.

In this study a method for assessing chemically and environmentally induced cell DNA damage was developed, using the single cell gel electrophoresis (SCGE) assay and compared these results with coenzyme Q concentrations in various tissue samples obtained by using a validated HPLC analysis with electrochemical detection.

Four groups of one-year-old C57BL/6 mice received a standard diet or a diet supplemented with Q_{10} (200mg/kg/day) for six weeks. After four weeks, one group that had received the standard diet and one group that had received the Q_{10} supplemented diet were treated additionally with one dosage of MPTP (40mg/kg).

The results showed that the $Q_{10}H_2$ as well as the Q_9H_2 concentrations were elevated in the plasma, brain, heart and liver of those groups receiving Q_{10} and Q_{10} + MPTP. This observation, as well as the phenomenon that the Q_9H_2 levels were higher than the $Q_{10}H_2$ levels in the controls indicated that Q_9 is the predominant Q homologue in mice and that oral intake of Q_{10} increased the levels of both Q_9H_2 and $Q_{10}H_2$ in tissue and blood.

The heart, brain and liver cells exhibited significantly higher DNA damage in the groups treated with MPTP. The group receiving MPTP plus Q_{10} displayed less DNA damage than the MPTP group indicating that Q_{10} most likely act as an ameliorating factor for MPTP neurotoxicity. The blood samples before and after treatment in contrast, showed very little difference in DNA damage. This might be explained by the fact that blood cells regenerate much faster than other tissue.

Our findings indicate that levels of Q_{10} and Q_9 can be increased in tissue by long-term supplementation with Q_{10} and that Q_{10} could attenuate/prevent DNA damage in various cells. This suggests that Q_{10} may be useful in disorders where there is impaired activity of complex I, which might lead to DNA damage of the cell, such as Parkinson's disease.

UITTREKSEL

Koënsiem Q_{10} (Q_{10}) is 'n baie belangrike *in vivo* anti-oksidant en word dikwels aanbeveel as 'n dieetaanvuller. Verhoogde Q_{10}-konsentrasies sal waarskynlik lei tot hoër energieproduksie en anti-oksidantkapasiteit, wat weer tot verminderde DNS- skade en seldood sal lei. Dit is nog onseker of orale toediening van Q_{10} betekenisvolle verhoging daarvan in weefselvlakke veroorsaak en of dit oksidatiewe stres (DNS-skade) *in vivo* kan moduleer.

Daar is ondersoek of orale Q_{10}-toediening in muise die vlakke van gereduseerde Q_{10}, $Q_{10}H_2$, in bloed en weefsel (brein, lewer en hart) kan verhoog. Die verwantskap tussen $Q_{10}H_2$ konsentrasies in die bloed en die onderskeie weefsels is ook bepaal. Hierdie konsentrasies is vergelyk met sel-DNS-skade in bloed en brein-, lewer- en hartweefsel.

In hierdie studie is daar ook nagevors of koënsiem Q_{10} die neurotoksiese effek van 1-metiel-4-feniel-1,2,3,6-tetrahidropyridine (MFTP) in ou muise kan verminder deur die verlaging in DNS-skade te meet.

'n Metode is ontwikkel om chemiese- en omgewingsgeïnduseerde sel-DNS-skade waar te neem met enkelsel-gel-elektroforese (ESGE) tegnologie. Hierdie resultate is met koënsiem Q konsentrasies in verskillende weefsels, wat met 'n gevalideerde HPLC-metode bepaal is, vergelyk.

Vier groepe een jaar oue C57BL/6 muise het elk vir ses weke óf 'n standaarddieet, óf 'n dieet met Q_{10} (200mg/kg) ontvang. Na vier weke is een groep wat die standaarddieet en een groep wat die Q_{10} dieet gevolg het, addisioneel met MFTP (40mg/kg) behandel.

Resultate het getoon dat die $Q_{10}H_2$, sowel as die Q_9H_2 konsentrasies verhoog was in die plasma, brein, hart en lewer van die groepe wat Q_{10} en Q_{10} + MFTP ontvang het. Hierdie waarneming, sowel as die verskynsel dat Q_9H_2-vlakke hoër was as die $Q_{10}H_2$-vlakke in die kontroles, dui daarop dat Q_9 die dominante Q homoloog is in muise. Die orale toediening van Q_{10} het die vlakke van beide Q_9H_2 en $Q_{10}H_2$ in weefsel en bloed verhoog.

Die hart-, brein- en lewerselle het merkwaardig groter DNS skade getoon in die groepe wat behandel is met MFTP. Die groep wat MFTP + Q_{10} ontvang het, het minder DNS-skade getoon as die MFTP-groep, wat impliseer dat Q_{10} heel waarskynlik die neurotoksisiteit van MFTP kan verminder. Hierteenoor het die bloedmonsters voor en na behandeling min verskil in DNS-skade vertoon. Dit kan moontlik verklaar word deur die feit dat bloedselle baie vinniger vorm as ander selle.

Ons resultate dui daarop dat Q_9 and Q_{10} vlakke verhoog met langtermyn Q_{10}-aanvulling. Q_{10} vertraag, of voorkom DNS skade in verskeie selle. Hierdie bevinding dui daarop dat Q_{10} waardevol mag wees vir die behandeling van afwykings waar daar beperkte aktiwiteit van kompleks I is, wat mag lei tot DNS-sel-skade, soos byvoorbeeld Parkinson se siekte.

CHAPTER 1

INTRODUCTION

1.1. General

Coenzyme Q (Q_{10}) is a component of the mitochondrial electron transport chain and also a constituent of various cellular membranes. Q_{10} acts as an important *in vivo* anti-oxidant and has widely been advocated to be a beneficial dietary adjuvant. It however, remains controversial whether oral administration of Q_{10} can significantly enhance its tissue levels and/or can modulate the level of oxidative stress (DNA damage) *in vivo.*

Clinical applications of Q_{10} are widespread (Strijks, 1997). In consideration of the prospects of Q_{10} as a remedy, it may, in the future be necessary to assess not only the clinical data but to also elucidate the modes of biochemical and biophysical action of Q_{10} to establish a scientific premise for treatment with this substance. Q_{10} is neither a protein nor a foreign substance. Thus, neither anaphylactic nor other side effects are expected. In this study Q_{10} will be evaluated as a therapeutic substance.

It has long been known that there is a significant relationship between the risk of the development of various neurodegenerative diseases, including Alzheimer's disease (AD) and Parkinson's disease (PD), and previous xenobiotic exposure. People with a history of occupational herbicide use, have an increased risk for developing PD of about three times that of the unexposed population (Perlmutter, 1999). If mitochondrial dysfunction plays a role in the development of PD and increased risk of developing PD with exposure to xenobiotics is valid, oxidative stress produced by mitochondrial dysfunction may lead to PD (Beal, 1996). Oxidative stress is defined as a shift in pro-oxidant-anti-oxidant balance in favour of the former, and has been implicated as a causative factor in aging and degenerative diseases such as heart attack, diabetes, cancer, PD, AD, Huntington's disease (HD) and amyotrophic lateral sclerosis (Yamashita & Yamamoto, 1997; Beal, 1996). It is also a pathogenic factor in several paediatric disorders, particularly in necrotising enterocolitis, bronchopulmonary dysplasia, intraventricular haemorrhage, and retinopathy of premature infants (Finckh *et al.*, 1995). One of the most promising agents for up-regulation of mitochondrial function is Q_{10}. Q_{10} transports electrons in the mitochondria for ATP production and it also has free-radical scavenging properties (Perlmutter, 1999).

A decrease of the ratio of ubiquinol ($Q_{10}H_2$) (the reduced form of coenzyme Q_{10}) to ubiquinone (Q_{10}) (the oxidised form of coenzyme Q_{10}) is also important and has been reported in patients with adult respiratory distress syndrome and pulmonary oedema (Yamashita & Yamamoto, 1997). These diseases are all linked to increased free radical formation (Menke *et al.*, 2000). In other findings the percentage of $Q_{10}H_2$ to total coenzyme Q_{10} (TQ_{10}) was decreased in the plasma of patients who developed PD prematurely and in patients with hyperlipidemia and liver disease (Tang *et al.*, 2001). The outcome of this study may lead to a better understanding of the mechanism by which xenobiotics cause extrapyramidal symptoms, the role of Q_{10} in the prevention of these symptoms, the role of Q_{10} in prevention of cell DNA damage and the effect of $Q_{10}H_2$ as an anti-oxidant.

1.2. Aim of this study

We hypothesize that Q_{10} would increase levels of $Q_{10}H_2$ in blood and in the tissue (brain, liver and heart), effecting a higher energy production and anti-oxidant capacity. This may lead to lower DNA damage and cell death. To test this hypothesis we will determine the relationship between $Q_{10}H_2$ concentrations in the blood and various tissues. These concentrations will be correlated with cell DNA damage found in the blood and tissues. We will also determine if $Q_{10}H_2$ could attenuate the damage to cell DNA in a suitable animal model.

We will measure concentrations of $Q_{10}H_2$ and monitor cell DNA repair. This will make it possible to evaluate the effectiveness of Q_{10} as a possible anti-oxidant and as protective agent against genetic damage.
To achieve these aims the following will need to be done:

- The development of a suitable, sensitive analytical method for the quantitative analysis of $Q_{10}H_2$ levels.
- The varying levels of $Q_{10}H_2$ induced in the plasma of experimental test animals (C57 BL/6J mice) will have to be correlated with $Q_{10}H_2$ concentrations in tissue.
- The extent of cell deoxyribonucleic acid (DNA) damage needs to be determined with a suitable method.

CHAPTER 2

UBIQUINONE

2.1. General

Coenzyme Q_{10} (ubiquinone) is of major importance as an endogenous anti-oxidant. It is well established as a transport mediator of reducing equivalents in the respiratory system located in the mitochondria where it is involved in electron transport and ATP synthesis (Menke *et al.*, 2000).

The reduced form of Q_{10}, known as ubiquinol-10 ($Q_{10}H_2$), is the only known lipid-soluble anti-oxidant that animal cells can synthesize *de novo* and for which enzymes for the regeneration of its oxidised state formed in the course of its anti-oxidant function exist (Frei *et al.*, 1990). In the $Q_{10}H_2$ capacity it can inhibit lipid peroxidation by scavenging chain propagating lipid peroxyl radicals and it can also reduce α-tocopheryl radicals because of its 10–fold greater molar concentration than α-tocopherol (Yamashita & Yamamoto, 1997). The anti-oxidant activity depends on the ratio of $Q_{10}H_2$ and Q_{10} in plasma, the concentration and the redox status (Total Q_{10} = $Q_{10}H_2$ and Q_{10}) (Wang *et al.*, 1999).

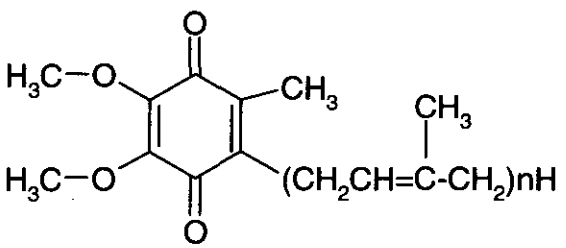

Coenzyme Q_{10} n=10

Coenzyme Q_9 n=9

Figure 2.1. Coenzyme Q_{10} (2,3-dimethoxy-5-methyl-6-decaprenylbenzoquinone).

In most mammals, including man, Q_{10} is the exclusive form of coenzyme Q. An exception is found in rat and mouse tissue where Q_9 is the prevalent isoprenolog. Q_{10} is found in human tissue like the heart, kidney and urine (Hatefi, 1963).

As Q_{10} exerts its major function in the respiratory chain, located in the mitochondria, a deficiency thereof or a defect in Q_{10} biosynthesis can result in reduced ATP production and decreased anti-oxidant activity that may have detrimental consequences.

2.2. The respiratory transfer chain

The main function of food is the production of energy. This is accomplished through its catabolism during which energy-rich hydrogen atoms are released and converted into ATP in the respiratory chain. The electron transfer chain is a vital part of the respiratory system as can be seen in figure 2.2.

The average adult human generates enough metabolic energy from nutrients to synthesize his or her own weight in ATP every day (Mathews & Van Holde, 1990). How this energy is produced, the involvement of this energy in aging and cell death, oxidative phosphorylation, the role of Coenzyme Q_{10}, the Q-pool, the role of DNA in cell death and Parkinsonism will be described in this chapter.

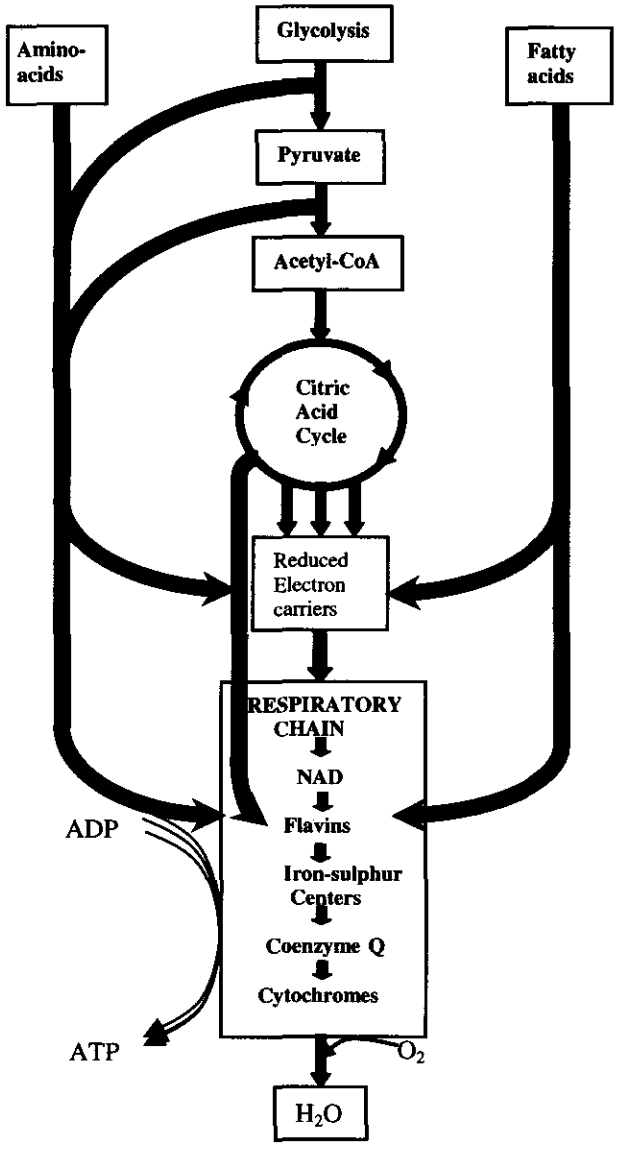

Figure 2.2. Overview of respiration in short (Mathews & Van Holde, 1990).

2.2.1 The mitochondrion

Mitochondria are the energy powerhouses of the cell. Mitochondria have their own DNA and manage the oxidative phosphorylation process. In this process, carbon-carbon double bonds are split to create pairs of energized electrons, the energy of which is converted to ATP (Kidd, 2000).

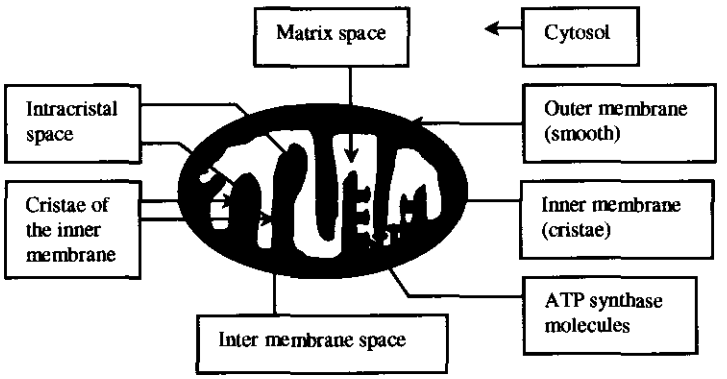

Figure 2.3. The mitochondria (Mathews & Van Holde, 1990).

The mitochondrion consists of four distinct sub regions shown in figure 2.3. The outer membrane, the inner membrane, the intermembrane space and the matrix. The inner membrane is highly folded into cristae throughout the interior of the mitochondrion. Since the respiratory proteins responsible for oxidative phosphorylation are bound to the inner membrane, the density of cristae is related to the respiratory activity of a cell. Heart muscle cells have very high rates of respiration and therefore contain densely packed cristae. In contrast, liver cells have lower respiratory rates with sparsely distributed cristae (Mathews & Van Holde, 1990).

The respiratory protein-lipid enzyme complexes involved in oxidative phosphorylation located in the mitochondrial inner membrane (figure 2.3.) are flavin adenine dinucleotide (FAD), flavin mononucleotide (FMN), quinoid compounds (coenzyme Q_{10}) and transition metal compounds (iron-sulphur clusters, hemes, protein-bound copper). These enzymes are designated:
Complex I (NADH: ubiquinone oxidoreductase),
Complex II (succinate:ubiquinone oxidoreductase),
Complex III (ubiquinol:ferrocytochrome c oxidoreductase),
Complex IV (ferrocytochrome c:oxidase),
Complex V (ATP synthase) (Ebadi *et al.*, 2001).

Q_{10} is present in mitochondria in molar amounts exceeding those of other respiratory chain carriers, resulting in a Q_{10}-pool. The Q_{10}-pool acts as a redox carrier between flavin dehydrogenase and the cytochrome system (Ernster & Dallner, 1995).

2.2.2. Oxidative phosphorylation and the Q-pool

2.2.2.1. Oxidative phosphorylation

Oxidative phosphorylation (figure 2.4.) begins with the entry of electrons into the respiratory chain. Most of these electrons arise from dehydrogenases that collect electrons from catabolic pathways of fats, proteins, and carbohydrates (Ebadi *et al.*, 2001).

Reduced nicotinamide nucleotides (NADH) passes its two electrons and one hydrogen atom to flavin mononucleotides (FMN). Since FMN carries two hydrogen atoms in addition to an electron pair, a second H^+ ion is absorbed from the medium inside the matrix to form $FMNH_2$. This carrier passes its electrons to the next carrier group in the chain, the iron sulphur proteins. The iron sulphur carriers are "pure" electron carriers and so the hydrogen atoms carried by $FMNH_2$ are released into the intermembrane, contributing the first two H^+ ions to the gradient (Wolfe, 1981). The Q-pool (section 2.2.2.2.) is involved in the uptake of additional $2H^+$ ions. Thus for each pair of electrons transferred, four protons are removed from the matrix (figure 2.5.) (Walker, 1992). Complex V uses the potential energy stored in the proton gradient of H^+ ions, set up by electron transport, to condense ADP (adenosine diphosphate) and inorganic phosphate (P) into ATP as the gradient runs down. The H^+ gradient depends on the fact that some of the carriers in the electron transport chain carry both hydrogen atoms and electrons during their cycles of oxidation and reduction, while some only carry electrons (Wolfe, 1981). The ATP is exchanged across the inner membrane with ADP by the adenine nucleotide translocase (ANT). Molecular oxygen is the final electron acceptor (Ebadi *et al.*, 2001). Oxygen in combination with the hydrogen atoms forms water as a final product of oxidative phosphorylation (figure 2.4.).

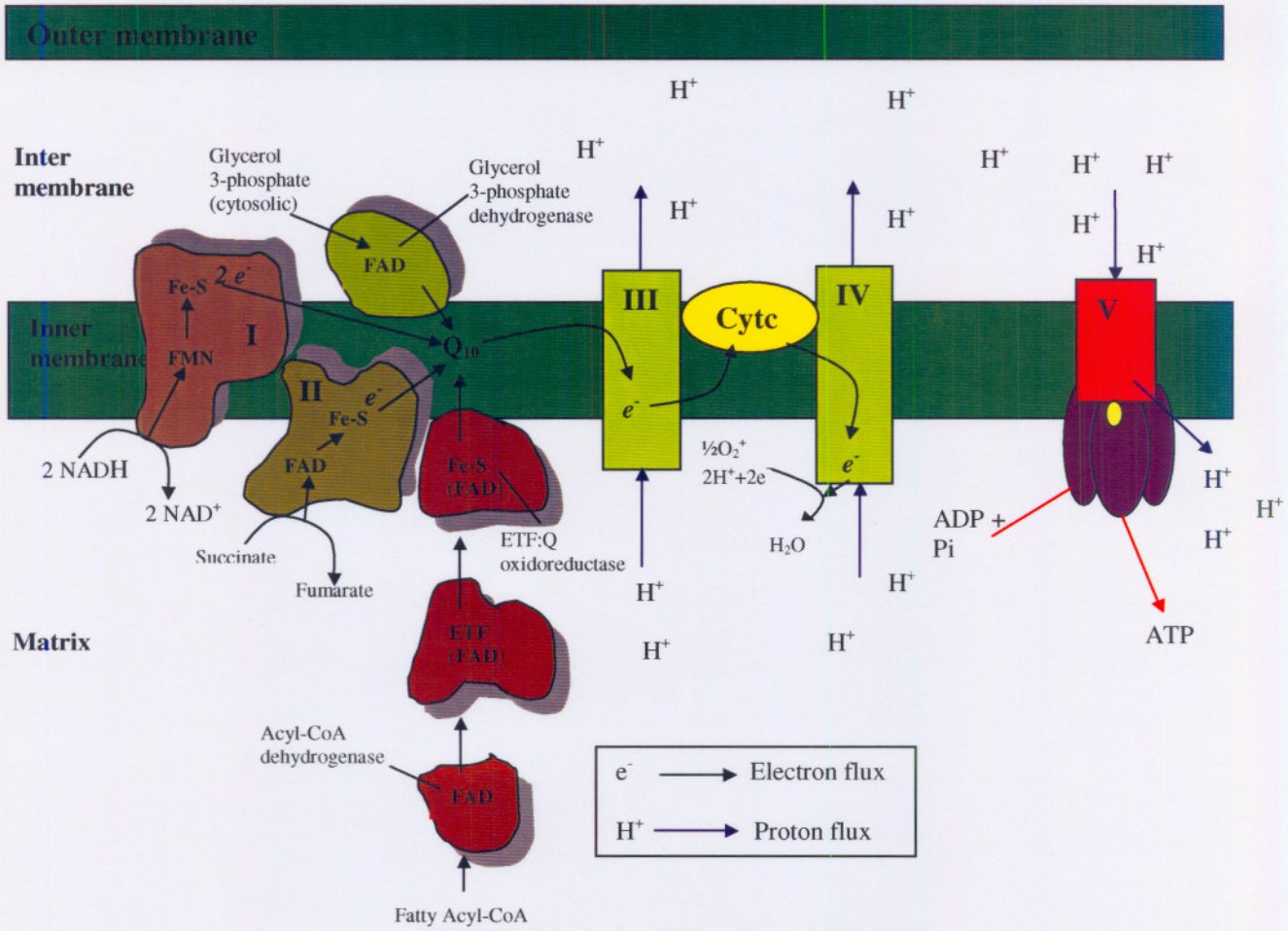

Figure 2.4. Complexes (I-V) in the mitochondrial inner membrane (Ebadi *et al*, 2001; Nelson & Cox, 2000).

2.2.2.2. Q-pool

In 1976 scientists proposed the proton motive Q_{10} cycle, which involves ubisemiquinone (QH). This cycle accounts for the energy conservation occurring in the respiratory chain (Ernster & Dallner, 1995).

In 1984 a model for the mitochondrial respiratory chain were postulated in which electron transfer depends on random collisions between enzyme complexes and small diffusing molecules (Q_{10} and cytochrome c) situated in the lipid bilayer of the mitochondria (figure 2.3. - 2.5.).

In the Q cycle (figure 2.5.), two electrons carried by the iron sulphur proteins are passed to two molecules of coenzyme Q - one to each Q molecule. These take up one H^+ each from the matrix at the same time to form QH. The two Q molecules accept another electron from the cytocrome b molecule to form the fully reduced ubiquinol (QH_2). The additional pair of H^+ atoms are taken up from the matrix. In the next step of the Q cycle, the two Q molecules pass on one electron each to the next carriers in the chain two molecules of cytochrome c. Since cytochromes are "pure" carriers, the Q molecules, in returning from QH_2 to QH, release one H^+ ion each to the intermembrane space. The second electron carried by each QH passes to each of the two cytochrome b molecules. As this transfer takes place, the two Q molecules return to the fully oxidised form and pass on their last H^+ ions, one each, to the intermembrane. The electrons pass on to the final acceptor O_2. As the oxygen molecule accepts the electrons, an additional $2H^+$ ion are passed from the matrix converting $½O_2$ to H_2O. The electrons passed to cytochrome b are now ready to enter another Q cycle (Wolfe, 1981).

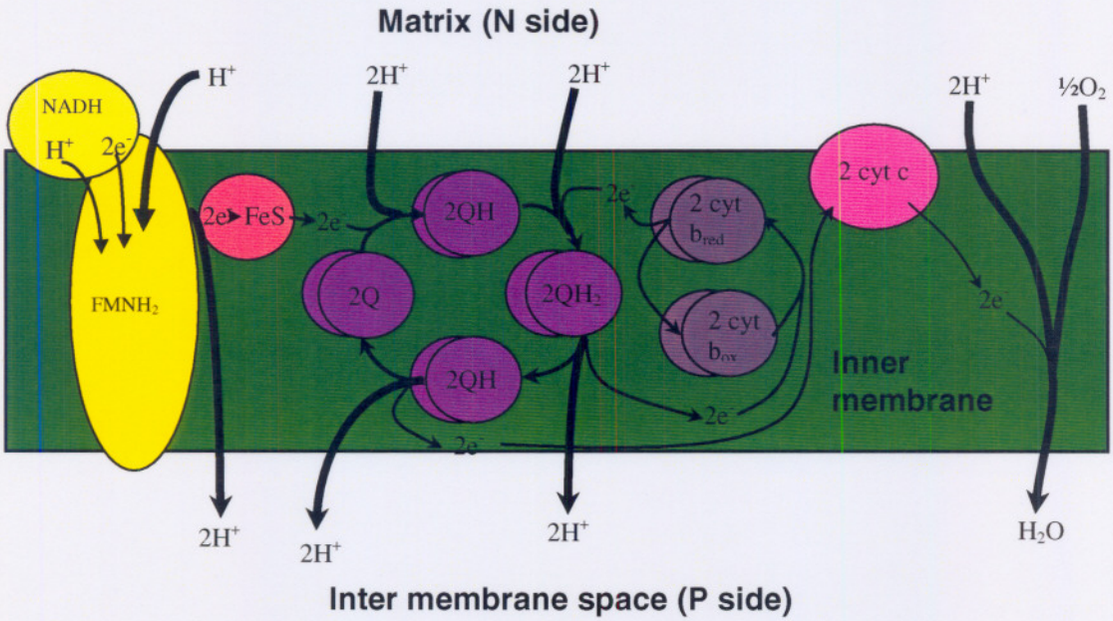

Figure 2.5. The proton motive Q_{10} cycle (Q pool) (N side negative, P side positive), (Nelson & Cox, 2000; Wolfe, 1981).

2.3. Oxidative stress and reactive oxygen species (ROS)

All the cells in the human body generate life-sustaining energy through the respiratory chain (section 2.2.). A by-product of aerobic respiration however, is the formation of oxygen containing radicals (oxyradicals) (Kidd, 2000).

The mitochondrion is situated at the site where oxyradicals are produced and where anti-oxidant defences are normally most challenged. 20% of all the oxygen consumed by the human goes to the brain, where 5% is converted to reactive oxygen species (ROS). Mitochondria metabolise 95% of molecular oxygen and convert 2% of the total oxygen to ROS. Mitochondria thus create 90 % of the oxyradicals that constitute the endogenous oxidative burden (Kidd, 2000).

Complexes I, II, III, IV and V (figure 2.4.) optimise electron transfer efficiency while minimizing electron leakage to oxygen that would generate oxyradicals. Damage to any one complex would reduce ATP production and worsen leakage of oxyradicals from the system. Nevertheless, during transfer through the five complexes, electrons do escape and give rise to ROS and free radicals (Kidd, 2000).

ROS denote superoxide, hydrogen peroxide, hydroxyl radicals and singlet oxygen. In a broader sense, peroxides, hydrogenperoxide, epoxide metabolites of endogenous lipids and xenobiotics, which have chemically reactive oxygen-containing functional groups, can be included as ROS. Free radicals are defined as any atom or molecule that has more than one unpaired electrons. The oxygen molecule too is a radical, two of its unpaired electrons are located separately in a π antibonding orbital. Therefore ROS and free radicals are not identical (Ebadi *et al.*, 2001).

Oxygen drives energy produced from food molecules through the production of oxyradicals, which is so reactive that it could destroy the whole living system.

The oxygen molecule is capable of accepting an electron to create superoxide (figure 2.6.), a reactive form of oxygen. One theory suggests that ubisemiquinone (figure 2.5.),

generated in the course of electron transport reactions in the respiratory chain, donate electrons to oxygen and provide a constant source of superoxide:
(Q_{10}^{-} + O_2 ⟶ O_2^{-} + Q_{10}) (Raha & Robinson, 2000). Later studies by Lenaz (2001) on Q_{10} depleted mitochondria however, indicated that endogenous Q_{10} is not required for superoxide generation and that it is not a source of ROS. The reason being that ubisemiquinone is stable when bound to protein and therefore the Q-pool is not involved when ROS is generated (Lenaz, 2001).

Superoxide is generated from oxygen by, among others, the respiratory chain complexes I and III or other cellular enzymes from oxygen. Superoxide itself can be toxic, especially through inactivation of proteins that contain iron-sulphur centres such as aconitase, succinate dehydrogenase and NADH-ubiquinone oxidoreductase. Hydrogen peroxide is the dismuted product of superoxide and is also toxic. A second much more damaging species, the hydroxyl radical, is very reactive and can cause peroxidative damage to proteins, lipids and DNA. Another very reactive species is peroxynitrite ($ONOO^{-}$) formed from superoxide (O_2^{-}) and nitric oxide (NO). Under normal circumstances, the rate of generation of superoxide from mitochondria is rather low and does little damage because of the efficient removal by superoxide dismutases. However, circumstances can arise (e.g. ingested chemicals, high concentrations of oxygen medically applied, or during ischemia) where high rates of superoxide production do occur (Raha & Robinson, 2000).

ROS can accumulate in the brain. Pathological consequences result from a disparity between the production of free radicals and the rate at which cells can eliminate them (Ebadi *et al.*, 2001). Anti-oxidant defences such as Q_{10} however, were developed to curb the toxic threat from oxyradicals and to help keep them integrated with the pathways of healthy metabolism (Kidd, 2000).

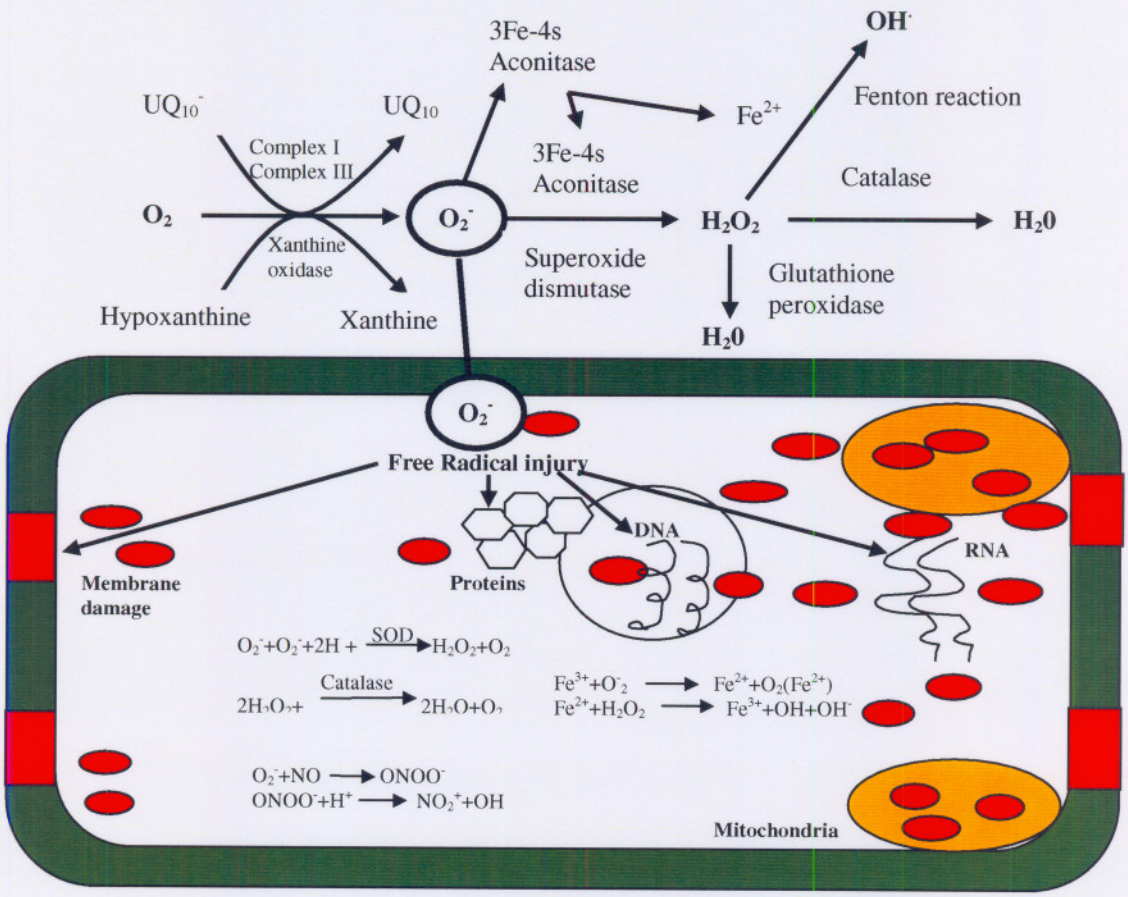

Figure 2.6. Reactions involved in the production and removal of oxygen free radicals in the cell (Ebadi *et al.*, 2001).

2.4. Q_{10} as anti-oxidant

Exogenous Q_{10} has been shown to protect against acute post-ischemic hepatic and myocardial injury and against carbon tetrachloride-induced lipid peroxidation. Frei *et al.* (1990) described that administration of Q_{10} to patients can increase tolerance of the heart to ischemia and that patients with respiratory distress syndrome, a condition associated with oxidant stress, have decreased plasma levels of $Q_{10}H_2$. The mechanism by which $Q_{10}H_2$ (reduced Q_{10}) acts as an anti-oxidant is as follows:

$$Q_{10}H_2 + L(OO)^{\cdot} \longrightarrow Q_{10}^{\cdot -} + H^+ + L(OO)H \qquad (1)$$

$Q_{10}H_2$ represents ubiquinol-10 with two fenolic hydrogen atoms, $Q_{10}^{\cdot -}$, the semiquinone and $L(OO)^{\cdot}$ the peroxyl radicals. The semiquinone radical can disproportionate to Q_{10} and $Q_{10}H_2$ or might scavenge another peroxyl radical.

$$2Q_{10}^{\cdot-} + 2H^{+} \longrightarrow Q_{10}H_2 + Q_{10} \quad \textbf{(2)}$$

$$Q_{10}^{\cdot-} + H^{+} + L(OO)^{\cdot} \longrightarrow Q_{10} + L(OO)H$$

$Q_{10}H_2$ and also semiquinone (QH) can undergo autoxidation:

$$Q_{10}H_2 + O_2 \longrightarrow Q_{10}^{\cdot-} + 2H^{+} + O_2^{\cdot-} \quad \textbf{(3)}$$

$$Q_{10}^{\cdot-} + O_2 \longrightarrow Q_{10} + O_2^{\cdot-} \quad \textbf{(4)}$$

The superoxide radicals ($O_2^{\cdot-}$) formed in these reactions can further oxidise $Q_{10}H_2$

$$Q_{10}H_2 + O_2^{\cdot-} \longrightarrow Q_{10}^{\cdot-} + H_2O_2 \quad \textbf{(5)}$$

Reactions 1 and 3 are radical trapping. Frei *et al.* (1990) also reported that in the presence of ascorbate the anti-oxidant potency of $Q_{10}H_2$ is diminished. It is also important to note that $Q_{10}H_2$ have a sparing effect on α-tocopherol. This sparing affect could reflect site-specific anti-oxidation within the membrane (figure 2.8.) (Frei *et al.*, 1990).

Figure 2.7. shows the three states in which Q_{10} appears in the above mechanism (Ernster & Dallner, 1995).

It appears that $Q_{10}H_2$ may prevent both the initiation and propagation (figure 2.8.) of lipid peroxidation whereas vitamin E acts exclusively as a chain-breaking anti-oxidant, inhibiting propagation. $Q_{10}H_2$ is in a favourable position to accomplish both of these functions, because of its location in the hydrophobic region of the membrane phospholipid bilayer and also due to its access to the protonmotive Q_{10} cycle, which is capable of regenerating $Q_{10}H_2$ from the ubisemiquinone radical (Ernster & Dallner, 1995) as has previously been described in figure 2.5.

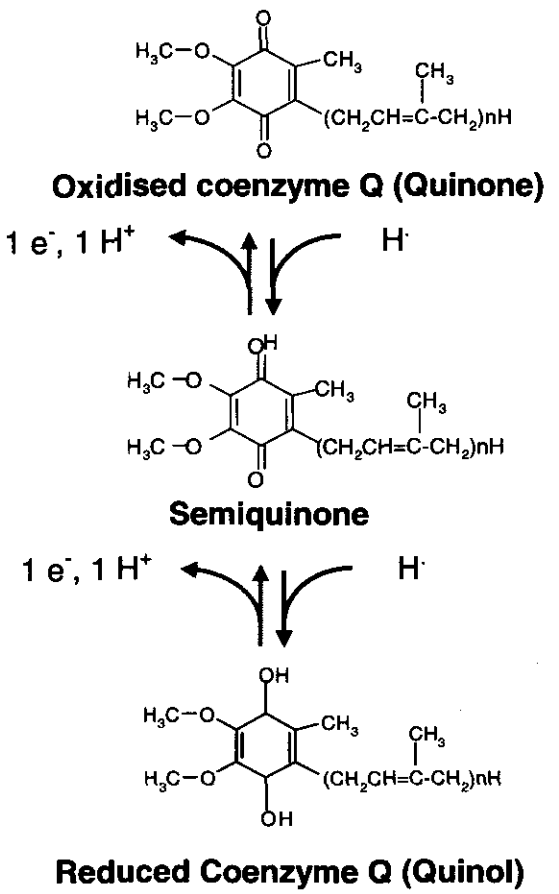

Figure 2.7. Complete reduction of ubiquinone requires two electrons and two protons, and occurs in two steps through the semiquinone radical intermediate (Mayes, 1993).

$Q_{10}H_2$ is the first anti-oxidant consumed when low density lipoproteins (LDL) is exposed to oxidants like peroxyl radicals, transition metals (Cu^{2+}, Fe^{3+}), hypochlorite, singlet oxygen and peroxynitrite (figure 2.8.). LDL from healthy people contains <1 molecule $Q_{10}H_2$ per particle, so how much should provide significant anti-oxidant protection? Each molecule $Q_{10}H_2$ scavenges two α-tocopherols and as such terminates two radical chains. This causes the rate of peroxidation to decrease 40-80 fold. The degree of inhibition decreases with the square root of the concentration of the anti-oxidant. This explains why even small amounts of $Q_{10}H_2$ offers protection against LDL peroxidation caused by low radical flux (Thomas *et al.*, 1997).

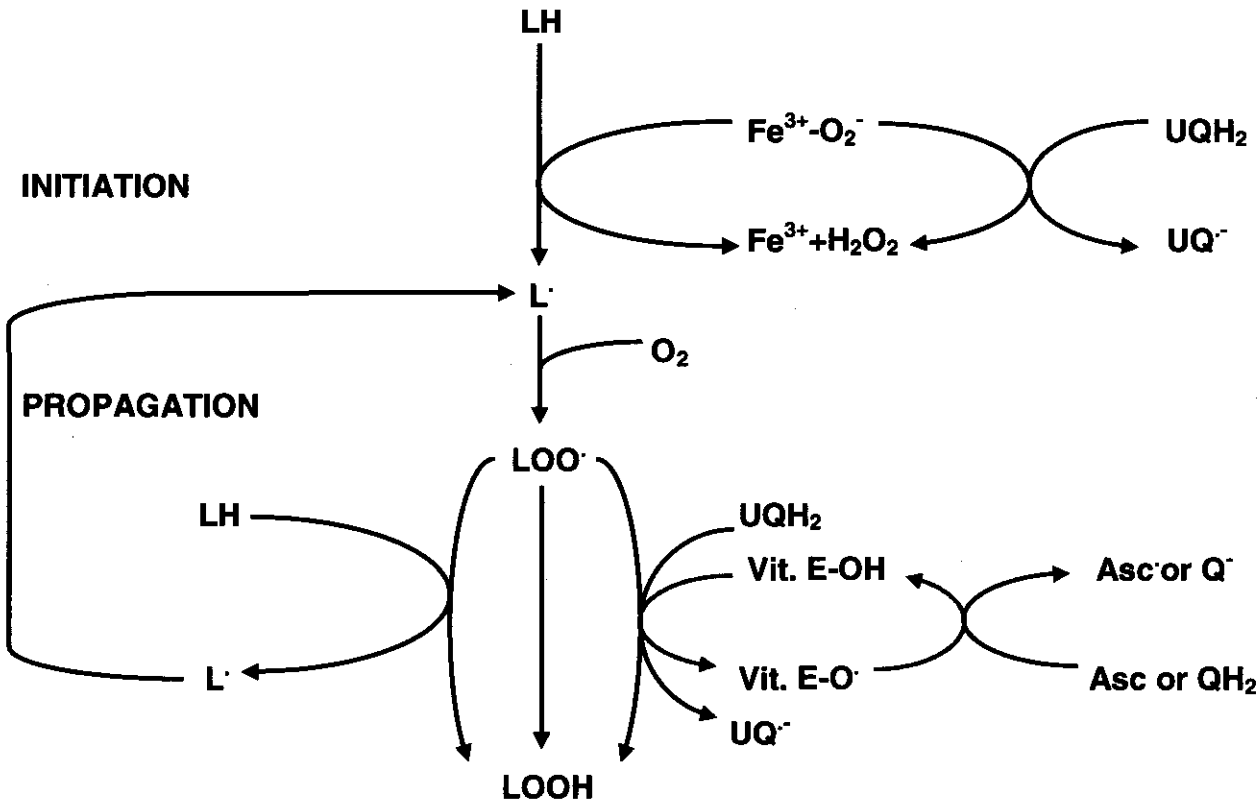

Figure 2.8. Schematic presentation of the action of Q_{10} H_2 as an inhibitor of lipid peroxidation and its relationship with vitamin E (Ernster & Dallner, 1995). (Abbreviations as in section 2.4.)

Decreased Q_{10} levels in plasma as well as a decreased ubiquinone /ubiquinol ratio have been reported in diseases with oxidative damage (Menke *et al.*, 2000). Electron leakage contributes to a defect in mitochondrial oxidative phosphorylation in terms of reduction in the activity of the NADH Q_{10} reductase (complex I). This leads to an increase in the oxidative burden. Such a reduced complex I activity has been reported in patients suffering from Parkinson's disease (Kidd, 2000; Ebadi *et al.*, 2001).

2.5. Properties of Q_{10}

2.5.1. Biosynthetic pathway

In mammalian cells the biosynthesis of Q_{10} involves two metabolic pathways (figure 2.9.). The first pathway involves the quinone ring, which is derived predominantly from tyrosine and in some instances from phenylalanine, which is converted to 4-

hydroxybenzoate (red lines) (Ernster & Dallner, 1995). This aromatic ring structure is always derived from dietary sources (Dallner & Sindelar, 2000).

The second pathway involves the polyprenyl side chain, which is synthesized from acetyl-CoA (blue lines) through the mevalonate pathway, leading to farnesyl-pyrophosphate. The latter, after conversion to decaprenyl-pyrophosphate (or in rodents solanesyl-pyrophosphate), condenses with 4-hydroxybenzoate acid to decaprenoyl- (or nonaprenoyl)-4-hydroxybenzoate, which is then converted to ubiquinone (Ernster & Dallner, 1995).

Little is known about the enzymes leading to synthesis of 4-OH benzoate. Most enzymes of the mevalonate pathway seem to have an intracellular distribution with different implications for the biosynthesis and transport of lipids. Q_{10} occurs in addition to mitochondria, in the endoplasmatic reticulum (ER), the Golghi apparatus, the lysosomes, the peroxisomes and the plasma membrane (Ernster & Dallner, 1995).

According to evidence, Q_{10} synthesis begins in the ER and is completed in the Golghi membranes, from where the quinone is transported to various cellular locations. It is also discharged across the plasma membrane to the blood, where it binds to serum lipoproteins. In contrast to cholesterol, Q_{10} does not distribute among different tissues via the circulation. In human and rat tissue and blood, Q_{10} is present partly in the reduced form ($Q_{10}H_2$), with the extent of reduction varying from one tissue to another. This is consistent with its function as an anti-oxidant (Ernster & Dallner, 1995).

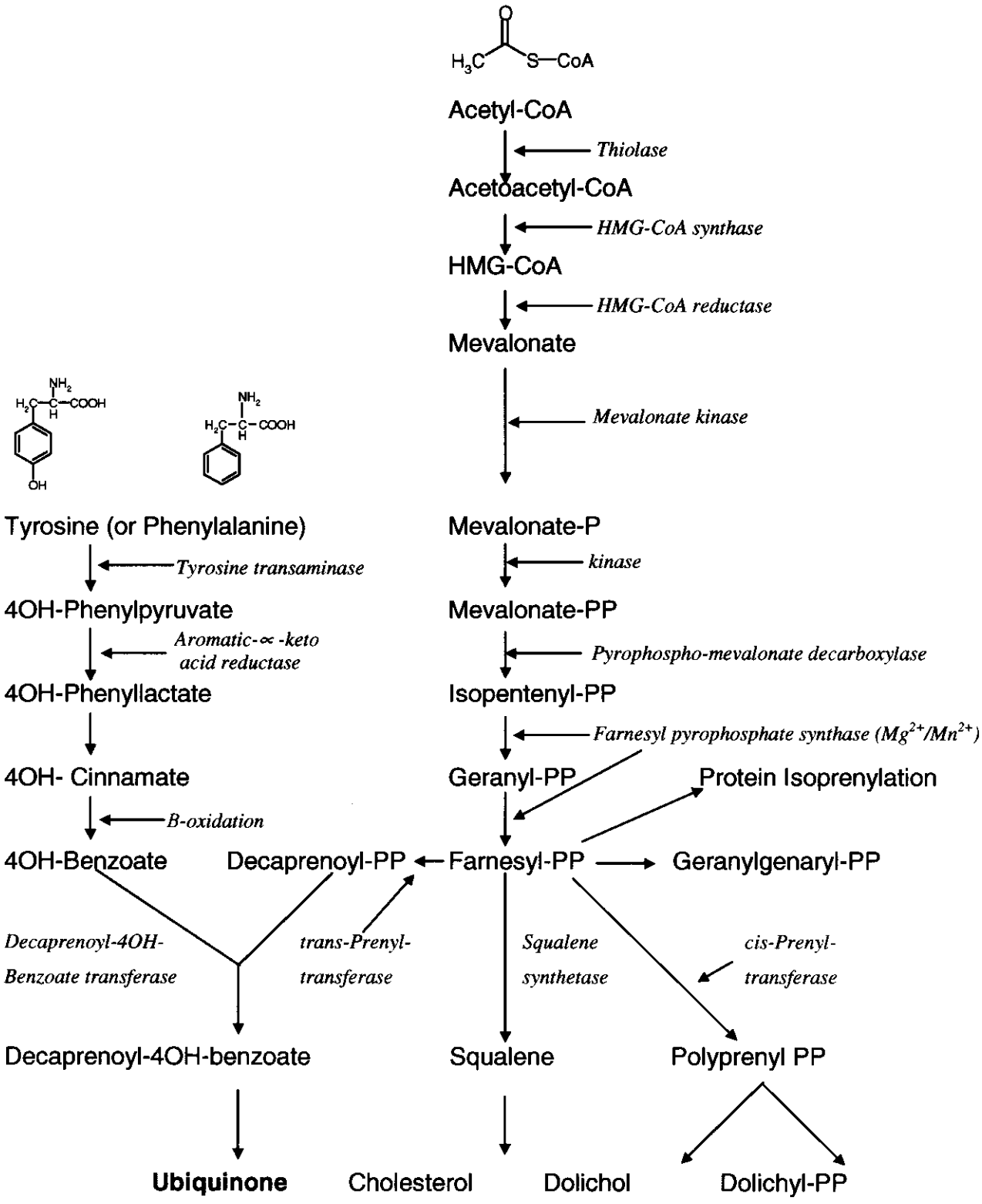

Figure 2.9. The pathway of biosynthesis of ubiquinone, cholesterol and dolichol (Ernster & Dallner, 1995).

The mechanism by which Q_{10} is reduced in membranes other than the inner membrane of the mitochondria is unclear. One possibility is that quinone reductases in membranes carry out this function. It has also been considered that the reduction may take place by way of temporary fusion between different membranes. The anti-oxidant effect of $Q_{10}H_2$ is probably not restricted to mitochondria. For instance, $Q_{10}H_2$ inhibits lipid peroxidation in isolated microsomes and prevents lipid peroxidation *in vivo* in mitochondrial and microsomal fractions of liver homogenates (Ernster & Dallner, 1995).

2.5.2. Half-life and catabolism

The half-life of Q_{10} in different tissues varies between 49 and 125 h and is in the same range as that of cholesterol, dolichol and phospholipids. A remarkable exception to this is found in the brain, where Q_{10} has a half-life of 90 h while cholesterol and dolichol exhibit extremely lower turnover rates than 90 h. Catabolism studies have been performed with the assumption that exogenously supplied Q_{10} mimics endogenous Q_{10} catabolism. The two major compounds in both urine and faeces had a quinone ring and a drastically shortened side chain with a carboxyl group. Both were in the conjugated form. Exogenously supplied Q_{10} did not influence the excretion of endogenous Q_{10} indicating that the two Q_{10} sources may represent two different pools (Dallner & Sindelar, 2000).

2.5.3. Uptake and distribution

Little is known about the uptake of ubiquinone in various human organs. Rats display a substantial uptake in the liver but this is mainly sequestered in the lysosomes. Dietary supplementation of ubiquinone may act primarily by elevating the ubiquinone levels in blood, where it serves important functions (Ernster & Dallner, 1995).

Q_{10} concentrations depend on a balance between 'inputs' and 'outputs'. With regard to 'inputs', Q_{10} levels are determined by the endogenous synthesis of Q_{10} and by the supply through the diet. The 'outputs' are those caused by oxidative stress and by cellular metabolism with regard to energy production (Mataix *et al.*, 1997).

Thomas *et al.* (1997) reported that when $Q_{10}H_2$ is present, formation of oxidised lipids are markedly suppressed. In humans not supplemented with Q_{10} only every second

LDL particle contains one molecule $Q_{10}H_2$. With dietary supplementation of 100-300 mg per day of $Q_{10}H_2$, increased concentrations of $Q_{10}H_2$ in plasma and all of its lipoproteins were noted. However, supplementation does not alter the redox ratio of $Q_{10}H_2$ to Q_{10} in LDL, which remains constant with 80% of the total Q_{10} present as $Q_{10}H_2$. This suggests that a reducing potential is available to keep Q_{10} in the reduced form but little is known of this process (Thomas *et al.*, 1997).

2.5.3.1. Stability of Q_{10}

$Q_{10}H_2$ is not stable and is oxidised easily in air. Ikenoya *et al.* (1981) reported that levels of $Q_{10}H_2$ decreased gradually with time. Ikenoya *et al.* (1981) evaluated the stability of $Q_{10}H_2$ in plasma under various storage conditions and found that the ratio of $Q_{10}H_2$ to the total sum of $Q_{10}H_2$ plus Q_{10} was constant for one day when kept at 2 and -10°C. At 24°C, 69% $Q_{10}H_2$ disappeared in one day. This indicated that blood samples from humans must be analysed on the same day or within 24 h even if stored below 2°C (Okamoto *et al.*, 1988). Investigation of $Q_{10}H_2$ in clinical studies have been hampered by instability during sample handling, storage, and processing. The concentration of $Q_{10}H_2$ decreases rapidly within one hour after phlebotomy. At room temperature it is oxidised at a rate of 3 nmol/l per min in the hexane extract of human plasma (Tang *et al.*, 2001).

2.5.4. Oxidative regulation

Studies on rats treated with thyroid hormone, revealed an increase of Q_{10} concentration in aerobic tissue. This increase in tissue Q_{10} occurred after the increase in metabolic rate caused by thyroid treatment, suggesting that it was an adaptation to, rather than a cause of, the increased oxidative activity (Ernster & Dallner, 1995).

Q_{10} administration has an effect on various myo- and neuropathies related to mitochondrial DNA depletion and other types of oxidative tissue injury. Evidence for regulation between oxidative stress and anti-oxidant capacity can be derived from studies of age-related changes in tissue Q_{10} levels. In 1985 scientists reported that the ubiquinone contents of several tissues of the rat increase after birth, reaching a maximum after 18 months after which it decreases with advancing age. In 1989 similar observations in human tissue was made with a maximal level of Q_{10} in most organs at

the age of 20 years followed by a decline. These findings indicate interplay among the three major biosynthetic products of mevalonate metabolism (ubiquinone, dolichol and cholesterol) (figure 2.9.) (Ernster & Dallner, 1995).

If Q_{10} decreases with age, dolichol increases in certain organs more than 100 fold, while cholesterol is unchanged. This decrease of Q_{10} content upon increasing age is consistent with the 'free radical theory of aging'. It may also account for the age-related increase in the extent of oxidative damage to proteins and DNA (especially the mitochondrial DNA) as well as increased incidence of degenerative diseases such as cancer and cardiovascular diseases. Aging and age-related degenerative diseases (AD and PD) may be related to a diminished capacity of the organisms to maintain adequate $Q_{10}H_2$ levels in relation to the prevailing need for anti-oxidant defence (Ernster & Dallner, 1995).

2.5.5. Clinical applications of dietary Q_{10} supplementation

In vitro supplementation of Q_{10} results in increased activity of the mitochondrial electron transfer system by enhancing complex I activity. Dietary supplementation of Q_{10} also protects LDL from the pro-oxidant effect of α-tocopherol supplementation alone (Thomas *et al.*, 1997). Q_{10} shows efficacy in the treatment of some other disorders of the mitochondrial electron transport system, it blocks neuronal lesions produced by the mitochondrial toxin, malonate. Q_{10} results in improvement in patients with encephalomypathies and also protects against glutamate neurotoxicity (Strijks, 1997).

Higher Q_{10} blood levels protect LDL from oxidation and prevent free radical damage caused by neutrophils in inflammatory diseases. It also prevents oxidative injury by endothelial cells and gives protection against free radical damage in the circulation. These are all effects of Q_{10} administration in experimental and clinical medicine (Ernster & Dallner, 1995).

In conclusion it can be said that Q_{10} is decreased in the brain with aging and that administration of Q_{10} may be useful in the treatment of mitochondrial disorders, causing neurodegenerative diseases such as Parkinson's disease where striatal activity of complex I is reduced.

2.6. Parkinson's disease (PD)

Alterations in the Q_{10} redox state may reflect changes in membrane electron transport and the effectiveness of defence against toxic reactive oxygen species such as hydrogen peroxide and superoxide (section 2.3.). This is noted for PD in which alterations in the activities of complex I have been reported in the substantia nigra (SN) (Gotz *et al.*, 2000; Walker, 1992). Complex I serves as a major entry point for electrons into the transport chain (section 2.2.3.). PD is an association between neurodegeneration and mitochondrial dysfunction or oxidative stress or both (Beal, 2000). Deficiencies of mitochondrial enzyme activities affect the electron transport process, which might be reflected by the Q_{10} redox state. Q_{10} redox ratios ($Q_{10}H_2$ to Q_{10}) and the ratio of $Q_{10}H_2$ compared to total Q_{10}, is significantly decreased in PD patients (Gotz *et al.*, 2000). PD is the second most common neurodegenerative disorder affecting 1% of the population older than 50 years and was first described by James Parkinson in 1871 (Ebadi *et al.*, 2001). Prior to this, the incidence of PD was very low, which led researchers to theorize that oxidative stress from environmental neurotoxins cause PD like symptoms. Evidence has of late converged to suggest that PD is primarily caused by oxidative stressors (Kidd, 2000).

The hallmark of PD is the degeneration of dopamine producing neurons in the SN (dopamine neurons outside the SN tend not to be affected) with the key factor being neuron death accompanied by the presence of Lewy bodies and Lewy neuritis. This reduces the overall supply of dopamine and compromises the brain's capacity to effectuate movement. PD therefore first becomes noticeable as tremors in the limbs and progresses to bradykinesia, rigidity and posture instability with impaired gait. During later phases the nerve supply to the heart degenerates, abnormalities of the liver occur and lower detoxification levels and lower mitochondrial oxidative phosphorylation are observed. PD is an age related disease and most cases do not have a familial contribution (Kidd, 2000).

2.6.1. PD and MPTP

The neurotoxic chemical, 1-methyl-4-phenyl-1,2,3,6-tetrahydropyridine (MPTP), induces symptoms that closely resemble PD (via inhibition of complex I), (Ebadi *et al.*, 2001) by causing damage to dopaminergic neurons. Investigators discovered this reaction in the

1980's when heroin addicts in California, who had taken an illegal drug contaminated with MPTP, began to develop severe Parkinsonism. A mechanism to explain the action of MPTP in nigrostrial cells in the brain is summarized in figure 2.10. (Walker, 1992).

Studies have elucidated that MPTP is metabolised by type B monoamine oxidase to the initial two-electron oxidation product, 1-methyl-4-phenyl-2,3-dihydropyridinium ($MPDP^+$), which undergoes further oxidation to the ultimate four-electron oxidation product, 1-methyl-4-phenylpyridinium (MPP^+) (figure 2.10.).

The MPP^+ is taken up selectively at dopaminergic synapses by the dopaminergic reuptake pump and then into the mitochondria by passive transport. In the neuronal mitochondria, MPP^+ inhibits respiration, blocking the oxidation of NADP by acting between Fe-S clusters and preventing electron transfer to ubiquinone (Walker, 1992) from NADH dehydrogenase, which results in defective oxidative phosphorylation (section 2.2.3.2.) (Strijks *et al.*, 1997).

This inhibition of complex I results in ATP depletion and cell death. Since the neurons do not regenerate, the damage is permanent. MPTP and idiopathic PD are similar in many respects, and it is possible that environmental xenobiotics act in a manner related to the etiology of the idiopathic disease (Walker, 1992). Q_{10} is able to attenuate the MPTP-induced loss of striatal dopaminergic neurons (Ebadi, 2001).

An alternative mechanism of MPTP toxicity may involve the generation of toxic active oxygen species (Walker, 1992). The $O_2^{\cdot}$ free-radical is formed in the below mechanism (figure 2.10.).

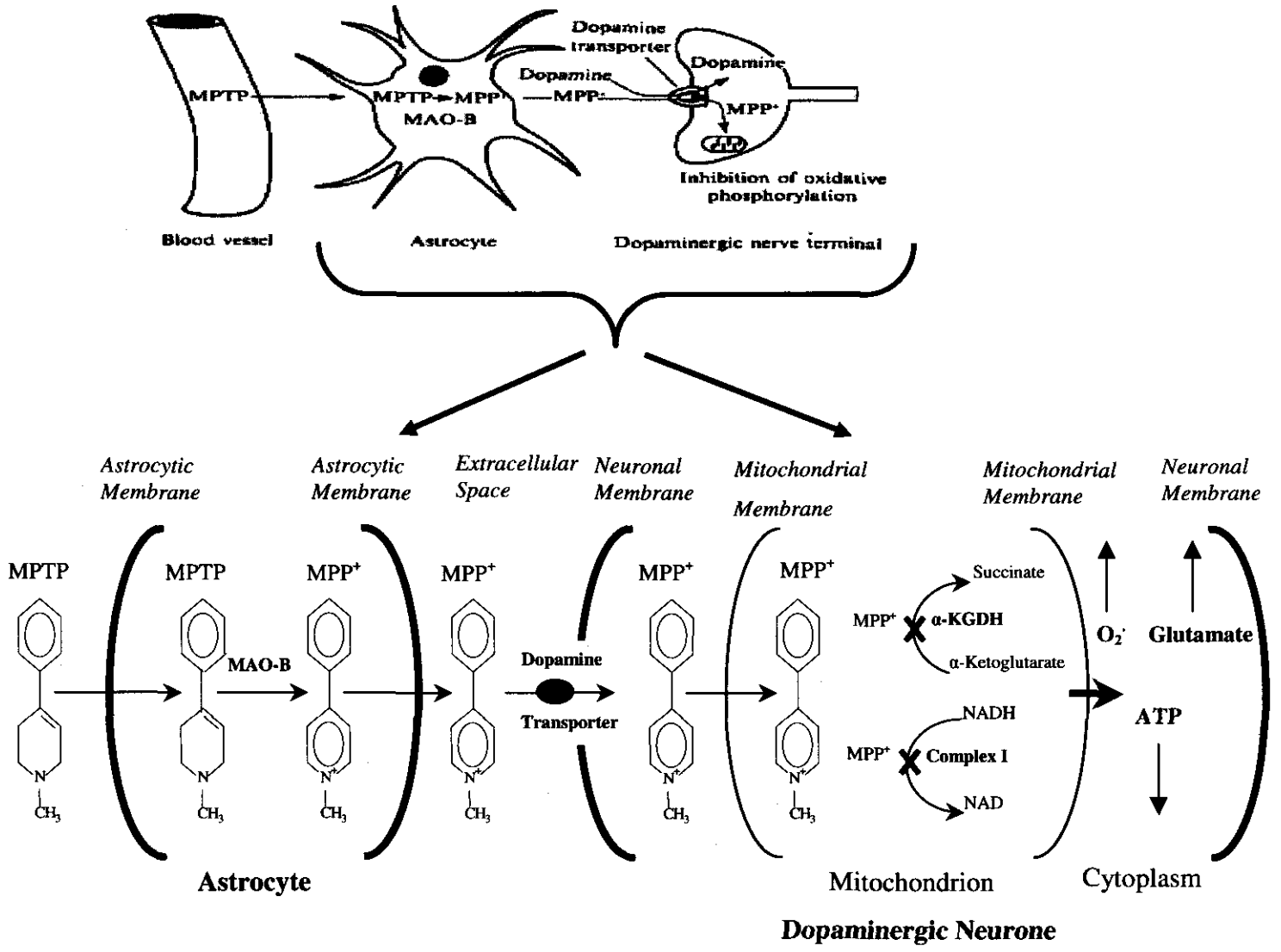

Figure 2.10. Uptake of the neurotoxin MPTP into the central nervous system (Walker, 1992; Kassie *et al.*, 2000; Tsuda *et al.*, 1998; Vaghef *et al.*1998).

2.6.2. DNA and oxidative damage

There is evidence that oxidative DNA damage may be a major cause of aging and age-associated neurodegenerative diseases like PD.

It is well established that oxidative damage in biological systems can also occur in other molecular species like DNA. DNA can be damaged by way of the hydroxyl radical, without a simultaneous lipid peroxidation. There are indications that DNA can be attacked by lipid peroxyl and alkoxyl radicals, resulting in base oxidations and strand breaks (Ernster & Dallner, 1995).

Oxidative damage to mitochondrial DNA has been estimated to be 10-fold higher than damage to nuclear DNA (Perlmutter, 1999). There is evidence that oxidative DNA damage may be a major cause of aging and age-associated degenerative diseases like PD (Ebadi *et al.*, 2001). This evidence includes the high level of oxidative damage and its accumulation with age, the correlation between oxidative damage and maximal life span potential, and the increased oxidative damage and premature aging found in people with Down's syndrome (Ebadi *et al.*, 2001).

A wide range of other human diseases is also associated with defects in the generation of ATP due to changes in the mitochondrial DNA sequence. About 38% of the mitochondrial genome codes for components of complex I. Defects in this enzyme are amongst the most common (Walker, 1992).

Neuronal cells of the central nervous system are more dependent on energy than cells of any other tissue and are therefore the most seriously affected by mitochondrial defects. Skeletal muscle is also seriously affected, followed by the heart, kidney and liver. Accumulation of mitochondrial mutations and cytoplasmic segregation of mutations during life, leads to progressive loss of respiratory function in cells and this is an important contributor to the process of aging and several degenerative diseases (Walker, 1992).

The reaction of ROS with DNA, either at the sugar-phosphate backbone or at the base, leads to strand fragmentation, which results in a chemically modified base. ROS are therefore potent intracellular mutagens. Numerous base modifications are detectable when ROS react with DNA. The most studied oxidised base is 8-hydroxydeoxyguanisine (8-OHdG), formed when hydroxyl radicals or singlet oxygen attacks DNA. In addition to being a useful marker for oxidative DNA damage the formation of 8-OHdG in DNA is also mutagenic (Ebadi *et al.*, 2001).

Ernster & Dallner (1995) showed that mitochondrial $Q_{10}H_2$ provides protection not only against lipid peroxidation but also against protein and DNA oxidation in membranes and lipoproteins and also suppresses DNA strand breaks in lymphocytes challenged with oxidative stress (Alleva *et al.*, 2001; Ernster & Dallner, 1995).

CHAPTER 3.

ANALYTICAL METHODS FOR UBIQUINONE

Procedures for the isolation and detection of ubiquinone in the past relied on spectrophotometry, fluorimetry or polarography and required lengthy isolation and purification steps to remove interfering compounds (Lang & Packer, 1987). Capillary zone electrophoresis, voltammetric, chemiluminescent, potentiometric, fluorometric and spectrophotometric methods are also described in the literature. Although some of these methods provide good sensitivity, most are complicated and time consuming (Karpinska *et al.*, 1998). The most popular methods currently, are HPLC analyses with ultra violet (UV) or electrochemical (EC) detection.

3.1. General separation and identification methods for ubiquinones

3.1.1. Colour reactions

Methods for the identification of quinines include colour reactions, paper chromatography and enzymatic reactions. Craven's test was considered to be specific for quinones containing a labile hydrogen or halogen atom attached to a quinone carbonyl group. A dark bluish-violet colour, which changes to blue, green and reddish brown develops when quinone is treated with cyanoacetate (ECA) and alcoholic ammonia during this test. ECA with gaseous ammonia gives a blue colour, which changes to green and tan upon standing. These colour changes can be attributed to the methoxyl groups, which undergo displacement with ECA (figure 3.1.).

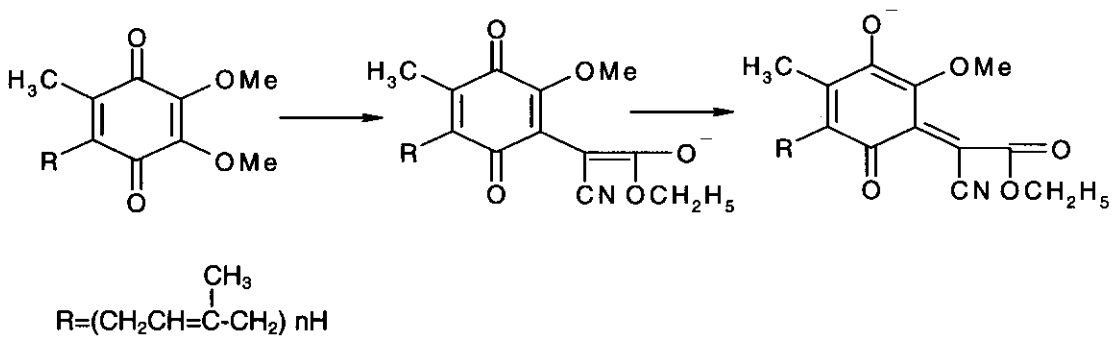

Figure 3.1. Reaction of ethyl cyanoacetate with coenzyme Q.

Other reactions involve the oxidation-reduction properties of Q_{10}. The oxidised quinone may be detected by interaction with leucomethylene blue and the reduced quinone by application of the Emerie-Engel test ($FeCl_3$, α, α- dipyridyl), described by Lester *et al.* (1958) (quoted by Hatefi, 1963) or it could be detected after interaction with tetrazolium dyes).

These colour tests suffer from a lack of specificity. They cannot be used unless the Q_{10} sample is relatively pure and uncontaminated by other quinones or compounds capable of interacting with the reagents (Hatefi, 1963).

3.1.2. Chromatography

Paper chromatography has been used for large-scale separation of Q_9 and Q_7. In addition this method is a convenient tool for identification of coenzyme Q. An excellent procedure was developed by Lester & Ramasarma (1959), (quoted by Hatefi, 1963) which involves the use of paper impregnated with silicone with two different solvent systems composed of n-propanol and water. In the first system, used to separate Q_{10}, the ratio n-propanol-water is 4:1(v:v). In the second system the ratio is 7:3 and is used to separate mixtures of Q_{10} and $Q_{10}H_2$ (Hatefi, 1963).

3.1.3. Enzymatic methods

Enzymatic reactions involving coenzyme Q can also be used for the assay of coenzyme Q and its synthetic homologs. In 1961 scientists have successfully employed coenzyme Q-depleted mitochondria (by acetone extraction) to survey various quinones with respect to coenzyme Q-like properties in the electron transport system (Hatefi, 1963). These reactions can be used for Q_{10} assay and its synthetic homologs.

3.2. Quantitave analysis of ubiquinone

3.2.1. Spectrophotometric

In 1968, scientists reported two methods for the quantitative analysis of Q_{10} in human blood, which eliminated the undesirable step of saponification. In both methods ECA was used to form a coloured product, suitable for colorimetric determination. However,

these methods were time consuming (Vadhanavikit *et al.*, 1984). For the determination of Q_{10} in biological samples, a dual wavelength spectrophotometric method developed by Chance (1951), Hatefi (1959) and Crane & Barr (1971) (quoted by Hatefi, 1963) has often been applied. Cyclohexane extracts of mitochondria in ethanol showed a UV spectrum similar to Q_{10}. With addition of KBH_4 the peak at 275 nm disappeared and a spectrum similar to $Q_{10}H_2$ appeared. The concentration of Q_{10} was calculated from the change in absorbancy (Hatefi, 1963). However, these methods cannot easily distinguish each homologue of Q_{10} and need a large amount of sample because of the low sensitivity (Okamoto *et al.*, 1988).

Ramasarma (1959) (quoted by Hatefi, 1963) described a method for the determination of total Q_{10} by spectrophotometric analysis. This method is based on the difference in absorbancy of the oxidised and reduced ubiquinone at 275 nm or in other words, a modified Craven 's test (section 3.1.). This method utilizes the quinone nuclei as the analytical principle but does not give satisfactory results for the individual homologues of ubiquinone (Imbayashi *et al.*, 1979).

The UV spectrophotometric methods have severe problems with plasma background, which makes determination very difficult. An alternative method was described by Karpinska *et al.* (1998), which utilizes derivative spectrophotometry. This eliminates the influence of the background and increases selectivity and sensitivity for coenzyme Q determination.

3.2.2. Liquid chromatography

HPLC offers several advantages, including speed, direct quantitive assays, ease of recovery of solutes and the absence of a requirement of volatility of the solute (Donnahey & Hemming 1975). In HPLC both the stationary phase and the mobile phase can interact selectively with the sample. HPLC is a much more versatile method than gas chromatography (GC), and can often achieve much more difficult separations (Lindsay, 1997).

Donnahey & Hemming (1975) reported that HPLC could be used for analytical and preparative chromatography of families of ubiquinones.

3.2.2.1. Fluorometric detection

Craven (1931) (quoted by Hatefi, 1963) reported that ubiquinones, which have a hydrogen or halogen substituent on the ring, give a blue colour in their reaction with ECA in the presence of a base. Kofler (1945) (quoted by Hatefi, 1963) reported that displacement of methoxyl substituents from the quinone ring by ammoniacal ECA give similar blue coloured products. Koniuszy *et al.* (1960) (quoted by Hatefi, 1963) applied this to the determination of ubiquinone in urine, replacing ammonia with potassium hydroxide. Redalieu *et al.* (1961) (quoted by Hatefi, 1963) developed a method that is sensitive to 1 nanomole of ubiquinone. Quite a number of quinones, including benzoquinone, chloranil, 2,5-dimethylbenzoquinone, 2,3-dichloronaphthoquinone and menadione give fluorescent products with alkaline ECA at a later stage of the Craven's reaction. Recovery experiments indicated that labeled tracers might be necessary to develop the method in biological samples (Rokos, 1973).

Abe *et al.* (1978) reported that other substances reactive with ECA were present in serum and liver. He extracted ubiquinone with n-hexane. Other fat-soluble vitamins in the extract did not react with ECA reagent. The minimum detectable quantity was 10 ng. This high-speed-liquid-chromatography (HSLC) -method with fluorometric detection was in good agreement with data obtained by HSLC-ultra violet detection at that stage. Overall it can be concluded that not all Q_{10} reacts with ECA to give fluorescent products and therefore poor recoveries occur. Although a fluorescence detector is highly sensitive, UV and EC detection give much better recoveries and selectivity.

3.2.2.2. Ultra violet detection

In the past, liquid chromatography with UV detection was seen as a useful method for determination of ubiquinone (Q_{10}) in serum and animal tissue because of its excellent selectivity and useful sensitivity (Okamoto *et al.*, 1988); (Grossi *et al.*, 1992). Q_{10} is detected at 275 nm absorbance maximum by UV detection (Lang & Packer, 1987). Wang *et al.* (1999) reported that when the concentration of Q_{10} is low, as in plasma, the sensitivity of UV detection is inadequate. Okamoto *et al.* (1988) reported that LC UV could not determine $Q_{10}H_2$ because of its low molar absorptivity, at wavelengths of 276-290 nm.

3.2.2.3. Electrochemical detection

Although more sensitive than UV detectors, the electrochemical (EC) detectors are not easy to use, and have a limited range of application. They are used for trace analyses where the UV detector does not have high enough sensitivity (Lindsay, 1997).

EC detectors for HPLC measure the conductance of the current (Lindsay, 1997) resulting from the application of a potential (voltage) across electrodes in a flow cell (Weston & Brown, 1997), associated with the oxidation or reduction of the solutes. To be capable of detection, the solutes must be easy to oxidise or reduce. EC detectors that measure current associated with the oxidation and reduction of solutes are called amperometric or coulometric detectors (Lindsay, 1997). A substance that can be electrochemically oxidised or reduced like ubiquinone (Q_{10}) is said to be electro active.

An amperometric EC detector is preferred for the determination of $Q_{10}H_2$ due to its high sensitivity although it is not applicable to Q_{10} (Wang *et al.*, 1999), except when all of the ubiquinone could be reduced to ubiquinol thus representing the total amount of Q_{10}. Several on-line postcolumn reduction methods for simultaneous measurement of $Q_{10}H_2$ by EC detection have been described. These methods however, required either an on-line reduction column or double cell EC detector (for achieving postcolumn reduction) or coupled-column with column switching valves or postcolumn two-way valves. The complication of the instrumentation limits the practical application of these methods in clinical use (Wang *et al.*, 1999). The amperometric detector's major advantage lies in the great reduction possible in the cell volumes and the very small dispersion produced (Knox, 1980). Another advantage of amperometric detectors is that detection is possible with a very small internal volume (Weston & Brown, 1997).

A coulometric EC detector is able to give a 100% yield of the electro chemical (EC) reaction and can detect the oxidised form. The $Q_{10}H_2$ is unstable at room temperature and quickly becomes oxidised (section 2.5.3.1.). With extraction, using a vacuum and subjecting the sample to prolonged air flushing, total conversion of $Q_{10}H_2$ to Q_{10} can be achieved, allowing the determination of total Q_{10} (Grossi *et al.*, 1992).

Ikenoya *et al.* (1981) developed a UV and EC detection method based on reversed-phase chromatography for Q_{10}. With measurement of the absorption at 290 nm, the

maximum for $Q_{10}H_2$, it was unsuccessful for tissue samples because of interference by UV-absorbing compounds, such as retinyl palmitate having similar retention times. EC detection was in the anodic mode for the determination of Q_9H_2 and $Q_{10}H_2$. UV detection was performed at 275 nm for Q_9 and Q_{10}. Conversion from $Q_{10}H_2$ to Q_{10} during analysis was less than 2% of the $Q_{10}H_2$ injected.

Edlund's (1988) detection system was comprised of three coulometric working electrodes and one UV detector coupled in series. Q_{10} was oxidised at the first electrode, reduced at the second and oxidised again at the third electrode. A precolumn switching system was used to prevent large solvent fronts of plasma components. The noise of a coulometric detector is dependent on the background current. Metal ions and oxygen are reduced at the same potential as Q_{10} and high background currents were obtained when Q_{10} was reduced by coulometry. High selectivity and sensitivity was obtained by this method (Edlund, 1988).

Grossi *et al.* (1992) introduced a precolumn oxidation cell for $Q_{10}H_2$ but their quantitative measurement was unsuccessful. Finckh *et al.* (1995) developed a micro method for simultaneous measurement of lipophilic anti-oxidants using HPLC with coulometric post column EC detectors. Poor recoveries were reported for Q_{10} and $Q_{10}H_2$. In 1996 a rapid HPLC-EC procedure was reported. The post column EC electrodes described by Edlund (1988) were used. The sample and solvent volumes were much greater than previous methods and the injection volume was increased fourfold. This method may be prone to analytical variation because it does not use an internal standard for quantifying Q_{10} (Tang *et al.*, 2001).

Wakabayashi *et al.* (1994) described a method with simultaneous determination of reduced and oxidised Q_{10} with a platinum catalyst reduction precolumn and EC detection with a glassy carbon electrode. Litescu *et al.* (2001) also found that Q_{10} is electro active at a glassy carbon electrode. Leray *et al.* (1998) described a procedure using two-isocratic step HPLC and EC detection in the oxidative mode. Zinc-catalysed reduction in a postcolumn reactor allows the detection. The high selectivity and sensitivity enabled use of low oxidation potentials giving little baseline noise (Leray *et al.*, 1998).

Yamashita & Yamamoto (1997) described a method for the simultaneous detection of $Q_{10}H_2$ and Q_{10} in human plasma. They used a post separation, on-line reduction column to convert Q_{10} to $Q_{10}H_2$ for EC detection. Wang *et al.* (1999) used sodium borohydride to reduce the Q_{10} to the $Q_{10}H_2$ for the determination of $Q_{10}H_2$ with EC detection. They reported that this method was useful in clinical investigation.

Tang *et al.* (2001) reported that in previous methods samples were converted to Q_{10} by the use of an oxidizing reagent such as ferric chloride, or to $Q_{10}H_2$ by reducing agents such as $NaBH_4$ or $Na_2S_2O_4$. These methods are inefficient because of pre-analytical degradation and potential for error because of the lability of $Q_{10}H_2$. They preferred EC coulometric detection for measurement of Q_{10} because of its high sensitivity. The EC reaction was measured at electrodes, which detected the current produced by the reduction of Q_{10} or by oxidation of $Q_{10}H_2$. The inline reduction procedure permitted transformation of Q_{10} into $Q_{10}H_2$ and avoided artifactual oxidation of $Q_{10}H_2$.

Mattila *et al.* (2000) compared in-line connected EC and diode array (DAD) detectors in reversed-phase HPLC for the analysis of Q_{10} and Q_9. Responses of the detection systems were linear in the range evaluated, 10-200 ng/injection and had correlation coefficients exceeding 0.999. Recoveries of added Q_{10} and Q_9 varied between 73-105% for DAD and 74-103% for EC detection respectively. Detection limits with DAD were 4 and 6 ng/injection, respectively, and 0.2 and 0.3 ng/injection by EC detection. The EC detector was 20-fold more sensitive, the selectivity was, in some cases poorer than with DAD.

CHAPTER 4

DETERMINATION OF DNA DAMAGE

During the last 20 years, many analytical techniques have been developed to monitor oxidative DNA damage. HPLC with EC and GC mass spectrometry (MS) are the two basic methods contributing to this field. Guanine in DNA is oxidised during derivatisation with GCMS and therefore the use of this method is limited. Currently, the arsenal of methods available include the HPLC-tandem MS technique, capillary electrophoresis, ^{32}P-postlabeling, fluorescence postlabeling, ^{3}H-postlabeling, antibody-base immunoassays, and assays involving the use of DNA repair glycosylases such as the comet assay, the alkaline elution assay and the alkaline unwinding method (Guetens *et al.*, 2001).

4.1. Methods used to determine DNA damage

4.1.1. Liquid chromatography (LC)

Guetens *et al.* (2001) introduced the use of LC-MS for the measurement of a number of oxidatively damaged DNA fragments. The bulk of available chromatographic methods aimed at measuring individual DNA base lesion require either chemical hydrolysis or enzymatic digestion of oxidised DNA, following extraction from cells or tissues. The effect of experimental conditions (DNA isolation, hydrolysis, and/or derivatization) on the levels of oxidatively modified bases in DNA is enormous and has been studied intensively in the last 10 years.

4.1.2. Spectrophotometry

Ahamad *et al.* (1998) used a monoclonal antibody (Mab) as an immunochemical probe to detect oxidative DNA damage *in vivo*. The absorbance of a DNA solution after the extraction and isolation was measured with a UV spectrophotometer at 260 and 280 nm to ascertain its purity and concentration.

4.1.3. Postlabeling

The protocol of Jones *et al.* (1997) has the advantage of allowing for the exclusive ^{32}P-labeling/detection of several oxidative DNA lesions. This development allows detection limits as low as 1.8 fmol of damage/µg of DNA assayed and has permitted an assessment of basal levels of damage in human peripheral blood lymphocyte DNA.

4.1.4. Viscometric method

Parodi *et al.* (1982) induced DNA damage with dimethylsulfate (DMS) and measured it with an oscillating crucible viscometer, having a U-shaped circular channel. A rapid increase in viscosity, indicated elevated DNA uncoiling.

4.1.5. DNA-DNA dot hybridisation technique

This technique was adapted by Müller *et al.* (1989) for use as a quantative DNA detection method during alkaline elution analysis of irradiated cell material. In comparison to standard microfluorometric methods, similar γ-ray-dose-response relationships were obtained with less than 1% of the cell material when the dot hybridisation assay was used (Müller *et al.*, 1989).

This method of detecting DNA in alkaline elution analysis is generally proposed for tissues which yield only low amounts of cell material and/or which are difficult to label by radioactive precursors.

4.1.6. Immunochemical assay

Van Loon *et al.* (1992) developed a simple, sensitive and fast immunochemical method to quantify the amount of DNA damage in cells of human blood after *in vitro* exposure to ionising radiation. The technique is based on the enhancement of the radiation-induced single–strandedness, which occurs in DNA regions flanking strand breaks, by a controlled further unwinding of the DNA in an alkaline solution. DNA damage is then quantified by determining the extent of single-strandedness with a monoclonal antibody, directed against single-stranded DNA.

4.1.7. Fluorometry

In 1996 Walles *et al.* used an alkaline elution assay in which cells were lysed and single stranded DNA subsequently eluted. The amount of DNA was measured by fluorometry after addition of fluorochrome.

In 1996 Walles *et al.* also used a DNA unwinding technique to determine single-strand breaks in cell nuclei. Single and double-stranded DNA was separated on a column of hydroxyapatite and the amount of DNA was also determined by fluorometry after addition of fluorochrome (Walles *et al.*, 1996).

4.1.8. Single cell gel electrophoresis (comet assay)

Deoxyribulose nucleic acid (DNA) damage can be determined with the single cell gel electrophoresis (SCGE) or comet assay technique by measuring the comet tail, the so-called tail moment (TM). DNA lesions produced by chemical and physical agents include strand breaks, modified bases, DNA-DNA crosslinks and DNA-protein crosslinks (Gutierrez, 1998). Strand breaks may be introduced directly by genotoxic compounds, through the induction of apoptosis or necrosis, or indirectly through the interaction with oxygen radicals or other reactive intermediates (Lee & Steinert, 2003). Gutierrez stated in 1998 that the comet assay is able to detect DNA damage induced by alkylating agents, intercalating agents, and oxidative damage (Gutierrez, 1998), which may be produced by MPTP (section 2.6.1. - 2.6.2.).

In 1978, Rydberg & Johanson estimated DNA damage in individual cells by a novel technique. They mixed human lymphocytes in agarose to make microgels on microscopic slides. They then lysed cells and unwound DNA using sodium hydroxide. The number of pieces of single stranded DNA that were generated under these alkaline conditions depended upon the number of breaks in the double stranded DNA. Using acridine orange (AO), an intercalating metachromatic dye, which emits a green fluorescence when bound to double stranded DNA, and red when bound to single stranded DNA at optimum concentrations, they quantified greenness and redness for estimating DNA damage.

In 1984, from the same laboratory, Östling & Johanson added a novel step to this technique. After lysis of cells in agarose microgels, they electrophoresed the DNA and after staining with AO they estimated the damage in cellular DNA by using the ratio of fluorescence intensity at two points along the migrated DNA (Östling & Johanson, 1984). The electric current pulled the charged DNA from the nucleus in the direction of the anode and resulted in characteristic images resembling a comet with a head and a tail. As a result of the loss of DNA supercoiling at low concentrations of genotoxins or DNA fragmentation at high concentrations, more fluorescence was observed in the tail relative to the head in damaged cells. DNA fragments migrate more freely in the gel than in the loops and cause the formation of more elongated tails. As the lyses was carried out at a neutral pH, only the detection of double-strand breaks was possible, since at this pH, DNA base paring is not disrupted and thus discontinuities in single-stand breaks cannot be detected (Kassie *et al.,* 2000). Singh *et al.* (1988) modified the assay by introducing a technique involving electrophoresis under alkaline conditions (pH > 13), which enabled the detection not only of frank strand breaks but alkalilabile sites, DNA crosslinking, and incomplete excision repair sites. Currently, this is the most commonly used method with slight modifications at different steps (Kassie *et al.,* 2000). This technique however, had two major disadvantages. Firstly, due to the significant amount of RNA present, estimation of the correct amount of DNA was not possible. Secondly, the sensitivity was limited due to the conditions used for dissociation of the chromatin, which allowed DNA to maintain its tertiary and quaternary structures (Singh *et al.*, 1988).

DNA, with the tertiary and quaternary structure intact, does not move in a predicted manner. Normally low molecular weight DNA moves farther in an electric current in an agarose matrix. In 1988, Singh *et al.* electrophoresed lysed cells under alkaline conditions (300 mM) to partially disrupt the DNA secondary structure and to remove the DNA tertiary and quaternary structure. This allowed a more predictable movement of DNA in the agarose. Alkaline conditions also degraded the RNA. They used ethidium bromide to visualise the electrophoresed DNA and were able to detect DNA damage caused by as low as 25 radicals (rad) of X-rays in freshly isolated human lymphocytes (Singh *et al.*, 1988).

In the technique used by Singh *et al.* (1994) most of the components for the lysis solution were incorporated from the lysing solution used in the nucleoid sedimentation

technique. Sodium lauryl sarcosine, a detergent, was added for rapid lysis of cells, since this detergent quickly penetrates the gel to reach embedded cells. Singh also recommended another agent, Triton X-100, a non-ionic detergent.

However, all of these revisions and adaptations did not provide enough sensitivity. To further enhance the sensitivity of the technique, Singh *et al.* (1994) made several modifications. To free nuclear DNA of proteins, they introduced a proteinase-K step after regular lysis. In order to apply a uniform electric field (which minimises variation in DNA migration from slide to slide and from cell to cell on the same slide), they modified the electrophoretic unit and used recirculating anti-oxidant rich alkaline electrophoretic solution consisting of 2% DMSO (dimethylsulfoxide), 0.1% 8-hydroxyquinoline, and 300 mM NaOH and 10 mM EDTA. To enhance sensitivity they used an intense fluorescent dye, YOYO-1, to detect electrophoretically migrated DNA. These changes enabled them to detect significant DNA damage after exposure to doses as low as 5 rad of X-rays. Slide to slide variations in DNA migration, due to the accumulation of salt towards the cathode and uneven distribution of electric current in the electrophoretic unit, were major problems. These were solved by using a recirculating electrophoretic solution and attaching dual electrical inputs to each electrode of the unit (Singh *et al.*, 1995).

Also in 1995, Singh *et al.* introduced the use of ethanol precipitation of migrated DNA in agarose to enhance the sensitivity of detection of DNA in microgels. This provided slides that were preserved for future use. Using a gamma ray source (Tc99m) to irradiate lymphocytes for 1 h at 4°C (low temperatures inhibit repair of strand breaks), the investigators were able to detect significant DNA damage at a dose as low as 0.1 rad. The researchers used frosted slides for better attachment of agarose. The shortcoming of the technique was the uneven background from the frosting on the slides. The uneven background made it difficult to analyse the migrated DNA using an image analysis system. Two changes were made to address this problem: In 1998 the use of a tray was introduced to simultaneously process eight slides from electrophoresis through the neutralisation to DNA precipitation (Singh, 1998) and, in 1999 newly designed clear window frosted slides were used. Collectively, these changes allowed visualisation for the first time of a single DNA double strand break in a single *Escherichia coli* DNA molecule using a fluorescent microscope (Singh *et al.*, 1999).

Many types of cells are suitable for detection of single strand breaks/alkali labile sites, using the alkaline microgel electrophoresis assay. Sperm cells, however, naturally carry abundant alkali labile sites (Singh *et al.*, 1989), so much so that it is not possible to see

the effects of even very high doses of radiation in well lysed and proteinase-K treated cells in microgels. In 1997, Singh & Stephens introduced a neutral version of the assay to detect X-ray induced DNA damage in human lymphocytes. In 1998, they also utilised the neutral microgel electrophoresis assay to detect DNA double strand breaks in sperm cells (Singh & Stephen, 1998).

4.2. Uses of SCGE

4.2.1. Dietary intervention studies

There are reports in which the comet assay was used for monitoring protective effects of antioxidant micronutrient supplements. These studies deal with the protective effects of antioxidant vitamin supplement or vegetable products towards oxidative DNA damage resulting form endogenous oxidative stress, exhaustive physical exercise or oxidative stress initiated *in vitro.* DNA damage was found to be reduced significantly upon a single dietary supplementation with vitamin C, short-term vitamin E supplementation, extended supplementation with a mixture of vitamins, or supplementation with a combination of vegetable products for 6 weeks (Kassie *et al.,* 2000).

4.2.2. Clinical studies

SCGE has been applied in a number of clinical studies to investigate the consequences of certain pathological conditions or therapeutical exposure to chemicals at the cellular level. Significantly elevated DNA damage was found in subjects with malnutrition and parasitic infection (Steinmetz & Potter, 1995), diabetes (Collins *et al.*, 1998), urinary bladder cancer (Mckelvey-Martin, 1997), and after an abortion (Baltaci *et al.*, 1998). Oxidative stress as a result of hyperglycaemia, local tissue damage or altered anti-oxidant status was incriminated as causes of increased damage in diabetic patients (Tangiguch *et al.*, 1996, Kassie *et al.,* 2000).

4.2.3. Occupational, lifestyle or environmental exposure to genotoxic agents

Since exposure to genotoxins at the work place or in the environment is usually low or even close to the background level, unequivocal positive results are rarely found in human bio monitoring studies with classical cytological tests such as sister chromatin

exchange, chromosomal aberration and micronucleus. On the other hand, the comet assay was shown to be able to identify low levels of exposure with great sensitivity (Betti *et al.*, 1995; Betti *et al.*, 1994; Hartmann *et al.*, 1998; Hartmann *et al.*, 1994) and as a result, a big interest arose in the use of this assay to bio monitor occupational, lifestyle, and environmental exposure to genotoxins.

Occupational exposure to pesticides, benzene, anaesthetic gases, radiation, vinyl chloride, and styrene caused a significant increase in DNA damage. Also, analysis of leukocytes from workers exposed to environmental pollutants at a waste disposal site exhibited significant DNA damage in the exposed group. However, workers at a municipal sewage plant did not show an increase in genetic damage. Whereas one study reported a significant increase in DNA strand breaks but not oxidized bases of lymphocytes of workers at a rubber factory, a higher but non-significant effect was found in another study using the same indicator cells. Comparison of white blood cells, buccal mucosa cells and nasal epithelial cells for their sensitivity to detect exposure to environmental pollutants showed that the latter are the most sensitive. This was explained by the fact that these cells are the first sites of contact with toxic pollutants. The effects of tobacco/cigarette smoking on DNA damage was investigated under two circumstances: either as a sole genotoxic factor or compounding factor. The habit of tobacco/cigarette smoking itself was found to cause a significant increase in DNA strand breaks. There was also a significant increase in DNA damage in farmers handling pesticides, hair colourists and health professionals exposed to anaesthetic agents (Kassie *et al.*, 2000).

CHAPTER 5

DETERMINATION OF UBIQUINONE CONCENTRATION AND DNA DAMAGE

This chapter discusses the determination of $Q_{10}H_2$ and Q_9H_2 levels in blood and tissue (brain, liver and heart), after oral administration of Q_{10}. It is postulated that an elevation of $Q_{10}H_2$ and Q_9H_2 could counter the compromised energy production caused by neurodegenerative agents or disease by its beneficial effect on the electron transport chain as well as its anti-oxidant capacity. This may lead to lower DNA damage and cell death. To test this hypothesis we will determine the relationship between $Q_{10}H_2$ concentrations in the blood and various tissues. These concentrations will be correlated with cell DNA damage found in the blood and tissues.

Because neurodegeneration and thus also the necessity for neuroprotection, is more frequent among the aged, old mice were used as animal model in this study. This will make it possible to evaluate the effectiveness of Q_{10} as a potential protective agent against genetic damage.

We used HPLC with EC detection to measure $Q_{10}H_2$ concentrations and SCGE technology to measure cell DNA damage and monitor DNA repair (Table 5.1.). This made it possible to evaluate the effectiveness of $Q_{10}H_2$ as a possible anti-oxidant against cell DNA damage.

Table 5.1. Samples determined

SAMPLE	METHOD	MOTIVATION (Determination)
Heparin blood/ Lymphocytes	HPLC (EC)	Concentration changes
	SCGE	DNA damage
Brain	HPLC (EC)	Concentration changes
	SCGE	DNA damage
Liver	HPLC (EC)	Concentration changes
	SCGE	DNA damage
Heart	HPLC (EC)	Concentration changes
	SCGE	DNA damage

5.1. Treatment regimen

The Ethics Committee of the Potchefstroom University for Christian Higher Education (PU for CHE) approved all experiments. The experimental animal centre at PU for CHE supplied the one-year-old C57BL/6 mice. The mice were each held in a separate cage of 10 cm x 30 cm at room temperature. The standard diet consisted of Epol rat chow, which was given ad lib. Four groups of mice were studied over six weeks:

Standard diet (Control), n = 48,

Q_{10} supplemented diet (Q), n = 48,

Standard diet with MPTP treatment (MPTP), n = 48,

Q_{10} supplemented diet with MPTP treatment (Q+MPTP), n = 48

The Q_{10} was sonicated until dissolved in sweet oil (SO), mixed with peanut butter (5:1) and administrated orally by applying the mixture onto a specimen glass. Peanut butter (PB) was added to enhance the viscosity of the mixture to place it in the cage for the mice to eat. The oral dosage for each mouse in 200 µl of the mixture was given daily, according to the average weight for the whole group and the concentration of our mixture. The control group also received 200 µl of PB and SO mixture per day.

Beal *et al.* (1998) showed that 200 mg/kg/day Q_{10} was enough to attenuate the MPTP induced loss of striatal dopamine and dopaminergic axons in aged mice. The treatment regimen is described in Table 5.2. Each mouse in the MPTP receiving groups were weighed and the dosage calculated accordingly.

Table 5.2. Group division and treatment scheduling.

	Treatment of various groups per day			
Week	**Control/day**	**Q_{10}/day**	**Q_{10} + MPTP/day**	**MPTP/day**
1	PB + SO	PB + SO + Q_{10} (200mg/kg)	PB + SO + Q_{10} (200mg/kg)	PB + SO
2	PB + SO	PB + SO + Q_{10} (200mg/kg)	PB + SO + Q_{10} (200mg/kg)	PB + SO
3	PB + SO	PB + SO + Q_{10} (200mg/kg))	PB + SO + Q_{10} (200mg/kg)	PB + SO
4	PB + SO	PB + SO + Q_{10} (200mg/kg)	PB + SO + Q_{10} (200mg/kg)	PB + SO
5	PB + SO + Saline solution (500µl) *(sc)* **on day one**	PB + SO + Q_{10} (200mg/kg) + Saline solution (500µl) *(sc)* **on day one**	PB + SO + Q_{10} (200mg/kg) + MPTP (40mg/kg)/ in Saline solution (500µl) *(sc)* **on day one**	PB + SO + MPTP (40mg/kg)/ in Saline solution (500µl) *(sc)* **on day one**
6	PB + SO	PB + SO + Q_{10} (200mg/kg)	PB + SO + Q_{10} (200mg/kg)	PB + SO

PB = Peanut butter, SO = Sweet oil, Q_{10} = Coenzyme Q_{10}, sc = subcutaneous

Four mice from each group were sacrificed every second day for six days, beginning two days after the subcutaneous injection of MPTP/Saline. Halothane was used to anaesthetise the animals.

Venous blood samples of each mouse were collected directly from the heart in tubes containing heparin. The blood samples were immediately centrifuged at 700 x g for 15 min at room temperature. The plasma was separated and stored at -75°C in polypropylene tubes. Heart, liver and brain tissue were removed and placed in polypropylene tubes and were also stored at -75°C. On the day assigned for analysis the samples were thawed at room temperature.

5.2. HPLC DETERMINATION OF Q_9H_2 and $Q_{10}H_2$

5.2.1. Extraction of Plasma.

An 8 ml amber glass tube containing an aliquot of 200 µl heparin plasma, 2000 µl absolute ethanol (for deproteination of Q_{10}) and 100 µl standard solution Q_8 (0.125 µg/ml absolute ethanol) (internal standard) was vortexed for one minute. No spiking of Q_9 or Q_{10} were necessary, since the sensitivity of the method was high enough to detect the levels found. The mixture was centrifuged at 700 x g for 10 min. with a Harmonic series centrifuge. Subsequently, 2000 µl of the supernatant was collected and evaporated under nitrogen. The residue was dissolved in 150 µl absolute ethanol and 30 µl $NaBH_4$ (0.5% methanol) was added for the reduction of Q_{10} and Q_9 to $Q_{10}H_2$ and Q_9H_2. After been vortexed for 10 seconds it was stored at -75ºC in amber vials for one week. 50 µl was injected into the HPLC system with EC detection.

5.2.2. Extraction of heart, liver and brain tissue

For tissue extractions, brain, liver and heart were used. The average weight for these tissues used were: heart 160 mg, brain 400 mg and liver 500 mg. The weights (in mg) were multiplied by three and that volume (in ml) of absolute ethanol was added, along

with 100 µl Q_8 internal standard solution, (0.125 µg/ml absolute ethanol). The absolute ethanol served to deproteinate the Q_9 and Q_{10}. The mixture was homogenised with ethanol for 5 min and centrifuged at 2450 x g (14000 rpm) for 20 min. with a Harmonic series centrifuge. Subsequently, the same volume of supernatant as the volume added was collected and evaporated under nitrogen. The residue was dissolved in 150 µl absolute ethanol and 30 µl $NaBH_4$ (0.5% methanol) was added for reduction of Q_{10} and Q_9 to $Q_{10}H_2$ and Q_9H_2. After been vortexed for 10 seconds it was stored at -75ºC in amber vials for one week. 50 µl was injected into the HPLC system with EC detection.

5.2.3. Chemicals and reagents

The chemicals and reagents used for HPLC determination of plasma and tissue Q_9H_2 and $Q_{10}H_2$ concentrations are summarised in Table 5.3.

Table 5.3. Chemicals and reagents.

CHEMICAL OR REAGENT	SUPPLIER
Ubiquinone-8	Nisshin chemicals, Japan
Ubiquinone-9	Fluka Chemie AG, Buchs, Switzerland
Ubiquinone-10	Sigma Chemical Co., St. Louis, MO
HPLC-grade methanol	Scharlau Chemie S.A., La Jota, Barcelona
Perchloric acid	BDH chemicals, Poole, England
Absolute ethanol	Scharlau Chemie S.A., La Jota, Barcelona
Sodium perchlarate monohydrate	Saarchem, Muldersdrift, S.A.
Sodium borohydrate	Saarchem, Muldersdrift, S.A.
Tert butanol	Sigma Chemical Co., St. Louis, MO
Dinitrogen gas	Afrox, Potchefstroom, S.A.

5.2.4. Instrumentation

The chromatographic conditions are summarised in Table 5.4.

Table 5.4. Instrumentation

CHROMATOGRAPHIC CONDITIONS	SPECIFICS
Software	Chemstation version 3D
HPLC pump	HPLC 1050 programmable solvent module pump
HPLC detector	HP 1049 A, Electrochemical Detector, Hewlett Packard
HPLC guard column	Phenomenex® C18, 5µm (4mm L x 3 mm) Phenomenex®, Torrance, CA
HPLC column	Lichrospher 100-S RP-18 ec. (125 x 4 mm) (Machery Nagel Cartrige column)
Manual injection loop	150 µl
Mobile phase	A: 100% methanol containing 50mM sodium perchlorate and 10mM perchloric acid. B: Mixture of ethanol and tertiary butanol (80:20,v/v)
Flow rate	Gradient flow: 1.5 ml/min for 6.5 min and then 1ml/min for 7min onwards
Temperature	Ambient: 25°C ± 2°C
Gradient flow	90% A - 10% B for 4 min. then 50% A - 50% B for 6 min. and then again 90% A – 10% B for 3 min.

5.2.5. Preparation of standards

1. Mice plasma and tissue samples.

Mixed plasma samples from untreated C57BL/6 mice were divided into 1.5 ml aliquots in polypropylene tubes and stored at -75°C. On the day assigned for analysis, one 1.5 ml plasma sample was thawed at room temperature providing seven 200 µl plasma samples that could be used for validation. If the mice plasma or tissue sample was prepared according to the method (section 5.2.1. and 5.2.2.) it was designated a "blank". If the mice plasma or tissue sample was prepared according to these methods, but an additional concentration of standard Q_9 or Q_{10} was added during the preparation to obtain a certain concentration, it was designated a "standard".

2. Standard solutions of Q_9 and Q_{10}

Two standard mother and two standard daughter solutions were prepared (figure 5.1.). Mother solutions were freshly prepared each week and stored at -75°C. Daughter solutions were freshly prepared from the mother solutions every day.

Each standard mother solution was prepared by weighing 5 mg of Q_9 and Q_{10} and diluting it to 20 ml with HPLC grade absolute ethanol in a volumetric flask giving a concentration of 250 µg Q_9 and Q_{10}/ml in absolute ethanol. Each of the daughter solutions were prepared by diluting 1 ml of a mother solution to 100 ml with HPLC grade absolute ethanol giving a concentration of 2.5 µg/ml in ethanol.

3. Standard solution of Q_8 (Internal standard).

A standard solution of Q_8 was prepared by weighing 5 mg of Q_8 and diluting it to 20 ml with HPLC grade absolute ethanol in a volumetric flask giving a concentration of 250 µg Q_8/ml absolute ethanol. Of this solution, 1 ml was diluted to 100 ml with HPLC grade absolute ethanol giving a concentration of 2.5 µg/ml ethanol. This solution was diluted

10-fold to 0.25 µg/ml and 100 µl was added to each plasma or tissue sample as internal standard to acquire a concentration of 0.125 µg Q_8/ml plasma (figure 5.4.).

5.2.6. Area under curve (AUC) as test parameter

The test parameters obtained by HPLC analysis should always be proportional, either directly or via a well defined mathematical transformation, to the concentration of the analyte given range. The plot of this proportional relationship serves as a standard curve from which the unknown concentration of a sample can be calculated if the test parameter had been determined.

In this study, the test parameter obtained by HPLC analysis was the ratio (AUC_{Q10}/AUC_{Q8}) and the ratio (AUC_{Q9}/AUC_{Q8}) to the concentrations of Q_{10} and Q_9 respectively. The AUC ratios were proportional to the concentrations Q_{10} and Q_9, since a plot of the AUC ratios against the concentrations Q_{10} and Q_9 provided linear curves (Appendix A1). These served as the standard curves from which the unknown Q_{10} and Q_9 concentrations could be calculated after the AUC ratios had been determined.

To construct a standard curve, seven mice plasma samples were required. One of these plasma samples served as a blank (Blank 1) and was prepared according to the method in section 5.2.1. The AUC ratio of this blank was representative of the total Q_9 and Q_{10}. The remaining six plasma samples were used to obtain standards of six different concentrations (C1, C2, C3, C4, C5, C6) and were prepared in a similar manner as the blanks except for being spiked with 70 µl, 84.8 µl, 101.6 µl, 120.2 µl, 229.6 µl, and 320.4 µl of the standard 2.5 µg/ml daughter solutions to acquire concentrations of 0.97 µg/ml, 1.176 µg/ml, 1.408 µg/ml, 1.666 µg/ml, 3.1818 µg/ml and 4.44 µg/ml. The AUC ratio obtained by each of these standards was representative of the total Q_9 or Q_{10} concentration added plus the Q_9 and Q_{10} content in the normal plasma samples of the mice. The AUC ratios were plotted against the concentrations to obtain a standard curve. Figure 5.1. gives a schematic representation of the preparation of the blank and standards from the standard solutions of Q_8, Q_9 and Q_{10}.

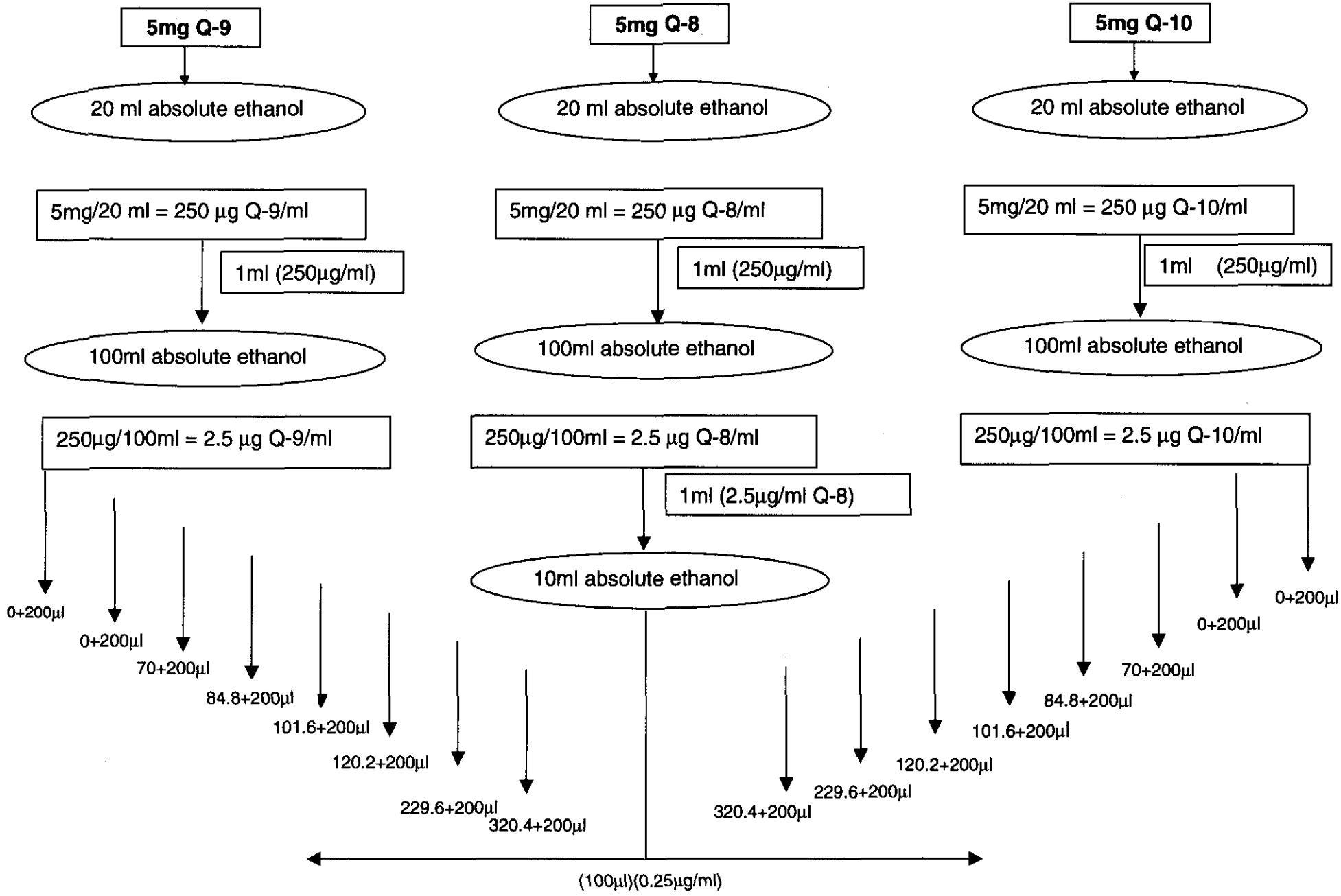

Figure 5.1. Schematic representation of the preparation of the blanks and standards.

Table 5.5. demonstrates the origin of the values for the x- and y- axes of the standard curves (chapter 6). The curves are defined by the following equation. Y = mX +c

Where

Y = AUC_{Q-10}/AUC_{Q-8} or AUC_{Q-9}/AUC_{Q-8}

X = concentration of Q_{10} or Q_9

m = slope of linear curve

c = Y-intercept of linear curve

Table 5.5.

SAMPLE	**Q_{10}**	**Q_9**	**Q_8**	**Y-AXIS**	**X-AXIS**
Base 1	Plasma	Plasma	Plasma +100 µl	(AUC_{Q-10}/AUC_{Q-8}) or (AUC_{Q-9}/AUC_{Q-8})	0 µg/ml
C1	Plasma +70 µl	Plasma +70 µl	Plasma +100 µl	(AUC_{Q-10}/AUC_{Q-8}) or (AUC_{Q-9}/AUC_{Q-8})	0.97 µg/ml
C2	Plasma +84.8 µl	Plasma +84.8 µl	Plasma +100 µl	(AUC_{Q-10}/AUC_{Q-8}) or (AUC_{Q-9}/AUC_{Q-8})	1.176 µg/ml
C3	Plasma +101.6 µl	Plasma +101.6 µl	Plasma +100 µl	(AUC_{Q-10}/AUC_{Q-8}) or (AUC_{Q-9}/AUC_{Q-8})	1.408µg/ml
C4	Plasma + 120.2 µl	Plasma + 120.2 µl	Plasma +100 µl	(AUC_{Q-10}/AUC_{Q-8}) or (AUC_{Q-9}/AUC_{Q-8})	1.666 µg/ml

C5	Plasma + 229.6 µl	Plasma + 229.6 µl	Plasma +100 µl	(AUC_{Q-10}/AUC_{Q-8}) or (AUC_{Q-9}/AUC_{Q-8})	3.1818 µg/ml
C6	Plasma + 320.4 µl	Plasma + 320.4 µl	Plasma +100 µl	(AUC_{Q-10}/AUC_{Q-8}) or (AUC_{Q-9}/AUC_{Q-8})	4.44 µg/ml

The standard curves (section 6) were used to determine Q_{10} and Q_9 concentrations in mice plasma and tissue samples, which were prepared according to the method in section 5.2.1. or section 5.2.2. The AUC ratio measured was representative of the total Q_{10} and Q_9 concentrations. This concentration was constituted by the Q_9 and Q_{10} content of the mice itself. For example:

$$\left(\frac{AUC_{Q-10}}{AUC_{Q-8}}\right)_{Mice\ Plasma} = m\ (Concentration\ Q\text{-}10) + c$$

$$\left(\frac{AUC_{Q-9}}{AUC_{Q-8}}\right)_{Mice\ Plasma} = m\ (Concentration\ Q\text{-}9) + c$$

5.3. HPLC Validation parameters

Validation is the process of establishing by means of a suitable protocol, that the performance characteristics of each procedure included in the method meet the previously stated requirements for the intended applications (Shah *et al.*, 1992).

In the development of HPLC methods the following must be recorded for method validation:

5.3.1. Linearity and range

The linearity assessment determines the procedure's ability to obtain test results, which are proportional to the concentration of the analyte in the sample within a given range, either directly or via a well-defined mathematical transformation. A procedure's range is proportional to its linearity. The range is the interval between the lower and the upper analyte concentrations for which it has been demonstrated that the analytical procedure has a suitable level of accuracy, precision and linearity (Jenke, 1996).

All samples were analysed in duplicate, thus each value represents the average of two values. Table 5.6. - 5.7. show the data obtained.

Table 5.6: Determination of linearity within chosen range of Q_9/Q_8.

	Concentration range (µg/ml)	**Regression coefficient**	**Slope**	**Y-intercept**
Linear curve 1	0.97 - 4.44	0.986	0.068	0.600
Linear curve 2	0.97 - 4.44	0.986	0.073	0.599
Linear curve 3	0.97 - 4.44	0.984	0.059	0.612
Mean (n=3)		0.985	0.067	0.604
SD		0.001	0.007	0.006
%CV		0.134	10.549	1.110

Table 5.7: Determination of linearity within chosen range of Q_{10}/Q_8.

	Concentration range (ng/ml)	Regression coefficient	Slope	Y-intercept
Linear curve 1	0.97 - 4.44	0.995	0.134	0.304
Linear curve 2	0.97 - 4.44	0.997	0.145	0.427
Linear curve 3	0.97 - 4.44	0.996	0.129	0.457
Mean (n=3)		0.996	0.136	0.396
SD		0.001	0.008	0.081
%CV		0.082	6.007	20.436

5.3.2. Precision

Precision can be defined as the closeness of agreement (degree of scatter) between a series of measurements obtained from multiple analyses of the same homogenous samples under the prescribed assay conditions (Jenke, 1996). Table 5.8. – 5.9. show the data obtained.

Tabel 5.8. Determination of precision for Q_9

Reference concentration (µg/ml)	Mean ratio Q_9 (n=3)	SD	%CV
1.176	0.697	**0.003**	0.402
1.666	0.709	0.008	1.133
4.44	0.903	0.027	3.023
Mean:		***0.012***	***1.519***

Tabel 5.9. Determination of precision for Q_{10}

Reference concentration (µg/ml)	Mean ratio Q_{10} (n=3)	SD	%CV
1.176	0.628	**0.016**	2.592
1.666	0.679	0.028	4.060
4.44	1.053	0.025	2.334
Mean:		***0.023***	***2.995***

5.3.3. Accuracy

Accuracy can be defined as the closeness of agreement between the values found by the method and the value, which is accepted, either as a conventional true value or a reference value (Jenke, 1996). Table 5.10. – 5.11. show the data obtained.

Tabel 5.10. Determination of accuracy for Q_9

Reference concentration (µg/ml)	Concentration found (Q_9) µg/ml (n=3)	SD	%CV	% Recovery
1.176	1.340	0.038	2.871	113.97
1.666	1.503	0.110	7.332	90.21
4.44	4.163	0.374	8.994	93.75
Mean:		***0.174***	***6.399***	***99.31***

Tabel 5.11. Determination of accuracy for Q_{10}

Reference concentration (µg/ml)	Concentration found (Q_{10}) µg/ml (n=3)	SD	%CV	% Recovery
1.176	1.410	0.083	5.875	119.90
1.666	1.745	0.191	10.923	104.75
4.44	4.321	0.169	3.927	97.34
Mean:		***0.148***	***6.908***	***107.33***

5.3.4. Specificity

Specificity can be defined as the ability of an assay to assess unequivocally the analyte of interest in the presence of compounds, which might be expected to be in the sample (Jenke, 1996). Baseline separation could be required as a criterion for specificity. A series of chromatograms (figure 5.2. - 5.7.) were prepared to visually compare them for interfering peaks near the peaks of interest.

Q_{10} (retention time = 9.076 min.), Q_9 (retention time = 7.861 min.), Q_8 (retention time = 6.558 min.)

1. The mobile phase and the reducing agent ($NaBH_4$)

Mobile phase

A: 100% methanol containing 50 mM sodium perchlorate and 10 mM perchloric acid.

B: Mixture of ethanol and tert butanol (80:20,v/v)

An aliquot of mobile phase and reducing agent (30 µl /0.5% methanol), prepared according to the method 5.2.5. was injected into the HPLC. The resulting chromatogram (figure 5.2.) registered peaks at 1.56 min.

These peaks, however, did not interfere with the respective peaks of Q_8, Q_9 and Q_{10} (see figure 5.3.).

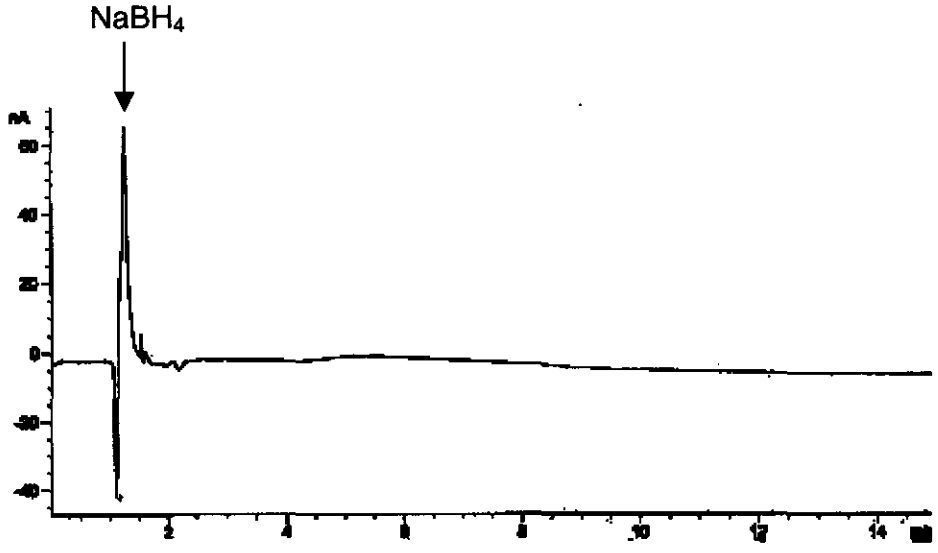

Figure 5.2. HPLC chromatograms of the mobile phase and the reducing agent ($NaBH_4$).

2. The internal standard (Q_8) and the assayed compounds (Q_9 and Q_{10}).

A solution was prepared by pipetting 100 µl of internal standard solution (Q_8) and adding 70 µl of Q_9 and Q_{10} standard solutions prepared according to the method in section 5.2.5. with added reducing agent. The UV (sig. 275 nm) detector showed no signals, indicating that ubiquinone was totally in the reduced form.

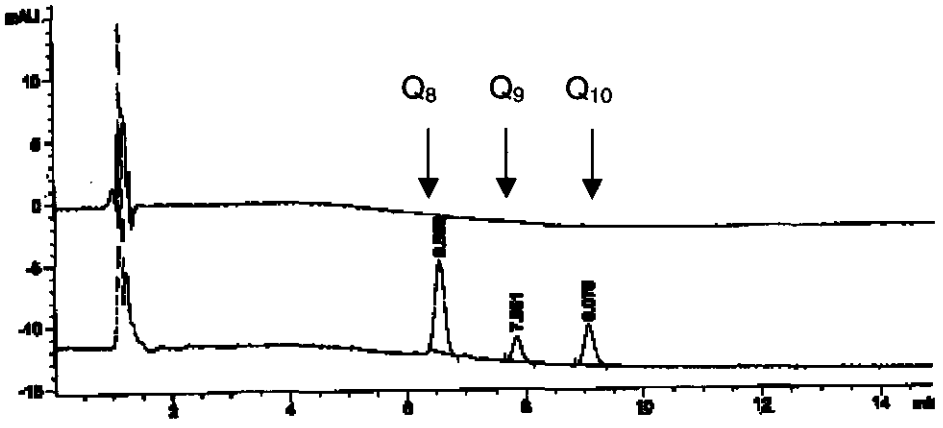

Figure 5.3. HPLC chromatograms of internal standard (Q_8) and the assayed compounds (Q_9 and Q_{10}).

3. A plasma sample without addition of Q_9 or Q_{10}

A mouse plasma sample was prepared according to the method in section 5.2.1. without adding Q_9 or Q_{10}. This procedure was followed to detect peaks in plasma during our study.

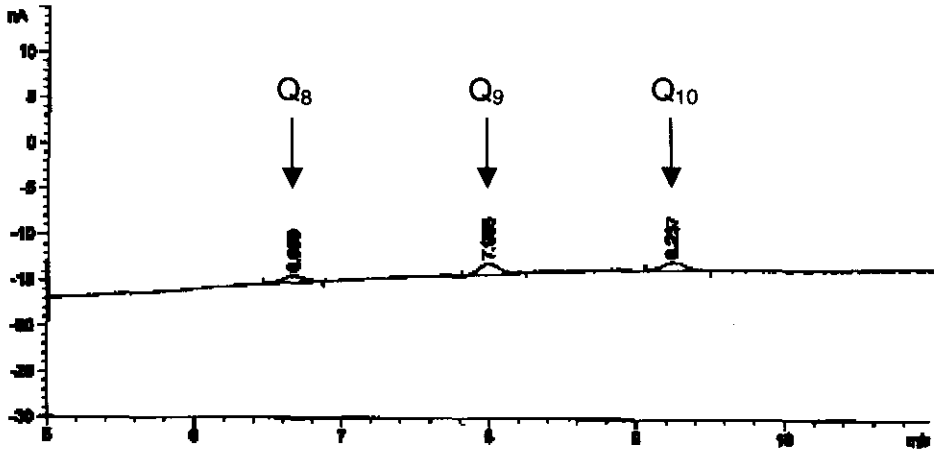

Figure 5.4. HPLC chromatograms of a mice plasma sample.

4. A heart tissue sample without addition of Q_9 or Q_{10}

A mouse heart sample was prepared according to the method in section 5.2.2. without adding Q_9 or Q_{10}. This procedure was followed to detect peaks in heart tissue during our study.

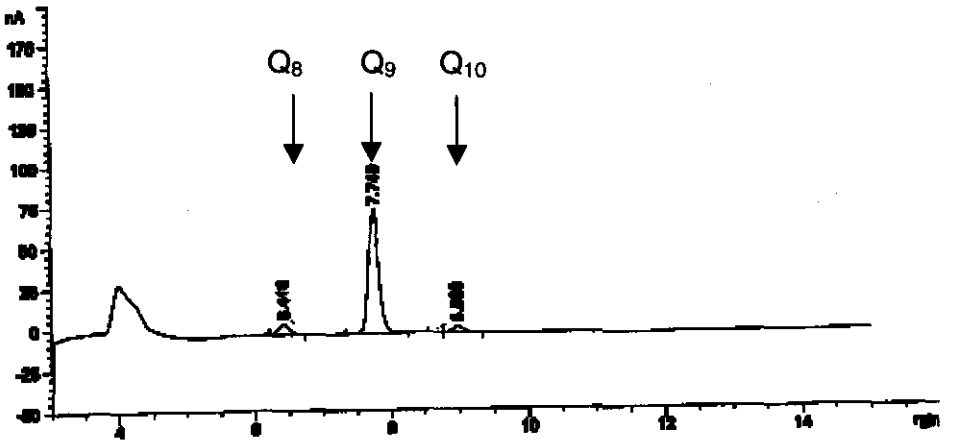

Figure 5.5. HPLC chromatograms of a mice heart sample.

5. A brain tissue sample without addition of Q_9 or Q_{10}

A mouse brain sample was prepared according to the method in section 5.2.2. without adding Q_9 or Q_{10}. This procedure was followed to detect peaks in brain tissue during our study.

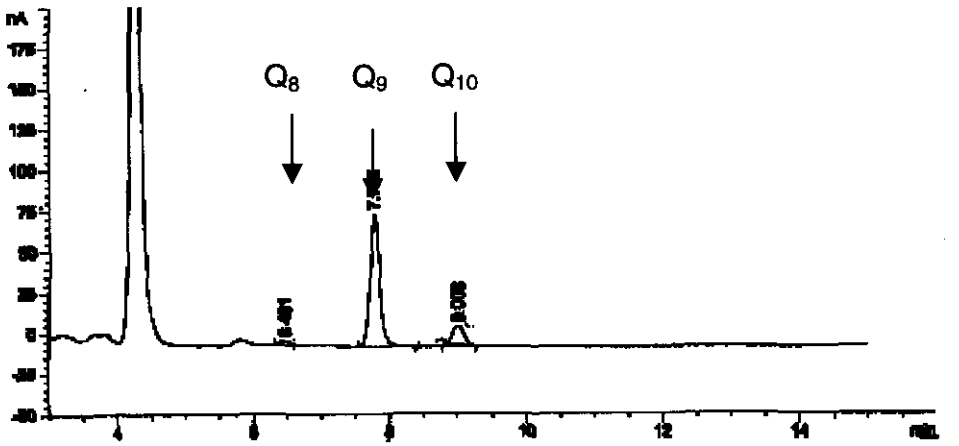

Figure 5.6. HPLC chromatograms of a mice brain sample.

6. A liver tissue sample without addition of Q_9 or Q_{10}

A mouse liver sample was prepared according to the method in section 5.2.2. without adding Q_9 or Q_{10}. This procedure was followed to detect peaks in liver tissue during our study.

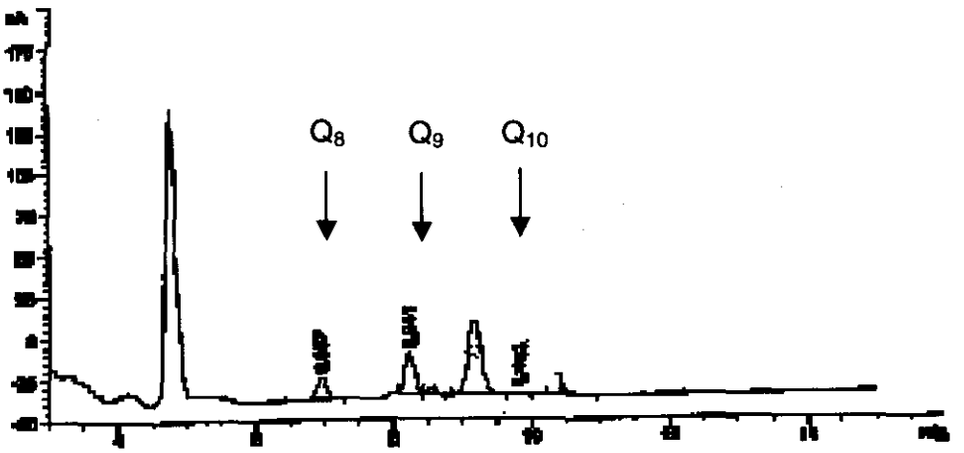

Figure 5.7. HPLC chromatograms of a mice liver sample.

5.4. Results of HPLC analysis of samples

The HPLC with EC detection system used in our experiment is shown in figure 5.8.

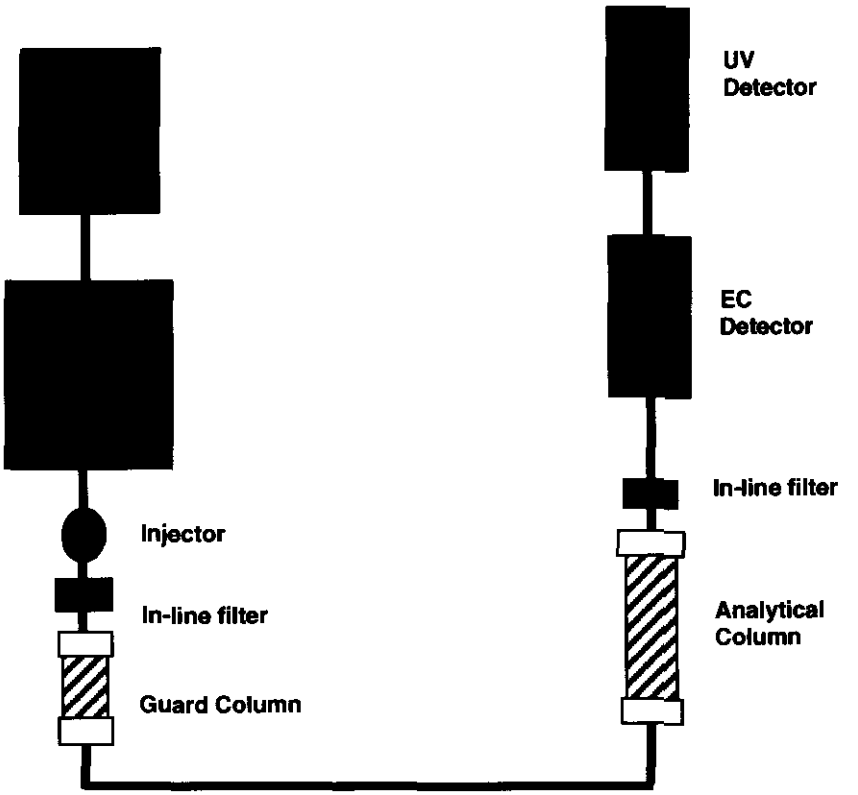

Figure 5.8. HPLC system used in our experiment.

Table 5.12. - 5.13. show the results of average Q_9H_2 and $Q_{10}H_2$ concentrations in the plasma and the organs of the various groups treated.

Table 5.12. Average results over six days for $Q_{10}H_2$ determination (Appendix A.2.). n = 12

Sample	Ave. [$Q_{10}H_2$] for Control group	Ave. [$Q_{10}H_2$] for MPTP group	Ave. [$Q_{10}H_2$] for Q_{10} + MPTP group	Ave. [$Q_{10}H_2$] for Q_{10} group
Plasma (µg/ml)	4.626	4.572	18.84	37.210
Liver (µg/mg)	20	21	37	29
Heart (µg/mg)	10	11	13	13
Brain (µg/mg)	98	91	117	129

Table 5.13. Average results over six days for Q_9H_2 determination (Appendix A.2.). n = 12

Sample	Ave. [Q_9H_2] for Control group	Ave. [Q_9H_2] for MPTP group	Ave. [Q_9H_2] for Q_{10} + MPTP group	Ave. [Q_9H_2] for Q_{10} group
Plasma (µg/ml)	18.590	17.992	22.982	24.59
Liver (µg/mg)	1046	1042	1084	1139
Heart (µg/mg)	945	936	1003	1056
Brain (µg/mg)	1107	1021	1281	1328

5.5. SCGE (COMET ASSAY) DETERMINATION OF DNA DAMAGE

The SCGE or comet assay was used for analysis of DNA cell damage found in the different groups treated in this experiment.

5.5.1. Chemicals and reagents

Table 5.14 lists the chemicals and reagents used for SCGE.

Table 5.14. The chemicals and reagents used for SCGE determination of DNA.

CHEMICAL OR REAGENT	SUPPLIER
Dimethylsulfoxide (DMSO)	Merck
Disodium salt EDTA	Sigma
Ethidium bromide	Boehringer Mannhiem
Propidium iodide	Sigma
Phosphate buffered saline $(KCl)+(Na_2HPO_4)+(KH_2PO_4)$	UniLAB

Sodium chloride (NaCl)	UnivAR
Sodium hydroxide (NaOH)	Merck
Triton X - 100	BDH
Trizma HCl	Sigma
EDTA disodium salt	Sigma
High melting point agarose	Techcomd LTD
Low melting point agarose	Seakem

5.5.2. Instrumentation

The SCGE microscopic conditions are summarised in Table 5.15.

Table 5.15. Instrumentation

MICROSCOPIC CONDITIONS	SPECIFICS
Fluorescent microscope	Olympus IX - 70
Sandblasted microscope slides 76 × 26mm	RESY
Power supply unit (28V; 300mA)	Bio-Rad Model 200/2.0 Power supply
Software	Olympus IX -70 system software

5.5.3. Procedures

5.5.3.1. Preparation of solutions

Homogenising buffer: 0.075 M NaCl with 0.024 M Na_2EDTA (pH 7.5)

Store at 4ºC

***Lysing solution*:** 2.5 M NaCl, 0.1 M Na_2EDTA, and 0.01 M Trizma HCl, 1%

DMSO in the lysing solution scavenges radials generated by the iron released from haemoglobin when blood or animal tissues are used. It is not needed for other solutions or where the slides will be kept in lysing for a brief time only.

Store at 4ºC

Cool for a minimum of 30 min before use.

Keep in dark storage.

***Phosphate buffered saline (PBS)*:** 1000 ml double distilled (dd) H_2O for 1 × PBS containing:

8 g NaCl, 0.2 g KCl, 0.2 g KH_2PO_4, 1.15 g Na_2HPO_4

Store at 4ºC

***Electrophoresis buffer*:** 0.3 M NaOH and 0.001 M Na_2EDTA

Store at 4ºC

Set pH>13

Use this buffer to selectively assess for strand breakage.

***Neutralisation buffer*:** 0.4 M Tris HCl

Store at 4ºC for at least 1 hour.

Set the pH as Tris has a temp/pH gradient.

***Staining solution*:** ethidium bromide (5µg/ml), propidium iodide (10µg/ml)

Store at 4ºC for at least 1 hour before use.

Kept in dark environment.

Caution: *Propidium iodide and ethidium bromides are mutagens and must be handled with care.*

5.5.3.2. Preparation of slides

1) 0.8% low melting point agarose (LMPA) (800 mg per 100 ml) and 1.0% high melting point agarose (HMPA) (1g per 100 ml) in 0.1 M EDTA were prepared. The mixture was then heated until the agarose dissolved. The LMPA container was placed in a 42°C water bath to cool and stabilise the temperature.

2) While the HMPA was hot, 100 µl was spread over the frosted slide and allowed to cool. The underside of the slide was wiped to remove excess agarose and was laid in a tray on a flat surface to dry. The slides were stored at room temperature until needed. High humidity conditions were avoided.

3) 800 µl of the LMPA (42°C) mixed with ~ 10,000 cells (~ 5 – 10 µl sample), were poured in the individual brackets on the frosted slide and refrigerated until the agarose gel became solid. ~ 10,000 cells in an area of 74 × 24 mm were used which resulted in ~ 1 cell per microscope field at 250 × magnification.

4) The slides were lowered into cold (4°C), freshly prepared lysing solution. The slides must be protected from light and refrigerated for a minimum of 1 hour. Slides may be stored for at least 4 weeks in cold lysing solution without affecting the results.

5) The amounts indicated (3) are based on using a 74 × 24 mm-perspex bracket. If the gels are not sticking to the slides properly, avoiding humidity and/or increasing the concentration of HMPA in the primary layer should eliminate the problem. From the point at which the slides are placed in the lysing solution, they should be kept under red or yellow light to prevent DNA damage.

5.5.3.3. Cell isolation

Whole heparin blood

Per gel block ~ 5 – 10 µl whole blood with 800 µl LMPA.

Tissue

The brain, liver, and heart were minced and suspended at a concentration of 1g/2 ml in chilled homogenising buffer (pH 7.5) containing 0.075 M NaCl and 0.024 M Na_2EDTA. It was then gently homogenised at 87.5 – 140 x g (500 - 800 rpm) in ice with a Harmonic series homogeniser. To obtain nuclei, the homogenate was centrifuged at 700 × g for 10 minutes at 4°C with a Harmonic series centrifuge. The precipitate was resuspended in chilled homogenising buffer (300 µl). The nucleus suspension was then processed.

5.5.4. Electrophoresis and storage of microgel slides

5.5.4.1. Procedure

1) After at least 1 hour at ~ 4°C, the slides were gently removed from the lysing solution and placed side by side on the horizontal gel box near one end, sliding them as together as possible.

2) The buffer reservoirs were then filled with freshly made pH > 13 electrophoresis buffer until the liquid level completely covered the slides (avoid bubbles over the agarose).

3) The slides were left in the alkaline buffer for 30 minutes to allow for unwinding of the DNA and the expression of alkali-labile damage.

4) The power supply was turned on to 28 volts and the current was adjusted to 300 milliamperes by raising or lowering the buffer level. The slides were then electrophorised for 40 minutes.

(The goal is to obtain migration among the control cells without it being excessive. The optimal electrophoresis duration differs for different cell types. If crosslinking is one of the endpoints being assessed then having controls with about 25% migrated DNA is useful. A lower voltage and a longer electrophoresis time may allow increased sensitivity).

5) The power was turned off and the slides were gently lifted from the buffer and placed on a drain tray. The slides were coated dropwise with neutralisation buffer ($Tris^{[HCl]}$), and left for 15 minutes until drained and then rinsed with dd H_2O.

6) The slides were then stained with 1000 ml ethidium bromide (5 μg/ml) or propidium iodide (10μg/ml) for 1 hour at 4°C and then scored. The slides can also be dried for storage.

7) When slides were required they were flooded with stain (~300 – 500 μl) to ensure even hydration and staining.

8) The electrophoresis process was carried out under a red/yellow light to prevent any further DNA damage. The procedure was performed at 4°C, for better repeatability of the experiment.

5.6. Results of the evaluation of the DNA damage

Fifty randomly selected cells were analysed per sample. Using the formula: Tail Moment = (Tail length)×(Migrated DNA intensity) a value was determined. Figure 5.9. shows a diagram of a typical comet.

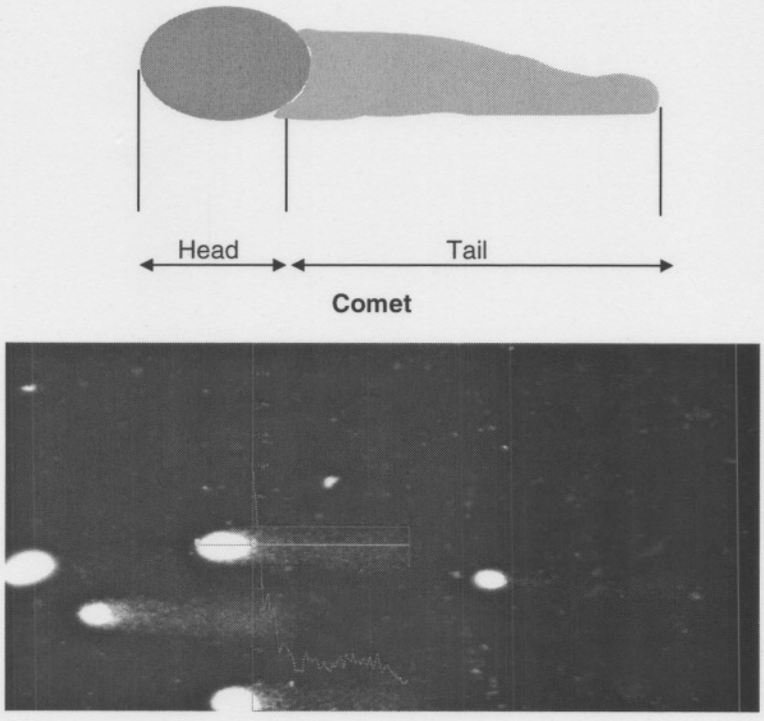

Figure 5.9. Diagram of typical comet.

Figure 5.10. briefly outlines the SCGE technique performed in our study.

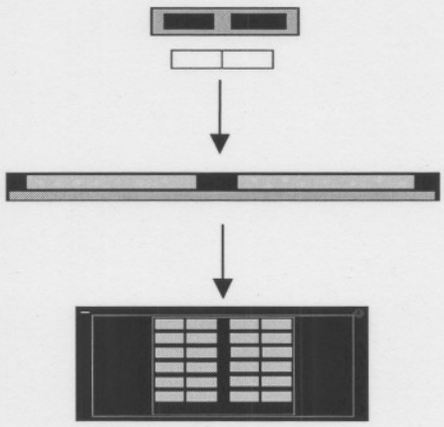

- Coat slide with 1% HMPA. Embed 10ml cells in 800 ml 0.8% LMPA on slide (42°C then refridge)
- Lyse cells *in situ* (1 hr, 4°C).
- "Unwind " damaged DNA in alkali (20 minutes at 4 °C)
- Electrophorese lysed cells under alkaline conditions.Stain slide (Propidium iodide/Ethidium bromide 5-10 µg for 1 hour at 4°C.

Figure 5.10. SCGE technique used

Table 5.16. lists the results of average DNA damage determined in the plasma and the organs of the various groups treated.

Table 5.16. Average results for TM (over six days) obtained by SCGE (Appendix B.3.)

n = 12

Sample	Ave. DNA damage for Control group ™	Ave. DNA damage for MPTP group ™	Ave. DNA damage for Q_{10} + MPTP group ™	Ave. DNA damage for Q_{10} group ™
Blood	4026.10	3744.80	3679.23	2882.64
Liver	5612.77	8696.91	6922.39	4956.30
Heart	3459.72	6402.64	4236.19	2659.27
Brain	4265.31	5467.93	3765.60	2975.81

CHAPTER 6

DISCUSSION AND CONCLUSION

We hypothesized that Q_{10} would increase levels of $Q_{10}H_2$ in blood and in the tissue (brain, liver and heart), effecting a higher energy production and anti-oxidant capacity. This may lead to lower DNA damage and cell death. To test this hypothesis we determined the relationship between $Q_{10}H_2$ levels in blood and various tissues with DNA damage found in blood and these tissues. Another important aspect of this study was to determine the possibility of $Q_{10}H_2$ attenuating the damage to cell DNA in mice.

The protocol of this study is discussed in chapter 5. During this investigation plasma and tissue samples were analysed for change in Q_9H_2 and $Q_{10}H_2$ concentrations as well as DNA damage after receiving MPTP and MPTP/Q_{10}. These results are summarised in appendices A and B and are presented in figures 6.5 - 6.12; 6.14. - 6.17. The reasons why certain methods were used will also be discussed.

It was expected that MPTP would cause a decrease in Q_9H_2 and $Q_{10}H_2$ concentrations and would lead to an increased DNA damage due to the lower anti-oxidant levels as well as the inhibition of complex I (section 2.6.2). It was furthermore postulated that groups receiving Q_{10} would exhibit reduced DNA damage as a result of increased $Q_{10}H_2$ concentrations.

6.1. Selection of the extraction method

Wang *et al.* (1999) reported that Q_{10} is readily soluble in hexane, insoluble in methanol, and slightly soluble in ethanol, 1-propanol and 2-propanol. Due to incompatibility of hexane with the mobile phase, injection volumes had to be limited (Yamashita & Yamamoto, 1997).

In the past detectability was improved through extraction with hexane after the plasma sample was deproteinated with alcohol. This is complicating and time consuming and may lead to oxidation of $Q_{10}H_2$ to Q_{10}. Wang *et al.* (1999) used absolute ethanol mediated protein precipitation to minimize oxidation. They reported no significant differences on peak heights for different plasma samples using ethanol, 1-propanol and 2-propanol. Contrary to solubility data, lower recovery values were obtained for hexane than for the alcohols. This confirmed the finding of Wang *et al.* (1999) that hexane was not an effective extraction agent for the HPLC analysis of Q_{10} as has previously been reported. We therefore used the extraction procedure suggested by Wang *et al.* (1999), which is a simple deproteinisation technique with 10 parts of absolute ethanol for plasma and 3 parts of absolute ethanol for tissue samples (Wang *et al.*, 1999).

Recently, a study was undertaken to compare the effects of heparin and EDTA on the stability of $Q_{10}H_2$ in blood and in plasma during the process of storage. Tang *et al.* (2002) discovered that concentrations of Q_{10} were slightly reduced in samples with EDTA compared with heparinised plasma. Variance in ratios of $Q_{10}H_2$ in EDTA indicated that heparinised plasma was superior to EDTA (Tang *et al.*, 2002). Therefore we decided to use heparinised tubes in our study.

According to Kaikkonen *et al.* (1999), plasma Q_{10} is stable for three years when stored at -80°C and remains stable even when thawed and frozen at least seven times. All samples in our study were stored at -80°C.

6.2. Determination of Q_9H_2 and $Q_{10}H_2$ concentrations in plasma and tissue

6.2.1. HPLC validation

The method described by Wang *et al.* (1999) was used to determine Q_9H_2 and $Q_{10}H_2$ concentrations in mice plasma and tissue because of the high sensitivity of the EC detector for the reduced ubiquinones. The method was validated using the acceptable criteria.

6.2.1.1. Linearity

Acceptance criteria for linearity differ from application to application. The correlation coefficient of the best linear least squares regression model should ideally be between 0.98 and 1.00. Since we analysed biological materials, we have set our acceptance level at 0.98. The agreement between the curves was calculated through a mean and %CV for the regression coefficients, slopes and y-intercepts of the curves. See data in appendix A1. (Table 1-3). The % CV's of the linearity and the slope of the calibration graph for between day analyses were 0.13% and 10.54%, respectively (n=3) for Q_9H_2 and 0.10% and 6.01% for $Q_{10}H_2$. Figures 5.1 – 5.2. show the linear curves for Q_9H_2 and $Q_{10}H_2$.

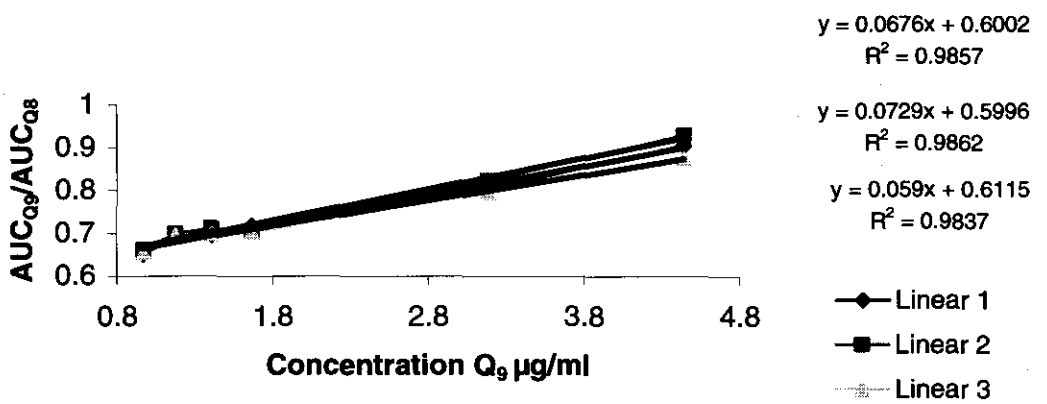

Figure 5.1. Linearity within chosen range of Q_9/Q_8

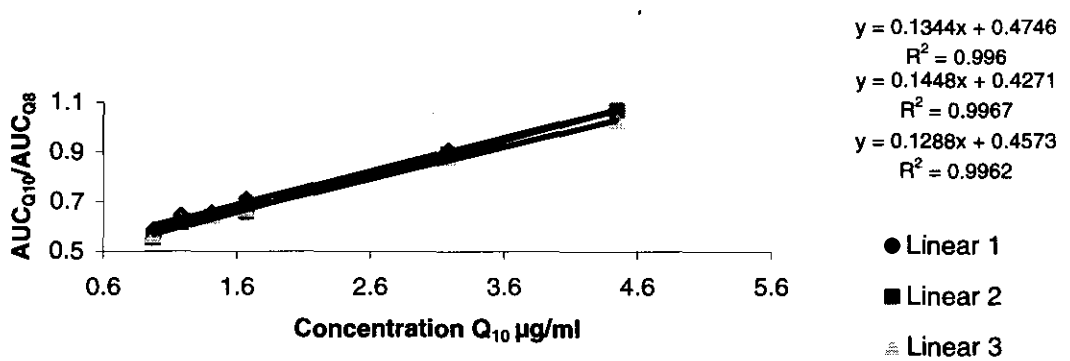

Figure 5.2. Linearity within chosen range of Q_{10}/Q_8

Most linear curve (out of the above curves), used for determining plasma and tissue $Q_{10}H_2$ and Q_9H_2 concentrations in our study.

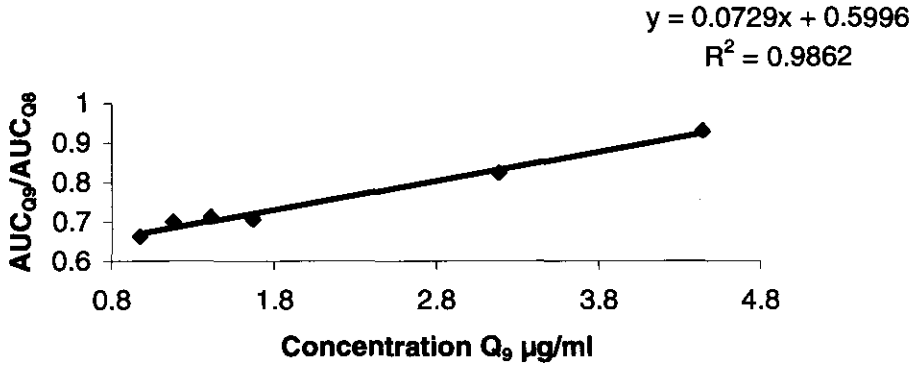

Figure 5.3. Curve of AUC ratio Q_9/Q_8

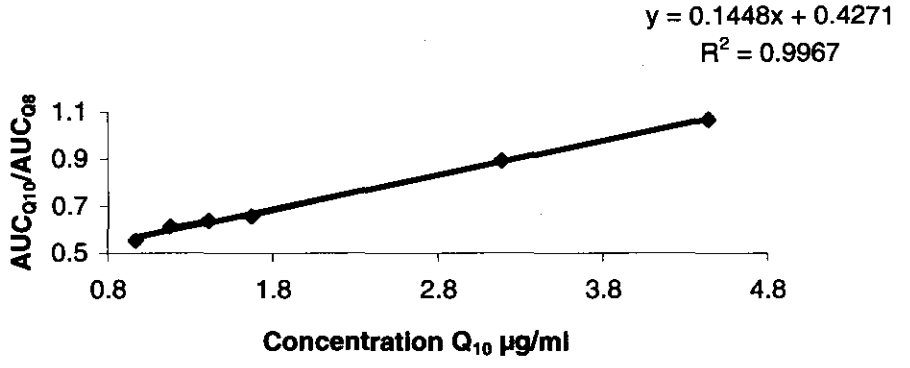

Figure 5.4. Curve of AUC ratio Q_{10}/Q_8

6.2.1.2. Precision

Precision can be subdivided into repeatability, intermediate precision and reproducibility. Repeatability (within day precision) reflects the variation in replicate procedures performed within a short period (same analytical run) with the same operational conditions. Intermediate precision (day-to-day precision) is related to analyses performed by different analysts on different instruments with different reagents at the same operating facility. Reproducibility (intra-laboratory precision) is related to the procedure being performed at two or more laboratories (Jenke, 1996). The mean C.V. of within-day and between-day assay was 1.52 % for Q_9H_2 and 2.99% for $Q_{10}H_2$. See data in appendix A1. (Table 7-9).

6.2.1.3. Accuracy

Accuracy requires six replicates of at least three concentrations within the specific range. The best conduct is to use the concentrations at the lowest point, midpoint and highest point of the standard curve (Jenke, 1996). The mean analytical recovery was 99.31% for Q_9H_2 and 107.33% for $Q_{10}H_2$ in the plasma. See data in appendix A1. (Table 4-6).

6.2.1.4. Selectivity

It can be concluded that the interfering peaks affecting specificity in our study, were from compounds in the plasma and not from the reactants and analytes used. These impurities are the result of the extraction procedure. See chapter 5.

6.2.1.5. Sensitivity

Sensitivity is the ability of a method to reliably respond in a consistent manner to decreasingly smaller amounts of analyte. Measures of sensitivity include the limit of detection (LOD) and limit of quantification (LOQ) (Jenke, 1996). For the method used in this study Wang *et al.* (1999) found a LOD of 0.002157 µg $Q_{10}H_2$/ml and a LOQ of 0.021575 µg $Q_{10}H_2$/ml. Because these values were significantly lower than the range experienced in this investigation, it was not deemed necessary to repeat determination of these sensitivity parameters.

6.2.2. Plasma and tissue Q_9H_2 and $Q_{10}H_2$ concentrations (Figure 6.5. – 6.12.)

Figure 6.5. – 6.12. depict the values obtained by HPLC analysis during week 5 and 6 of treatment. The top graph in each figure depicts the average Q_9H_2 or $Q_{10}H_2$ concentration while the graphs below depict the day to day concentration of these two

compounds. These results show that the Q_9H_2 and $Q_{10}H_2$ concentrations in the plasma, brain, heart and liver were elevated in the groups that received Q_{10} (Q_{10} and MPTP/Q_{10}) orally for six weeks compared to the controls.

The Q_9H_2 in the serum of the control was ± four-fold higher than that of $Q_{10}H_2$ (figure 6.5.-6.6.). This accords with previous findings (Lass *et al.*, 1999) that the predominant Q homologue in mice is Q_9. Administration of Q_{10} to mice resulted in a ± seven-fold increase in the $Q_{10}H_2$ (figure 6.6.) and also an elevation of Q_9H_2 concentrations by ± 40% in serum (figure 6.5.). The fact that Q_{10} administration resulted in a higher increase of $Q_{10}H_2$ in the serum than in other tissue (figure 6.8, 6.10, 6.12.) could be explained by the phenomenon that Q_{10} is converted to Q_9 in the liver, which is the predominant form. Q_{10} is transported by the portal vein to the liver before it is transported to other tissues via the circulatory system. Thus, the hypothesis that exogenous Q enters the endogenous pool of Q in the liver, and that the liver therefore controls the ratio between Q_9 and Q_{10} in the serum could explain why Q_{10} levels in peripheral tissue like the heart and brain (figure 6.8, 6.10.) were not elevated to the same extent as in the plasma when compared to the respective controls.

Higher Q_9H_2 than $Q_{10}H_2$ concentrations were also found in the tissue samples. The difference in Q_9H_2 and $Q_{10}H_2$ concentrations in the brain was ± 10 fold (figure 6.7. – 6.8.) whereas in the liver it was ± 50 fold (figure 6.11. - 6.12.) and in the heart ± 90 fold (figure 6.9. – 6.10.).

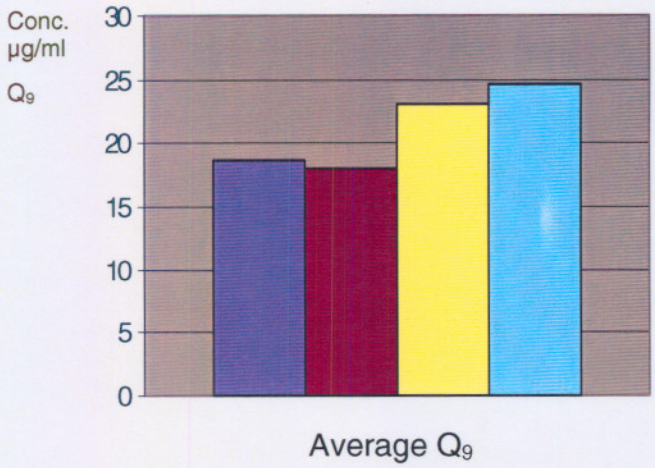

Average Q_9

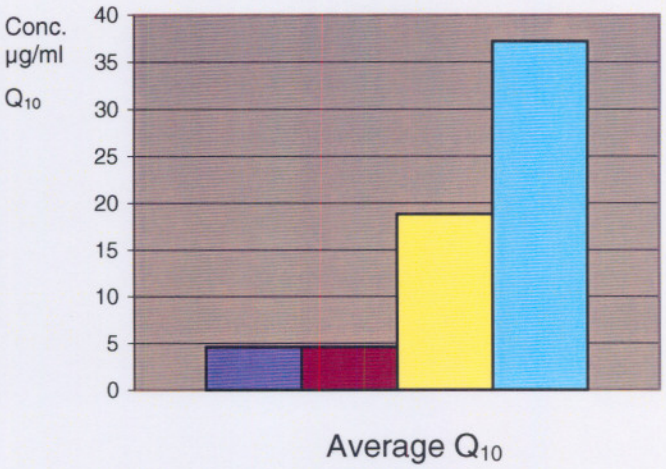

Average Q_{10}

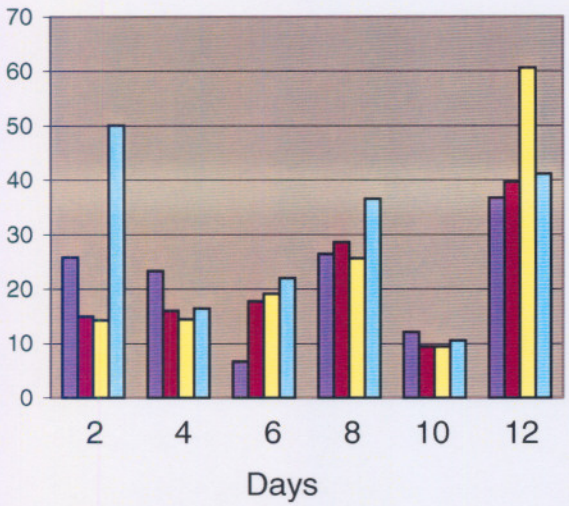

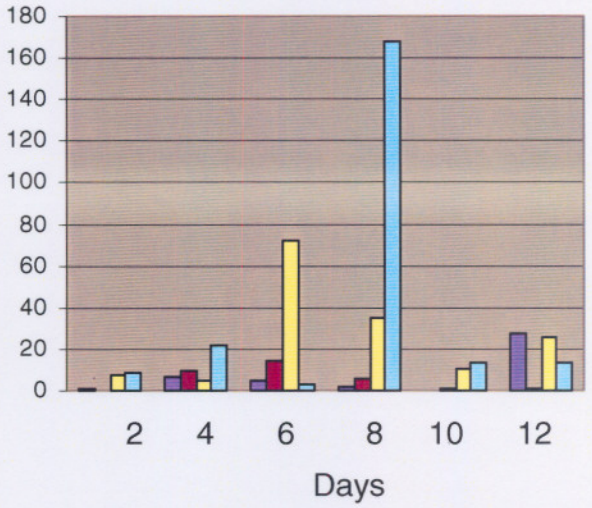

Figure 6.5.

Figure 6.6.

Average and day-to-day plasma Q_9H_2 and $Q_{10}H_2$ concentrations respectively.

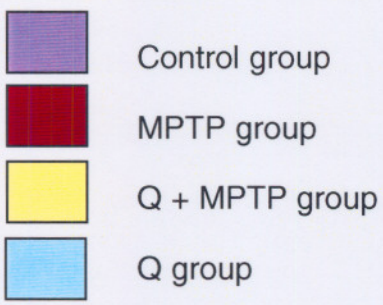

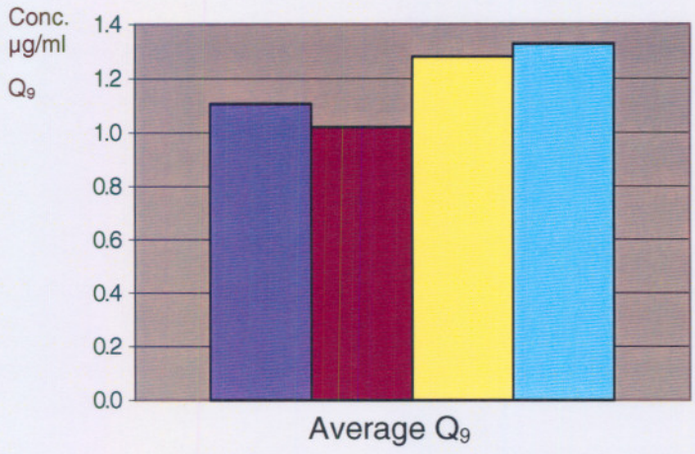

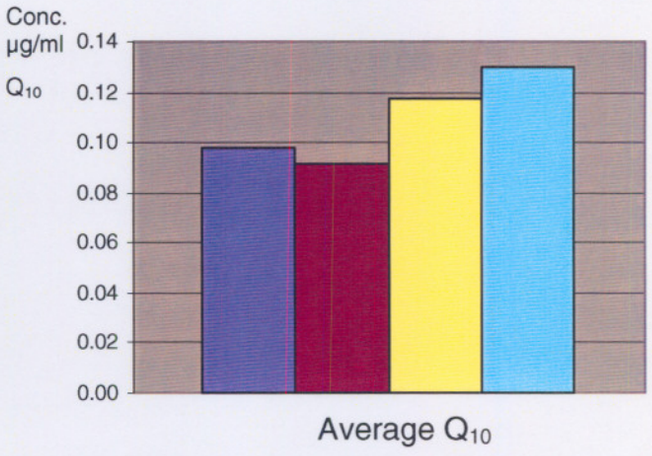

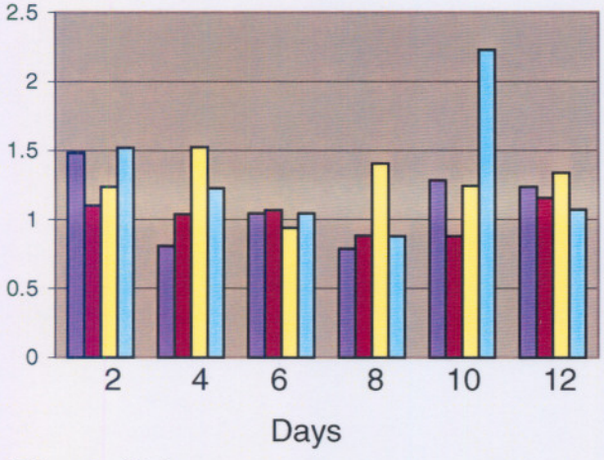

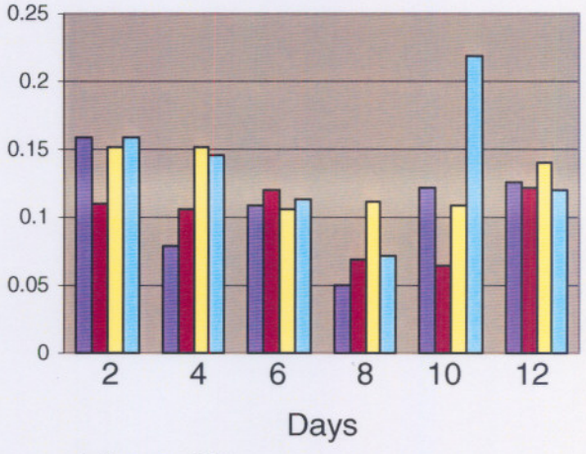

Figure 6.7.

Figure 6.8.

Average and day-to-day brain Q_9H_2 and $Q_{10}H_2$ concentrations respectively.

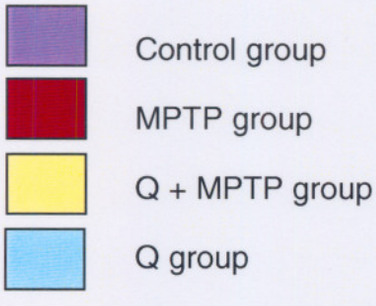

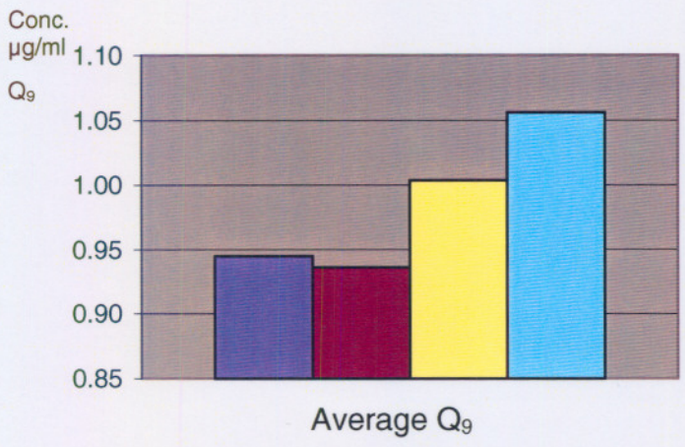

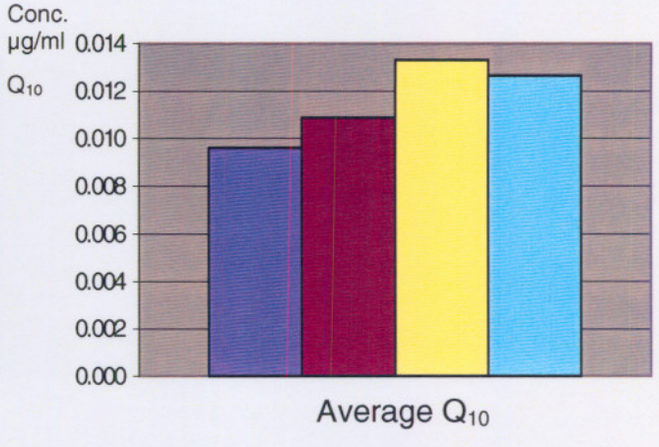

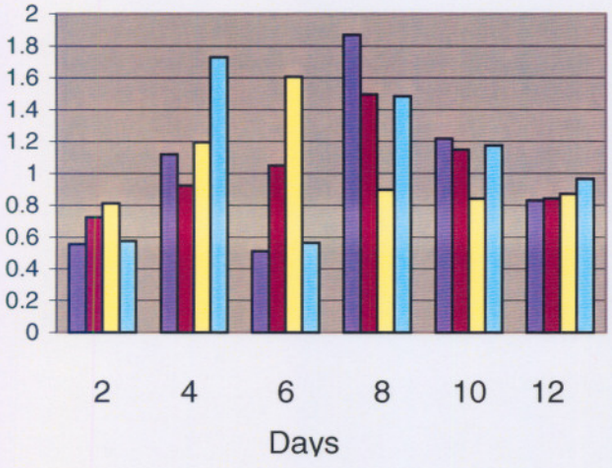

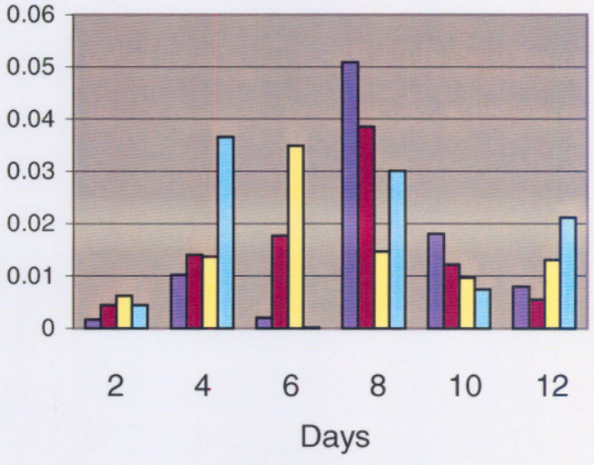

Figure 6.9.

Figure 6.10.

Average and day-to-day heart Q_9H_2 and $Q_{10}H_2$ concentrations respectively.

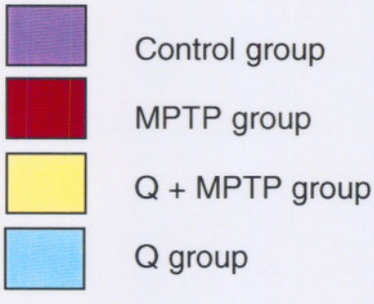

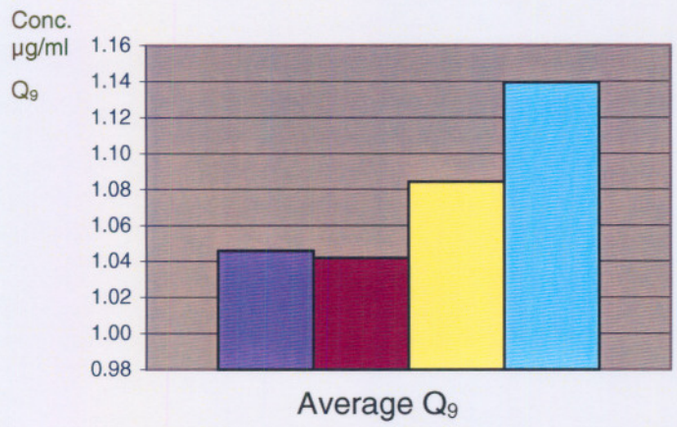

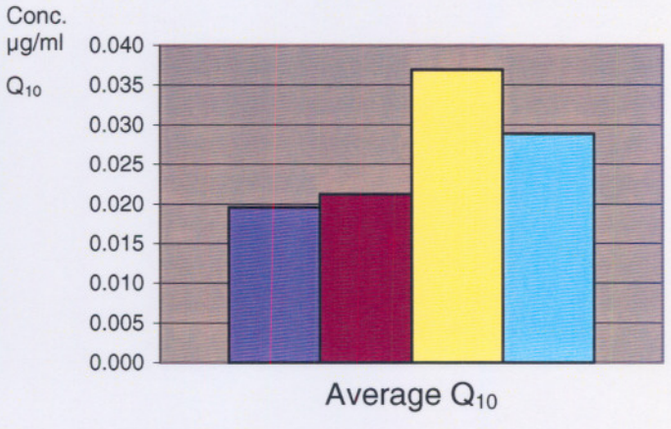

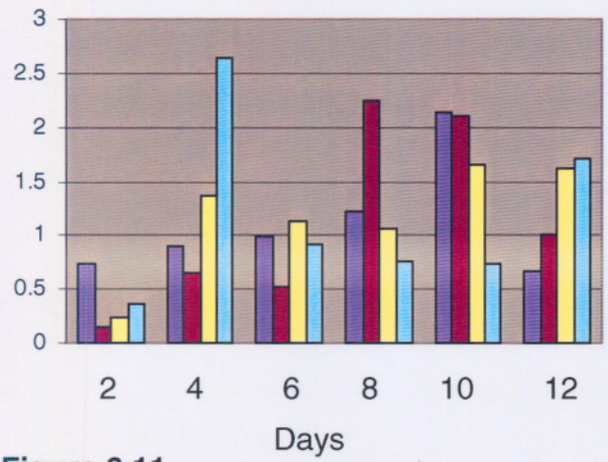

Figure 6.11.

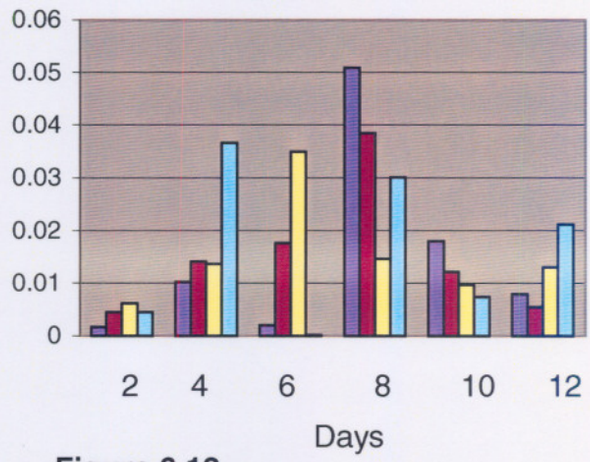

Figure 6.12.

Average and day-to-day liver Q_9H_2 and $Q_{10}H_2$ concentrations respectively.

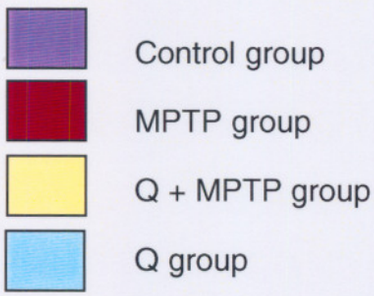

The test animals that did not receive Q_{10} (control and MPTP) showed lower levels of both Q_9H_2 and $Q_{10}H_2$ in the plasma and tissue. The groups receiving MPTP and MPTP + Q_{10} exhibited slightly higher levels of $Q_{10}H_2$ in the liver and heart than the control and Q_{10} groups respectively (figure 6.10. and 6.12.). This very interesting phenomenon might be explained by the theory of Shi *et al.* (1999) (figure 6.13 and next paragraph).

The same anomaly was not observed for Q_9H_2 which led us to hypothesize that this reaction occurs only prior to the Q_{10} - Q_9 conversion in the liver. This reaction may occur in the liposomes or in the cytoplasm of the cell or the brain synaptosomes. With dietary supplementation, Q_{10} ends up in the extramitochondrial fraction. It is likely that under nondeficient Q_{10} conditions, dietary supplementations affects luminal Q pools, the function of which is unknown (Dallner & Sindelar, 2000).

Shi *et al.* (1999) stated that ubiquinone could act as an electron acceptor from $MPDP^+$ and promotes the conversion from $MPDP^+$ to MPP^+ *in vivo*, thus accelerating the neurotoxicity of MPTP (figure 6.13). The $Q_{10}H_2$, formed in this reaction however, probably ameliorates the toxicity of MPTP by acting as an efficient anti-oxidant (section 2.4.) thus neutralizing the role of Q_{10} in facillating the formation of toxic MPP^+. A reduction in DNA damage may therefore prove to be the end result of these two seemingly opposing mechanisms.

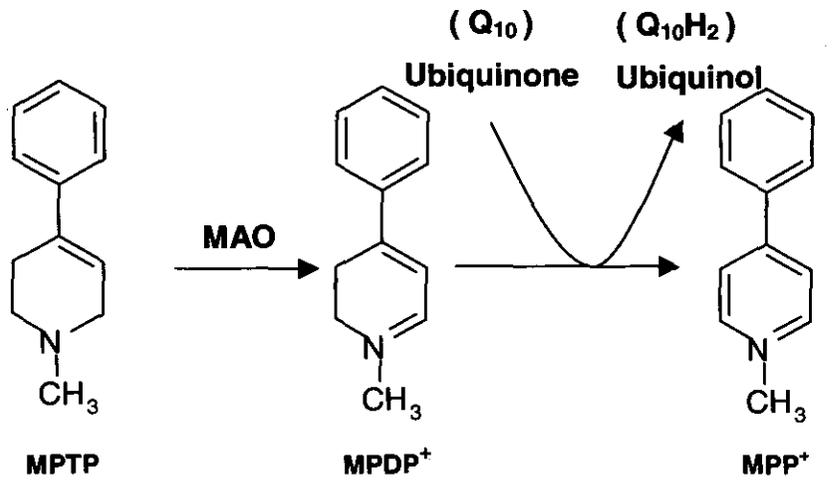

Figure 6.13. The proposed mechanism of MPTP in vivo (Shi *et al.*, 1999).

The average Q_9H_2 concentrations in the control groups for tissue (figure 6.7, 6.9, 6.11) varied only between 1.2 µg/mg (in the brain) and 0.91 (in the heart). $Q_{10}H_2$ concentrations were however 10 times higher in the brain (figure 6.8.) than in the heart (figure 6.10.) and liver (figure 6.12.). The MPTP + Q_{10} groups showed the highest Q_9H_2 and $Q_{10}H_2$ levels between day 4 and 6. This is in agreement with findings by Przedborski & Vila (2001) that MPP^+ levels reach a maximum between 3-6 days (MPP^+

is responsible for the conversion of Q_{10} to $Q_{10}H_2$). These results also confirm the findings of Shi *et al.* (1999) that Q_9H_2 and $Q_{10}H_2$ concentrations were at its highest levels on day 6.

The main findings were that addition of Q_{10} to the diet caused an increase in the $Q_{10}H_2$ and Q_9H_2 levels in plasma and heart, liver and brain tissue of mice (the magnitude of increase varied in different tissue). These results support the notion that there is a general uptake of supplemented Q_{10} by all tissues, although specific amounts of the uptake may vary in different tissues. Our results support the supposition that administration of Q_{10} to rodents can lead to tissue specific increases in both Q_9H_2 and $Q_{10}H_2$ concentrations in plasma and tissues. Dietary Q_{10} supplementation does not appear to have an effect on the endogenous biosynthesis of Q_9 (Lass *et al.*, 1999). The observed increase of Q_9 may thus be due to the *in vivo* modification of the isoprene moiety and/or the anti-oxidative protection of mitochondrial Q_9 by exogenous Q_{10}.

6.3. Determination of cell DNA damage

6.3.1. Single cell gel electrophoresis

Apart from the appeal of the images the comet assay produces, it is quick, simple sensitive, reliable and a fairly inexpensive way of measuring DNA damage (Collins *et al.*, 1997). The comet assay offers considerable advantages over other cytogenic methods for DNA damage detection, like chromosome aberration, sister chromatid exchanges (SCEs), micronucleus test (MN) and alkali elution because of its high sensitivity (< 5 cGy gamma rays). The cells studied need not to be mitotically active. Also important is that this technique requires a small number of cells (< 10,000) and is applicable to a broad spectrum of cell types because virtually any eukaryotic nucleated cell can be used (Pavlica *et al.*, 2001; Lee & Steinert, 2003).

The scope of the applications of the comet assay makes it an invaluable tool for investigating fundamental aspects of DNA damage and cellular responses to this damage. The alkaline comet assay resolves break frequencies up to a few thousand

per cell, so the distances between breaks are of the order of 10^9 Da, well beyond the range of fragment size for which conventional electrophoresis is suitable. The length of such a fragment is about 1 mm; the length of the tail of a comet is a few hundreds of this. If DNA was broken by irradiation, supercoiling was relaxed and loops spilled out into a 'halo' around the nucleoid core. We can therefore assume that the comet tail is made up of relaxed loops, and that the number of loops in the tail (or, the relative tail intensity) indicates the number of DNA breaks. This model fits observations that with increasing amount of damage, the tail intensity rather than the length increases, this was determined by the length of the loops (Collins *et al.*, 1997).

"Comets" are viewed by fluorescence microscopy after staining with a suitable fluorescence DNA-binding dye. The relative intensity of fluorescence in the tail is a function of DNA breaks and can be assessed either visually or using a computer based image analysis (Kassie *et al.*, 2000).

Tomaseti *et al.* (1999) used H_2O_2 to induce DNA damage *in vitro* and supplemented cells with $Q_{10}H_2$ and Q_{10} to evaluate the DNA strand breaks with the comet assay. Their results showed that the amount of DNA strand breaks were less and cell viability was significantly higher in $Q_{10}H_2$-enriched cells compared to control (Tomaseti *et al.*, 1999).

6.3.1.1. SCGE analysis

The objective was to develop an improved method for SCGE as compared to the already established methods. This was achieved by changing the dimensions of the gel slide and it's frosting, and the use of a gel bracket over the slide. The agarose matrix varies in composition, in the popular layered technique, which is time consuming and complicated to master. In this investigation a single thick layer of agarose was used, which proved as effective as the triple layer method. A primary thin layer was applied to the slide to promote adhesion of the single thick gel layer (influenced the polarity of the glass slide). There was also no noticeable variation in comet structure and size as a result of the single thick layer. Cells did not diffuse out of the gel even in the absence of

a third agarose layer. Staining the gel with ethidium bromide or propidium iodide proved as effective, the thickness of the layer had no effect.

The second objective was the isolation of cells from various organs and the use of whole blood in heparin tubes for analysis. The results (Appendix B) showed that it was possible to isolate enough cells from the various organs to allow for analysis. The use of a simple homogenising buffer and homogenising the samples by hand, proved that separation and isolation of cells, from individual organs need not be expensive and complicated.

Analysis of comet size and tail length showed that the electrophoresis method was sound. From the point of lyses to staining conforms generally to published methods. Adjustments were made for the experimental environment. Examples of this would be the temperature, which was maintained at 4°C to allow for repeatability, voltage differed according to container size (1v/cm) and all SCGE runs were completed under red light to reduce excessive external influences to the DNA.

For visualisation of DNA damage the Olympus IX -70 system and WISSAM analysis software package were used to quantitate the length of DNA migration and the percentage of migrated DNA. To distinguish between populations of cells differing in size (e.g. parenchymal versus nonparenchymal cells), nuclear diameter measurements were used. Using a combination of the tail length and migrated DNA in the tail, it is possible to determine the tail moment (TM).

Using the formula: Tail Moment (TM) = (Tail length) × (Migrated DNA intensity) values for DNA damage were calculated (Lee & Steinert, 2003) (see figure 5.9.).

6.3.2. Plasma and tissue cell DNA damage (figure 6.14. – 6.17.)

Figures 6.14. – 6.17. depict the values obtained by SCGE during week 5 and 6 of treatment. The top graph in each figure depicts the average TM - values obtained while the graphs below depict the day to day TM - values.

The heart, brain and liver cells (figure 6.15. – 6.17.) exhibited significant differences between the controls and the groups treated with MPTP, MPTP/Q and Q, showing a difference that varied between 1000 TM - value and 2500 TM - value for the various tissues. The blood samples before and after treatment (figure 6.14.) in contrast, showed very little variation in DNA damage – the difference between the highest and lowest TM - value was only 1000. This might be explained by the fact that blood cells regenerate much faster than other tissue and that new cells have replaced the damaged cells, where in tissue the damage is of a more permanent nature.

The facilitating of the $Q_{10}H_2$ formation will act as an anti-oxidant reducing DNA damage in the tissue. The average in all of the tissues (figure 6.15. – 6.17.) showed DNA damage to be most severe in groups treated only with MPTP and the lowest in groups treated with Q_{10} only. Groups that received both Q_{10} and MPTP showed lower DNA damage than those only receiving MPTP (figure 6.15 – 6.17.), leading us to postulate that Q_{10} administration could attenuate oxidative stress in mice.

On an overall day-to-day basis a decline in damage due to MPTP could be seen in figures 6.14. – 6.16. which may be an indication of other defence mechanisms being activated, for example, the cytochrome P450 system. Lower DNA damage in the Q groups when compared to the controls in all tissue samples indicates that Q_{10} may also lower DNA damage caused by exogenous factors.

The most severe cell DNA damage in the brain occurred on day 4-6. This correlates with findings by Przedborski & Vila (2001) that the peak of cell death after MPTP

administration occurs after 3-6 days. This may indicate lower defence mechanisms in the brain compared with other tissue.

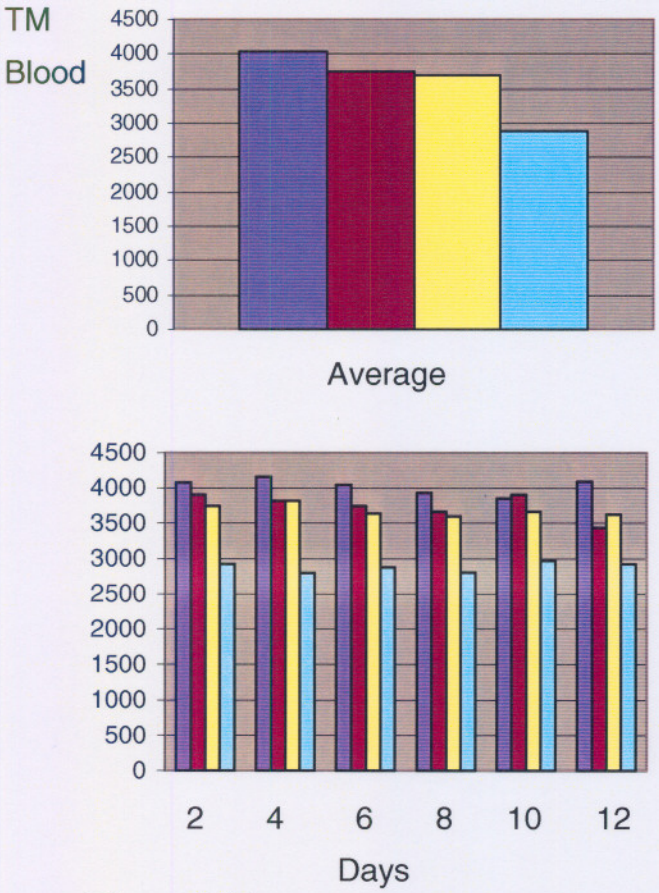

Figure 6.14.

DNA damage found in the lymphocytes

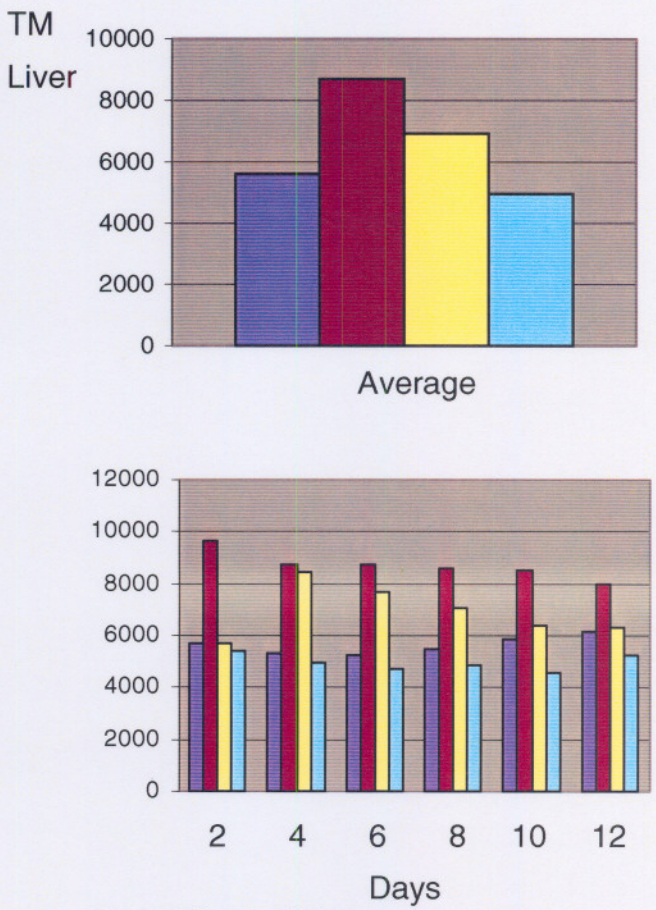

Figure 6.15.

DNA damage found in liver tissue

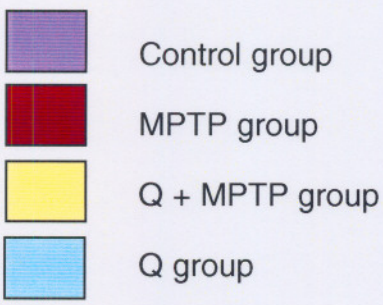

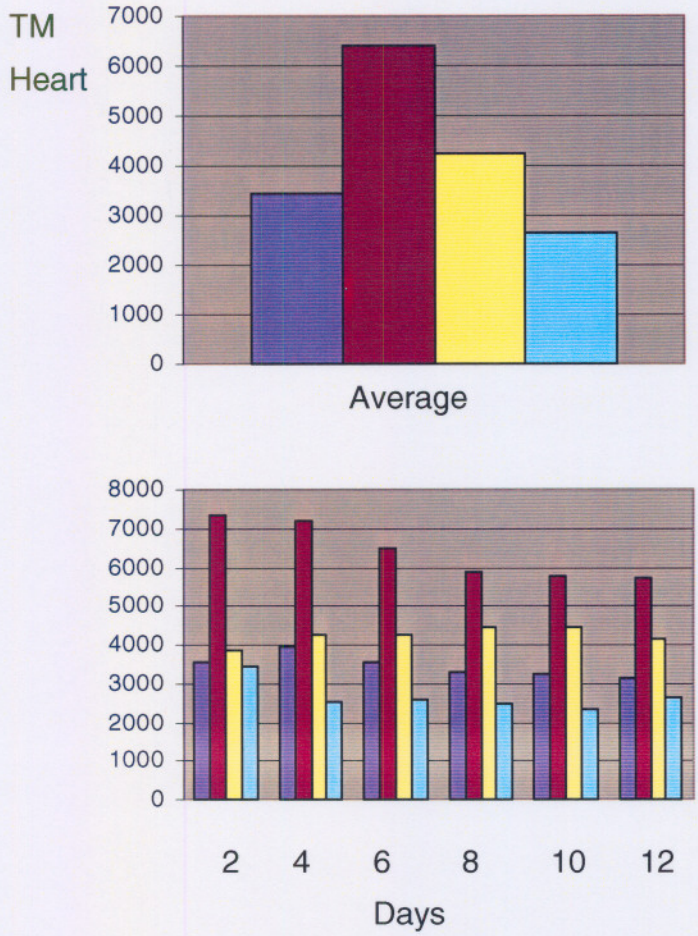

Figure 6.16.

DNA damage found in the heart tissue

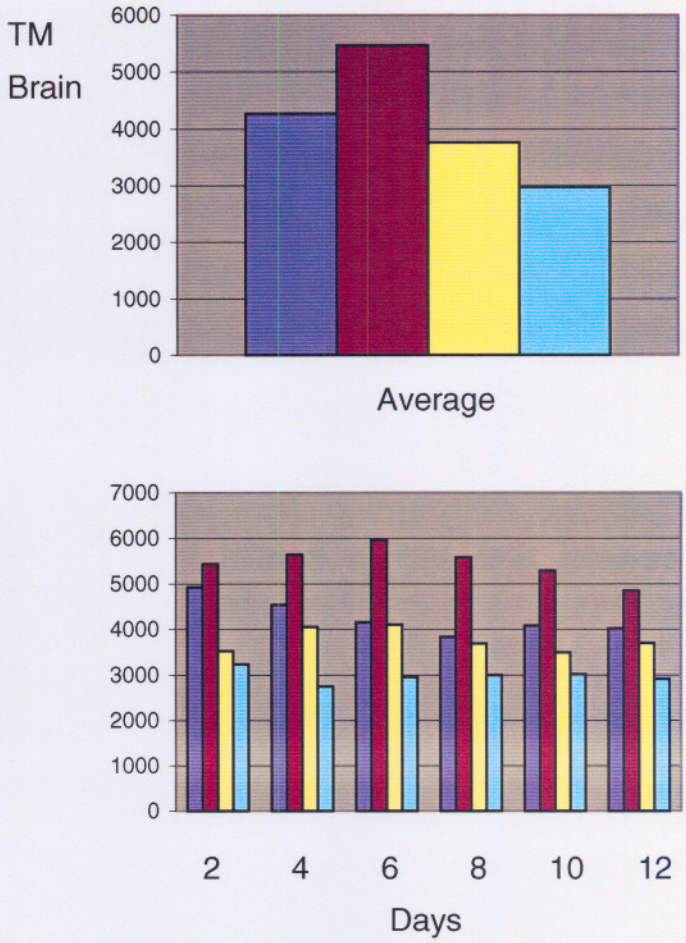

Figure 6.17.

DNA damage found in the brain tissue

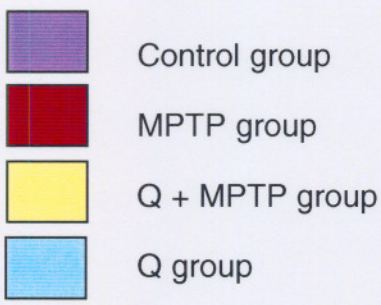

6.4. Summary

Comparing the results of the DNA damage obtained with the SCGE method with the concentration of $Q_{10}H_2$ measured by HPLC, it was possible to see that there was an effective correlation between lower DNA damage and higher $Q_{10}H_2$ or Q_9H_2 concentrations in isolated tissue samples (section 5.4, 5.6.).

MPTP impairs complex I activity (complex I activity is reduced in the substantia nigra of PD patients) and increases the production of reactive oxygen species. We assume that Q_{10} acts by enhancing mitochondrial function (complex I activity is stimulated and ATP synthesis is stimulated) and/or by reducing the levels of ROS in damaged tissue, after MPTP-induced generation of ROS (figure 2.10), due to its anti-oxidant function (section 2.4.).

The heart and liver showed that $Q_{10}H_2$ levels were higher after MPTP administration in the Q + MPTP group. This could be explained by Shi. *et al.* (1999) (section 6.2.2.). The lower levels of DNA damage found after Q_{10} treatment led us to assume that the anti-oxidant capacity was higher in all tissue because of the higher levels of $Q_{10}H_2$ and Q_9H_2 (section 2.4.). Our results also indicated that oral Q_{10} administration may lower the damage to cell DNA in C57 BL/6J mice by lowering *in vivo* oxidative stress by tripping the pro-oxidant/anti-oxidant balance of Q_{10} towards the anti-oxidants (section 2.4.).

Our findings that Q_{10} could attenuate/prevent DNA damage in various cells could suggest that Q_{10} may be useful in disorders where there is impaired activity of complex I which might lead to DNA damage of the cell, like in PD. Oxidative damage to mitochondrial DNA has been estimated to be 10-fold higher than damage to nuclear DNA (Perlmutter, 1999). Q_{10} could improve mitochondrial oxidative metabolism in these patients and thus prevent oxidative damage due to free radicals.

In summary, we found that the oral treatment of aged mice with Q_{10} caused a significant decline of DNA damage caused by MPTP. In addition Q_{10} may be shown as an

effective anti-oxidant. Our findings indicate that levels of Q_9 and Q_{10} can be increased in tissue by long-term supplementation with Q_{10} and that Q_{10} may be a useful therapy to ameliorate the progression of PD and other neurodegenerative diseases.

REFERENCES

ABE, K., ISHIBASHI, K., OHMAE, M., KAWABE, K. & KATSUI, G. 1978. Determination of ubiquinone in serum and liver by high-speed liquid chromatography. *Journal of nutritional science and vitaminology*, 24:555-567.

AHAMAD, J., ASHOK, B.K. & RASHID, A. 1998. Detection of oxidative damage by a monoclonal antibody: role of lysyl residues in antigen binding. *Immunology letters*, 62:87-97.

ALLEVA, R., THOMASETTI, M., ANDERA, L., GELLERT, N., BORGHI, B., WEBER, C., MURPHY, M.P. & NEUZIL, J. 2001. Coenzyme Q block biochemical but not receptor mediated apoptosis by increasing mitochondrial anti-oxidant protection. *FEBS letters*, 503:46-50.

BALTACI, V., AYGAN, N., AKYOL, D., KARAKAYA, A.E. & SARDAS, S. 1998. Chromosomal aberrations and alkaline comet assay in families with habitual abortion. *Mutation research*, 417:47-55.

BEAL, M.F. 1996. Mitochondria, free radicals, and neurogeneration. *Current opinion in neurobiology*, 6:661-666.

BEAL, M.F. 2000. Energetics in the pathogenesis of neurodegenerative diseases. *Trends in neurosciences*, 23:298-304.

BEAL, M.F., MATTHEWS, R.T., TIELEMAN, A. & SHULTS, C.W. 1998. Coenzyme Q_{10} attenuates the 1-methyl-4-phenyl-1,2,3,6-tetrahydropyridine (MPTP) induced loss of striatal dopamine and dopaminergic axons in aged mice. *Brain research*, 783:109-114.

BETTI, C., DAVINI, T., GIANNESSI, L., LOPRIENO, N & BARALE, R. 1995. Comparative studies by comet test and SCE analysis in human lymphocytes from 200 healthy subjects. *Mutation research*, 343:201–207.

BETTI, C., DAVINI, T., GIANNESSI, L., LOPRIENO, N & BARALE, R. 1994. Microgel electrophoresis assay comet test and SCE analysis in human lymphocytes from 100 normal subjects. *Mutation research*, 307:323–333.

COLLINS, A.R., DOBSON, V.L., DUšINSKá M., KENNEDY, G. & STěTINA, R. 1997. The comet assay: what can it really tell us? *Mutation research,* 375:183-193.

COLLINS, R., RASLOVA, K., SOMOROVSKA, M., PETROVSKA, H., ONDRUSOVA, A., VOHNOUT, B., FABRY, R. & DUSINSKA, M. 1998. DNA damage in diabetes: correlation with a clinical marker. *Free radical biology and medicine*, 25:373–377.

DALLNER, G. & SINDELAR, P.J. 2000. Regulation of ubiquinone metabolism. *Free radical biology & medicine*, 29:285-294.

DONNAHEY, P.L. & HEMMING, F.W. 1975. High performance chromatography of ubiquinones, ficaprenols and dolichols. *Biochemical Society transactions,* 3:775-776.

EBADI, M., GOVITRAPONG, P., SHRAMA, S., MURALIKRISHNAN, D., SHAVALI, S., PELLETT, L., SCHAFER, R., ALBANO, C. & EKEN, J. 2001. Ubiquinone (Coenzyme Q_{10}) and mitochondria in oxidative stress of Parkinson's disease. *Biological signals and receptors,* 10:224-253.

EDLUND, P.O. 1988. Determination of coenzyme Q_{10}, α-tocopherol and cholesterol in biological samples by coupled-column liquid chromatography with coulometric and ultraviolet detection. *Journal of chromatography,* 425:87-97.

ERNSTER, L. & DALLNER, G. 1995. Biochemical, physiological and medical aspects of ubiquinone function. *Biochimica et biophysica acta*, 1271:195-204.

FINCKH, B., KONTUSH, A., COMMENTZ, J., HÜBNER, H., BURDELSKI, M. & KOHLSCHÜTTER, A. 1995. Monitoring of ubiquinol-10, ubiquinone-10, cartenoids, and tocopherols in neonatal plasma microsamples using high-performance liquid chromatography with coulometric electrochemical detection. *Analytical biochemistry*, 232:210-216.

FREI, B., MIKE, C. & AMES B.N. 1990. Ubiquinol-10 is an effective lipid-soluble anti-oxidant at physiological concentrations. *Proceedings of the National Academy of Sciences*, 87:4876-4883.

GOTZ, M.E., GERSTNER, A., HARTH, R., DIRR, A., JANETZKTY, B., KUHN, W., RIEDERER, P. & GERLACH, M. 2000. Altered redox state platelet coenzyme Q_{10} in Parkinson's disease. *Journal of neural transmission*, 107:41-48.

GROSSI, G., BARGOSSI, P.L., FIORELLA, P.L. & PIAZZI, S. 1992. Improved high-performance liquid chromatographic method for the determination of coenzyme Q_{10} in plasma. *Journal of chromatography*, 593:217-226.

GUETENS, G., DE BOECK, G., HIGHLEY, M., VAN OOSTEROM, A. T. & DE BRUIJN, E. A. 2001. Oxidative DNA damage: biological significance and methods of analysis. *Critical reviews in clinical laboratory sciences*, 39:331-457.

GUTIERREZ, S., CARBONELL, E., GALOFRE, P., CREUS, A. & MARCOS, R. 1998. The alkaline single-cell gel electrophoresis (SCGE) assay applied to the analysis of radiation-induced DNA damage in thyroid cancer patients treated with ^{131}I. *Mutation research*, 413:111-119.

HARTMANN, S., PFUHLER, C., DENNOG, D., GERMDNIK, A. & PILGER, G. 1998. Exercise-induced DNA effects in human leukocytes are not accompanied by increased formation of 8-hydroxy-2-deoxyguanosine or induction of micronuclei. *Free radical biology and medicine*, 24:245–251.

HARTMANN, U., PLAPPERET, K., RADDATZ, M. & GRUNERT-FUCHS, G. 1994. Does physical activity induce DNA damage? *Mutagenesis,* 9:269–272.

HATEFI, Y. 1963. Coenzyme Q (ubiquinone). *Advances in enzymology and related subjects of biochemistry*, 25:275-328.

IKENOYA, S., MASAHIRO, T., YERUAKI, Y., ABE, K. & KATAYAMA, K. 1981. Studies on reduced and oxidised ubiquinones. I. Simultaneous determination of reduced and oxidised ubiquinones in tissues and mitochondria by high performance liquid chromatography. *Chemical and pharmaceutical bulletin*, 29:158-164.

IMABAYASHI, S., NAKAMURA, T., SAWA, Y., HASEGAWA, J., SAKAGUCHI, K., FUJITA, T., MORI, Y. & KAWABE, K. 1979. Determination of ubiquinone homologues by mass spectrometry and high performance liquid chromatography. *Analytical chemistry*, 51:534-536.

JENKE, D.R. 1996. Chromatographic method validation: a review of current practices and procedures. II. Guidelines for primary validation parameters. *Journal of liquid chromatography and related technology*, 19:737-757.

JONES, G., BENNETT, N., PODMORE, I. & ROUTLEDGE, M. 1997. Development of a postlabeling assay as a biomonitor of oxidative damage in humans. *Mutation research*, 379:S167.

KARPINSKA, J., MIKOLUC, B. & PIOTROWSKA-JASTRZEBSKA, J. 1998. Application of derivative spectrophotometry for determination of coenzyme Q_{10} in pharmaceuticals and plasma. *Journal of pharmaceutical and biomedical analysis*, 17:1345-1350.

KASSIE, F., PARZEFALL, W. & KNASÜLLER, S. 2000. Single cell gel electrophoresis assay: a new technique for human biomonitoring studies. *Mutation research,* 463:13-31.

KAIKKONEN, J., NYYSSONEN, K. & SALONEN, J.T. 1999. Measurement and stability of plasma reduced, oxidised and total coenzyme Q_{10} in humans. *Scandinavian journal of clinical and laboratory investigation*, 59:457-466.

KIDD, P.M. 2000. Parkinson's disease a multifactorial oxidative neurodegeneration: implications for integrative management. *Alternative medicine review: a journal of clinical therapeutic,* 5:502-529.

KNOX, J.H. 1980. High performance liquid chromatography. Edinburgh:Brown. 205p.

LANG, J.K. & PACKER, L. 1987. Quantitative determination of vitamin E and oxidised and reduced coenzyme Q by high-performance liquid chromatography with in-line ultraviolet and electrochemical detection. *Journal of chromatography*, 385:109-117.

LASS, A., FORSTER, M.J. & SOHAL, R.S. 1999. Effects of coenzyme Q_{10} and α-Tocopherol administration on their tissue levels in the mouse: elevation of mitochondrial α-Tocopherol by coenzyme Q_{10}. *Free radical biology and medicine*, 26:1375-1382.

LEE, R.F. & STEINERT, S. 2003. Us of the single cell gel elctrophoresis/comet assay for detection DNA damage in aquatic (marine and freshwater) animals. *Mutation research, Article in press.*

LENAZ, G. 2001. A critical appraisal of the mitochondrial coenzyme Q_{10} pool. *FEBS letters*, 509:151-155.

LERAY, C., ANDRIAMAMPANDRY, M.D., FREUND, M., GACHET, C. & CAZENAVE, J. 1998. Simultaneous determination of homologues of vitamin E and coenzyme Q and products of α-tocopherol oxidation. *Journal of lipid research*, 39:2099-2150.

LINDSAY, S. 1997. High performance liquid chromatography. 2nd ed. New York:Wiley. 337p.

LITESCU, S-C., DAVID, I-G., RADU, G-L & ABOUL-ENEIN, HY. 2001. Voltammetric determination of coenzyme Q_{10} at a solid glassy carbon electrode. *Instrumentation science and technology,* 29:109-116.

MATAIX, J., MANAS, M., QUILES, J., BATTINO, M., CASSINELLO, M., LOPEZ-FRIAS, M. & HUERTAS, J.R. 1997. Coenzyme Q content depends upon oxidative stress and dietary fat unsaturation. *Molecular aspects of medicine*, 18:129-135.

MATHEWS, C.K. & VAN HOLDE, K.E. 1990. Biochemistry. Redwood City, Calif.:Benjamin/Cummings. 1129p.

MATTILA, P., LEHTONEN, M. & KUMPULAINEN, J. 2000. Comparison of in-line connected diode array and electrochemical detectors in the high performance liquid chromatographic analysis of coenzymes Q_9 and Q_{10} in foodmaterials. *Journal of agricultural and food chemistry*, 48:1229-1233.

MAYES, P.A. 1993. The respiratory chain & oxidative phosphorylation. (*In* Murray, R.K., Granner, D.K., Mayes, P.A. & Rodwell, V.W., *eds.* Harper's biochemistry. 23rd ed. London:Prentice-Hall International. p.119-130.)

McKELVEY-MARTIN, V.J., MELIA, N., WALSH, I.K., JOHNSTON, S.R., HUGHES, C.M., LEWIS, S.E.M. & THOMPSON, W. 1997. Two potential clinical applications of the alkaline single-cell gel electrophoresis assay: 1 human bladder washings and transitional cell carcinoma of the bladder; and 2 human sperm and male infertility. *Mutation research*, 375:93–104.

MENKE, T., NIKLOWITZ, P., ADAM, S., WEBER, M., SCHLüTER, B. & ANDLER, W. 2000. Simultaneous detection of ubiquinol-10, ubiquinone-10, and tocopherols in human plasma micro samples and macro samples as a marker of oxidative damage in neonates and infants. *Analytical biochemistry*, 282:209-217.

MüLLER, T., ACHTEN, S., WALK, R.A., & DOERFLER, W. 1989. DNA-DNA dot hybridization technique used as DNA determination method in the alkaline elution analysis of DNA damage. *Mutation research*, 215:205-211.

NELSON, D.L. & COX, M.M. 2000. Lehninger principles of biochemistry. 3 rd ed. New York:Worth Publishers. 1152p.

OKAMOTO, T., FUKUNAGA, Y., IDA, Y. & KISHI, T. 1988. Determination of reduced and total ubiquinones in biological materials by liquid chromatography with electrochemical detection. *Journal of chromatography*, 430:11-19.

ÖSTLING, O. & JOHANSON, K.J. 1984. Microelectrophoretic study of radiation-induced DNA damage in individual mammalian cells. *Biochemical and biophysical research communications*, 123:291-298.

PARODI, S., BALDI, C., TANINGHER, M., ABELMOSCHI, M.L., PALA, M., PARODI, G. & SANTI, L. 1982. Comparison between sensitivity of a viscometric method and sensitivity of the alkaline elution assay for the determination of DNA damage induced by dimethylsulfate *in vitro. Toxicology letters*, 10:3501-358.

PAVLICA, M., KLOBUCAR, G.I.V., MOJAŠ, N., ERBEN, R., & PAPEŠ, D. 2001. detection of DNA damage in haemocytes of zebra mussel using comet assay. *Mutation research,* 490:209-214.

PERLMUTTER, D. 1999. Functional therapeutics in neurodegenerative disease. [Web:] **http://www.pcrm.org/health/preventive_medicine/parkinsons.html** [Date of access: 7 Aug. 2002].

PRZEDBORSKI, S. & VILA, M. 2001. MPTP: a review of its mechanisms of neurotoxicity. *Clinical neuroscience research*, 1:407-418.

RAHA, S. & ROBINSON, B.H. 2000. Mitochondria, oxygen free radicals, disease and ageing. *Trends in biochemical sciences,* 25:502-508.

ROKOS, J.A.S. 1973. Determination of ubiquinone in subnanomole quantities by spectrofluorometry of its product with alkaline ethylcyanoacetate. *Analytical biochemistry*, 56:26-33.

RYDBERG, B. & JOHANSON, K.J. 1978. Estimation of DNA strand breaks in single mammalian cells. Academic Press: New York. 505p.

SHAH, V.P., MIDHA, K.K., DIGHE, S., MCGILVERAY, I.J., SKELLY, J.P., YACOBI, A., LAYLOFF, T., VISWANAHAN, C.T., COOK, C.E., MCDOWALL, R.D., PITTMAN, K.A. & SPECTOR, S. 1992. Analytical methods of validation: Bioavailability, bioequivalence and pharmacokinetic studies. *Pharmaceutical research,* 9:588-592.

SHI, H., NORIKO, N., YUEXIAN, X. & ETSUO, N. 1999. 1-Methyl-4-phenyl-2,3-dihydropyridinium is transformed by ubiquinone to the selective nigrostriatal toxin 1-methyl-4-phenylpyridinium. *FEBS letters*, 461:196-200.

SINGH, N.P., STEPHENS, R.E., SINGH, H. & LAI, H. 1999. Visual quantification of DNA double-strand breaks in bacteria. *Mutation research,* 429:159-168.

SINGH, N.P. 1998. Sodium ascorbate induces DNA single-strand breaks in human cells in vitro. *Mutation research*, 375:195-203.

SINGH, N.P. & STEPHEN, R.E. 1998. X-ray induced DNA double-strand breaks in human sperm. *Mutagenesis*, 13:75-79.

SINGH, N.P. & STEPHEN, R.E. 1997. Microgel electrophoresis: mechanism, sensitivity and electrostretching. *Mutation research*, 383:167-175.

SINGH, N.P., GRAHAM, M.M., SINGH, V. & KHAN, A. 1995. Induction of DNA single strand breaks in human lymphocytes by low doses of Gamma Rays. *International journal of radiation biology,* 68:563-570.

SINGH, N.P., STEPHENS, R.E. & SCHNEIDER, E.L. 1994. Modifications of alkaline microgel electrophoresis for sensitive detection of DNA damage. *International journal of radiation biology,* 66:23-28.

SINGH, N.P., DANNER, D.B., TICE, R.R., McCOY, M.C., COLLINS, G.D. & SCHNEIDER, E.L. 1989. Abundant alkali labile sites in DNA of human and mouse sperm. *Experiments in cellular research*, 184:461-470.

SINGH, N.P., TICE, R.R., McCOY, M.C. & SCHNEIDER, E.L. 1988. A simple technique for quantitation of low levels of DNA damage in individual cells. *Experiments in cellular research*, 175:184-191.

STRIJKS, E., KREMER, H.P.H. & HORSTINK, M.W.I.M. 1997. Q_{10} therapy in patients with idiopathic Parkinson's disease. *Molecular aspects of medicine,* 18:237-240.

STEINMETZ, K.A. & POTTER, D. 1995. Vegetables, fruits and cancer, assessment of DNA damage in leukocytes from infected and malnourished children by single cell gel electrophoresis/comet assay. *Mutation research*, 331:65–77.

TANG, P.H., MILES, M.V., DEGRAUW, A., HERSHEY, A. & PESCE, A. 2001. HPLC analysis of reduced and oxidised coenzyme Q_{10} in human plasma. *Clinical chemistry*, 47:256-265.

TANG, P.H., MILES, M.V., STEELE, P., DEGRAUW, A., CHUCK, G., SCHROER, L. & PESCE, A. 2002. Anticoagulant effects on plasma coenzyme Q_{10} estimated by HPLC with coulometric detection. *Clinica chimica acta*, 318:127-131.

TANGIGUCH, N., KANETO, H., ASAHI, M., TAKAHASHI, M., WENYI, C., HIGASHIYAMA, S., FUJII, J., KEIICHIRO, S., & KAYNOKI, Y. 1996. Involvement of glycation and oxidative stress in diabetic macroangiopathy. *Diabetes,* 45:81–83.

THOMAS, S.R., NEUZIL, J. & STOCKER, R. 1997. Inhibition of LDL oxidation by ubiquinol-10. A protective mechanism for coenzyme Q in artherogenesis? *Molecular aspects of medicine*, 18:85-103.

TOMASETI, M., LITTARRU, G.P., STOCKER, R. & ALLEVA, R. 1999. Coenzyme Q_{10} enrichment decreases oxidative DNA damage in human lymphocytes. *Free radical biology & medicine,* 27:1027-1032.

TSUDA, S., KOSAKA, Y., MURAKAMI, M., MATSUO, H., MATSUSAKA, N., TANIGUCHI, K. & SASAKI, Y.S. 1998. Detection of nivalenol genotoxicity in cultured cells and multiple mouse organs by the alkaline single-cell gel electrophoresis. *Mutation research,* 415:191-200.

VADHANAVIKIT, S., SAKAMOTO, N., ASHIDA, N., KISHI, T., & FOLKERS, K. 1984. Quantitative determination of coenzyme Q_{10} in human blood for clinical studies. *Analytical biochemistry*, 142:155-158.

VAGHEF, H. & HELLMAN, B. 1998. Detection of styrene and styrene oxide-induced DNA damage in various organs of mice using the comet assay. *Pharmacology & Toxicology,* 83:69-74.

VAN LOON, A.A.W.M., GROENENDIJK, R.H., TIMMERMAN, A.J., VAN DER SCHANS, G.P., LOHMAN, P.H.M. & BAAN, R.A. 1992. Quantative detection of DNA damage in cells after exposure to ionising radiation by means of an improved immunochemical assay. *Mutation research,* 274:19-27

WAKABAYASHI, H., YAMATO, S., NAKAJIMA, M & SHIMADA, K. 1994. Simultaneous determination of oxidised and reduced coenzyme Q_{10} and α-tocopherol in biological samples by high performance liquid chromatography with platinum catalyst reduction and electrochemical detection. *Biological and pharmaceutical bulletin,* 17:997-1002.

WALKER, J.E. 1992. The NADH: ubiquinone oxidoreductase (complex I) of respiratory chains. *Quarterly reviews of biophysics,* 25:253-324.

WALLES, A.S., ZHOU, R. & LILIEMARK, E. 1996. DNA damage induced by etoposide; a comparison of two different methods for determination of strand breaks in DNA. *Cancer letters*, 105:153-159.

WANG, Q., LEE, B.L. & ONG, C.N. 1999. Automated high-performance liquid chromatographic method with precolumn reduction for the determination of ubiquinol and ubiquinone in human plasma. *Journal of chromatography B*, 726:297-302.

WESTON, A. & BROWN, P.R. 1997. HPLC and CE principles and practice. London:Saunders. 280p.

WOLFE, S.L. 1981. Biology of the cell. 2nd ed. Belmont, Calif.:Wadsworth. 544p.

YAMASHITA, S. & YAMAMOTO, Y. 1997. Simultaneous detection of ubiquinol and ubiquinone in human plasma as a marker of oxidative stress. *Analytical biochemistry*, 250:66-73.

APPENDIX A. 1: HPLC VALIDATION

1. LINEARITY

Curve 1:

Table 1.

Sample	HPLC parameter		AUC ratio (Y-axis) Q_9/Q_8	AUC ratio (Y-axis) Q_{10}/Q_8	Concentration (µg/ml) (X-Axis)
	Q	AUC			
Blank	Q_8	0	0	0	0
	Q_9	38.50215			
	Q_{10}	15.61532			
1	Q_8	92.05246	0.651067	0.588418096	0.97
	Q_9	59.93231			
	Q_{10}	54.165335			
2	Q_8	88.78439	0.694523	0.645132756	1.176
	Q_9	61.66283			
	Q_{10}	57.277715			
3	Q_8	90.21279	0.695847	0.656266715	1.408
	Q_9	62.77434			
	Q_{10}	59.20365			
4	Q_8	93.43245	0.718246	0.710748193	1.666
	Q_9	67.10746			
	Q_{10}	66.406945			
5	Q_8	94.24071	0.803824	0.906328404	3.1818
	Q_9	75.75295			
	Q_{10}	85.413035			
6	Q_8	88.52591	0.905418	1.06634905	4.44
	Q_9	80.15299			
	Q_{10}	94.39952			

Linear curve 1.1:

$y = 0.0676x + 0.6002$

$R^2 = 0.9857$

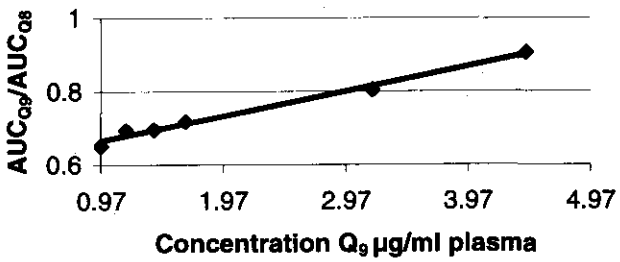

Curve of ratio Q_9/Q_8

Linear curve 1.2:

$y = 0.134x + 0.3044$

$R^2 = 0.9951$

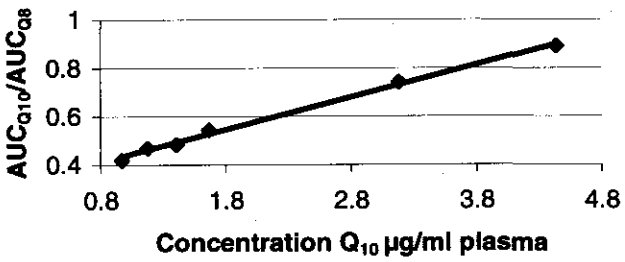

Curve of ratio Q_{10}/Q_8

Curve 2:

Table 2.

Sample	HPLC parameter		AUC ratio (Y-axis) Q_9/Q_8	AUC ratio (Y-axis) Q_{10}/Q_8	Concentration (µg/ml) (X-Axis)
	Q	AUC			
Blank	Q_8	0	0	0	0
	Q_9	41.32514			
	Q_{10}	13.81026			
1	Q_8	94.7091	0.662368	0.552907	0.97
	Q_9	62.7323			
	Q_{10}	52.36533			
2	Q_8	92.072075	0.700134	0.613065	1.176
	Q_9	64.46282			
	Q_{10}	56.44615			
3	Q_8	92.091735	0.712055	0.639275	1.408
	Q_9	65.57434			
	Q_{10}	58.87192			
4	Q_8	98.98108	0.706271	0.657704	1.666
	Q_9	69.90746			
	Q_{10}	65.1003			
5	Q_8	95.413435	0.82329	0.891989	3.1818
	Q_9	78.552954			
	Q_{10}	85.1077458			
6	Q_8	89.281325	0.929119	1.067854	4.44
	Q_9	82.952987			
	Q_{10}	95.339377			

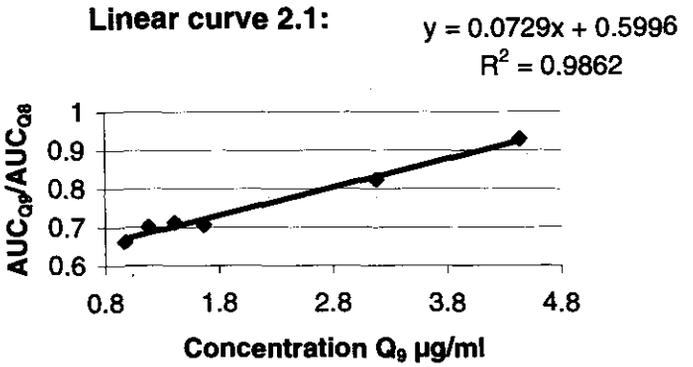

Curve of ratio Q_9/Q_8

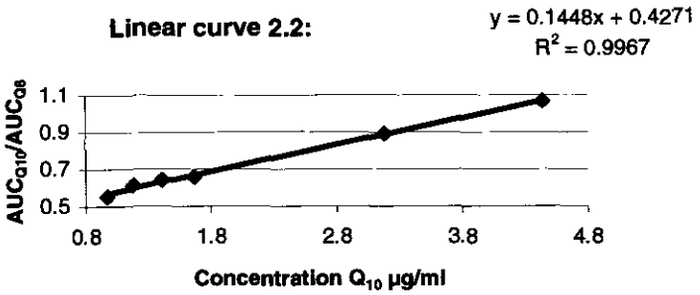

Curve of ratio Q_{10}/Q_8

Curve 3:

Table 3.

Sample	HPLC parameter		AUC ratio (Y-axis) Q_9/Q_8	AUC ratio (Y-axis) Q_{10}/Q_8	Concentration (µg/ml) (X-Axis)
	Q	AUC			
Blank	Q_8	0	0	0	0
	Q_9	39.52065			
	Q_{10}	14.20342			
1	Q_8	93.395825	0.654893	0.564965	0.97
	Q_9	61.164263			
	Q_{10}	52.765334			
2	Q_8	89.496695	0.697277	0.624355	1.176
	Q_9	62.404015			
	Q_{10}	55.877714			
3	Q_8	90.33384	0.700164	0.639889	1.408
	Q_9	63.24854			
	Q_{10}	57.80365			
4	Q_8	96.88382	0.702981	0.670978	1.666
	Q_9	68.107464			
	Q_{10}	65.006944			
5	Q_8	96.26799	0.797284	0.8727	3.1818
	Q_9	76.752949			
	Q_{10}	84.013035			
6	Q_8	90.770495	0.874678	1.024557	4.44
	Q_9	79.3949305			
	Q_{10}	92.999519			

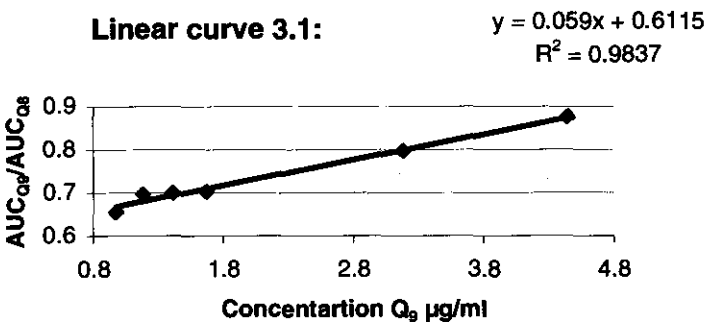

Curve of ratio Q_9/Q_8

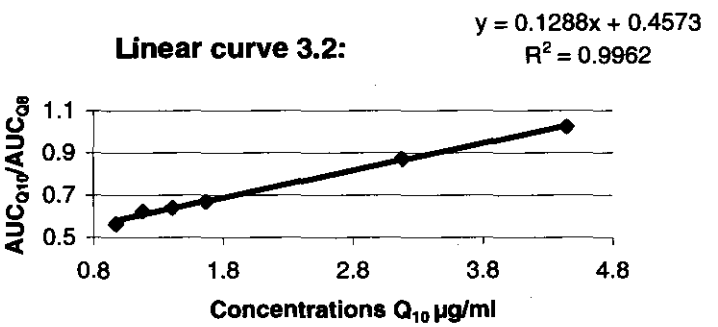

Curve of ratio Q_{10}/Q_8

2. ACCURACY

Accuracy according to linear curves 2 for both Q_9 and Q_{10}:

Slope (m) of Q_9/Q_8 linear curve: 0.0729

Y-intercept of Q_9/Q_8 linear curve: 0.5996

Slope (m) of Q_{10}/Q_8 linear curve: 0.1448

Y-intercept of Q_{10}/Q_8 linear curve: 0.4271

Sample 2: 1.18 µg/ml (Table 4)

Sample	HPLC parameter		AUC ratio (Y-axis) Q_9/Q_9	AUC ratio (Y-axis) Q_9/Q_{10}	Concentration Q_9/Q_8 (µg/ml)	Concentration Q_{10}/Q_8 (µg/ml)
	Q	AUC				
1	Q_8	88.78439	0.694523	0.645132756	1.302098765	1.505751077
	Q_9	61.66283				
	Q_{10}	57.277715				
2	Q_8	92.072075	0.700134	0.613065	1.379067215	1.362258287
	Q_9	64.46282				
	Q_{10}	56.44615				
3	Q_8	89.496695	0.697277	0.624355	1.339876543	1.362258287
	Q_9	62.404015				
	Q_{10}	55.877714				

Average of Q_9 concentration (µg/ml plasma): 1.340347508

SD of Q_9 concentration (µg/ml plasma): 0.038486386

%CV of Q_9 concentration (µg/ml plasma): 2.871373712 %

% Recovery: 113.9740 %

Average of Q_{10} concentration (µg/ml plasma): 1.410089217

SD of Q_{10} concentration (µg/ml plasma): 0.0828456

%CV of Q_{10} concentration (µg/ml plasma): 5.875202718 %

% Recovery: 119.9055 %

Sample 4: 1.67 µg/ml (Table 5)

Sample	HPLC parameter		AUC ratio (Y-axis) Q_8/Q_9	AUC ratio (Y-axis) Q_8/Q_{10}	Concentration Q_9/Q_8 (µg/ml)	Concentration Q_{10}/Q_8 (µg/ml)
	Q	AUC				
1	Q_8	93.43245	0.718246	0.710748193	1.627517147	1.95889636
	Q_9	67.10746				
	Q_{10}	66.406945				
2	Q_8	98.98108	0.706271	0.657704	1.463251029	1.592569061
	Q_9	69.90746				
	Q_{10}	65.1003				
3	Q_8	96.88382	0.702981	0.670978	1.418120713	1.684240331
	Q_9	68.107464				
	Q_{10}	65.006944				

Average of Q_9 concentration (µg/ml plasma): 1.502961963

SD of Q_9 concentration (µg/ml plasma): 0.110202064

%CV of Q_9 concentration (µg/ml plasma): 7.33232067 %

% Recovery: 90.213863 %

Average of Q_{10} concentration (µg/ml plasma): 1.745235251

SD of Q_{10} concentration (µg/ml plasma): 0.190628454

%CV of Q_{10} concentration (µg/ml plasma): 10.92279416 %

% Recovery: 104.75601 %

Sample 6: 4.44 µg/ml (Table 6)

Sample	HPLC parameter		AUC ratio (Y-axis) Q_8/Q_9	AUC ratio (Y-axis) Q_8/Q_{10}	Concentration Q_9/Q_8 (µg/ml)	Concentration Q_{10}/Q_8 (µg/ml)
	Q	AUC				
1	Q_8	88.52591	0.905418	1.06634905	4.195034294	4.414703384
	Q_9	80.15299				
	Q_{10}	94.39952				
2	Q_8	89.281325	0.929119	1.067854	4.520150892	4.425096685
	Q_9	82.952987				
	Q_{10}	95.339377				
3	Q_8	90.770495	0.874678	1.024557	3.773360768	4.126084254
	Q_9	79.3949305				
	Q_{10}	92.999519				

Average of Q_9 concentration (µg/ml plasma): 4.162848652

SD of Q_9 concentration (µg/ml plasma): 0.374433985

%CV of Q_9 concentration (µg/ml plasma): 8.994657659 %

% Recovery: 93.75785 %

Average of Q_{10} concentration (µg/ml plasma): 4.321961441

SD of Q_{10} concentration (µg/ml plasma): 0.169714199

%CV of Q_{10} concentration (µg/ml plasma): 3.926786514 %

% Recovery: 97.34147 %

3. PRECISION

Sample 2: 1.18 µg/ml (Table 7)

Sample	HPLC parameter		AUC ratio (Y-axis) Q_8/Q_9	AUC ratio (Y-axis) Q_8/Q_{10}
	Q	AUC		
1	Q_8	88.78439	0.694523	0.645132756
	Q_9	61.66283		
	Q_{10}	57.277715		
2	Q_8	92.072075	0.700134	0.613065
	Q_9	64.46282		
	Q_{10}	56.44615		
3	Q_8	89.496695	0.697277	0.624355
	Q_9	62.404015		
	Q_{10}	55.877714		

Average of Q_9 AUC ratio: 0.697311333

SD of Q_9 AUC ratio: 0.002805157677

%CV of Q_9 AUC ratio: 0.402281859 %

Average of Q_{10} AUC ratio: 0.627517585

SD of Q_{10} AUC ratio: 0.016266121

%CV of Q_{10} AUC ratio: 2.59213787 %

Sample 4: 1.67 µg/ml (Table 8)

Sample	HPLC parameter		AUC ratio (Y-axis) Q_9/Q_8	AUC ratio (Y-axis) Q_9/Q_{10}
	Q	AUC		
1	Q_8	93.43245	0.718246	0.710748193
	Q_9	67.10746		
	Q_{10}	66.406945		
2	Q_8	98.98108	0.706271	0.657704
	Q_9	69.90746		
	Q_{10}	65.1003		
3	Q_8	96.88382	0.702981	0.670978
	Q_9	68.107464		
	Q_{10}	65.006944		

Average of Q_9 AUC ratio: 0.709166

SD of Q_9 AUC ratio: 0.0080337304

%CV of Q_9 AUC ratio: 1.132841958 %

Average of Q_{10} AUC ratio: 0.679810064

SD of Q_{10} AUC ratio: 0.027603

%CV of Q_{10} AUC ratio: 4.060398847%

Sample 6: 4.44 µg/ml (Table 9)

Sample	HPLC parameter		AUC ratio (Y-axis) Q_8/Q_9	AUC ratio (Y-axis) Q_8/Q_{10}
	Q	AUC		
1	Q_8	88.52591	0.905418	1.06634905
	Q_9	80.15299		
	Q_{10}	94.39952		
2	Q_8	89.281325	0.929119	1.067854
	Q_9	82.952987		
	Q_{10}	95.339377		
3	Q_8	90.770495	0.874678	1.024557
	Q_9	79.3949305		
	Q_{10}	92.999519		

Average of Q_9 AUC ratio: 0.903071666

SD of Q_9 AUC ratio: 0.027296231

%CV of Q_9 AUC ratio: 3.022598541 %

Average of Q_{10} AUC ratio: 1.052920017

SD of Q_{10} AUC ratio: 0.024574616

%CV of Q_{10} AUC ratio: 2.33394898 %

APPENDIX A.2: RAW DATA FOR HPLC

Abbreviations for appendix A.2 (Tables):

Sample:	Example: *P 1.1.C* (Plasma, day one, mice 1, Control group)
	Example: *L 1.2.MP* (Liver, day one, mice 2, received MPTP only)
	Example: *B 2.1.Q+M* (Brain, day two, mice 1, received Q_{10} + MPTP)
	Example: *H 2.2.Q* (Heart, day two, mice 2, received Q_{10} only)
ml/mg	millilitre plasma or milligram tissue
$Q_{8/9/10}$(AUC)	Area under curve for Q_8 or Q_9 or Q_{10}
$Q_{9/10}/Q_8$	Ratio Q_9/Q_8 or Q_{10}/Q_8
Ave.	Average for two mice.
X	Concentration Q_9 or Q_{10} determined through linear curves 2 (section 5.5.4.2).
Ave. X	Average concentration for two mice.
$Q_{9/10}$/ml/mg	Concentration Q_9 or Q_{10} in one millilitre plasma or one milligram tissue.

Sample	ml	Q8(AUC)	Q9(AUC)	Q10(AUC)	AUC Q9/8	AVE.	X	AVE. X	µg/ml	AVE.	AUC Q10/8	AVE.	X	AVE. X	µg/ml	AVE.
	-	-	-	-	-	-	-	-	-	-	-	-	-	-	-	-
P1.1 C	1000	**26.85**	**42.12**	**11.490**	1.569	1.914	13.294	18.033	13.294	18.033	0.428	0.384	0.006	-0.294	0.006	0.000
P1.2 C	1000	**27.68**	**62.55**	**9.440**	2.260		22.773		22.773		0.341		-0.594		-0.594	
P2.1 C	1000	**11.83**	**39.43**	**10.410**	3.333	2.777	37.496	23.279	37.496	23.279	0.880	1.219	3.128	5.471	3.128	5.471
P2.2 C	1000	**5.53**	**12.28**	**8.620**	2.221		22.236		22.236		1.559		7.815		7.815	
P3.1 C	1000	**29.66**	**61.26**	**44.210**	2.065	1.300	20.107	9.614	20.107	9.614	1.491	0.911	7.344	3.339	7.344	7.344
P3.2 C	1000	**6.2**	**3.32**	**2.050**	0.535		-0.880		-0.880		0.331		-0.666		0.000	
P4.1 C	1000	**10.46**	**20.39**	**5.670**	1.949	1.958	18.515	18.637	18.515	18.637	0.542	0.271	0.794	-1.078	0.794	0.794
P4.2 C	1000	**4.57**	**8.99**	**0.000**	1.967		18.760		18.760		0.000		-2.950		0.000	
P5.1 C	1000	**33.53**	**33.26**	**19.640**	0.992	1.612	5.382	13.881	5.382	13.881	0.586	0.404	1.096	-0.160	1.096	1.096
P5.2 C	1000	**32.19**	**71.82**	**7.150**	2.231		22.380		22.380		0.222		-1.416		-1.416	
P6.1 C	1000	**49.74**	**123.53**	**29.650**	2.484	2.651	25.842	28.134	25.842	28.134	0.596	4.037	1.167	13.049	1.167	13.049
P6.2 C	1000	**17.55**	**49.45**	**70.850**	2.818		30.426		30.426		4.037		24.931		24.931	

Sample	ml	Q8(AUC)	Q9(AUC)	Q10(AUC)	AUC Q9/8	AVE.	X	AVE. X	µg/ml	AVE.	AUC Q10/8	AVE.	X	AVE. X	µg/ml	AVE.
P1.1 MP	1000	**29.75**	**30.54**	**10.550**	1.027	1.188	5.857	8.077	5.857	8.077	0.355	0.273	-0.501	-1.065	-0.501	-1.065
P1.2 MP	1000	**27.21**	**36.74**	**5.200**	1.350		10.297		10.297		0.191		-1.630		-1.630	
P2.1 MP	1000	**25.88**	**42.43**	**54.480**	1.639	2.222	14.265	21.715	14.265	21.715	2.105	1.514	11.588	7.506	11.588	7.506
P2.2 MP	1000	**10.12**	**28.38**	**9.340**	2.804		30.243		30.243		0.923		3.424		3.424	
P3.1 MP	1000	**18.56**	**33.52**	**3.170**	1.806	1.376	16.549	10.654	16.549	10.654	0.171	1.222	-1.770	5.491	-1.770	5.491
P3.2 MP	1000	**4.86**	**4.6**	**11.050**	0.947		4.759		4.759		2.274		12.753		12.753	
P4.1 MP	1000	**8.43**	**18.25**	**3.820**	2.165	2.106	21.472	20.668	21.472	20.668	0.453	1.054	0.180	4.327	0.180	4.327
P4.2 MP	1000	**8.59**	**17.59**	**14.210**	2.048		19.865		19.865		1.654		8.475		8.475	
P5.1 MP	1000	**14.28**	**38.81**	**6.550**	2.718	1.764	29.056	15.973	29.056	15.973	0.459	1.495	0.218	7.378	0.218	7.378
P5.2 MP	1000	**9.17**	**7.43**	**23.220**	0.810		2.890		2.890		2.532		14.538		14.538	
P6.1 MP	1000	**24.62**	**70.16**	**38.280**	2.850	3.096	30.866	34.250	30.866	30.866	1.555	0.977	7.788	3.797	7.788	3.797
P6.2 MP	1000	**18.3**	**61.18**	**7.300**	3.343		37.635		37.635		0.399		-0.195		-0.195	

Sample	ml	Q8(AUC)	Q9(AUC)	Q10(AUC)	AUC Q9/8	AVE.	X	AVE. X	µg/ml	AVE.	AUC Q10/8	AVE.	X	AVE. X	µg/ml	AVE.
P1.1 Q+M	1000	**29.29**	**22.19**	**46.890**	0.758	1.136	2.167	7.355	2.167	7.355	1.601	1.287	8.106	5.936	8.106	5.936
P1.2 Q+M	1000	**38.91**	**58.91**	**37.830**	1.514		12.543		12.543		0.972		3.765		3.765	
P2.1 Q+M	1000	**8.16**	**9.11**	**0.000**	1.116	1.154	7.089	7.604	7.089	7.604	0.000	0.131	-2.950	-2.042	-2.950	-2.042
P2.2 Q+M	1000	**14.68**	**17.49**	**3.860**	1.191		8.118		8.118		0.263		-1.134		-1.134	
P3.1 Q+M	1000	**3.21**	**4.72**	**32.350**	1.470	4.365	11.945	51.657	11.945	51.657	10.078	6.892	66.649	44.646	66.649	44.646
P3.2 Q+M	1000	**2.65**	**19.24**	**9.820**	7.260		91.369		91.369		3.706		22.642		22.642	
P4.1 Q+M	1000	**9.24**	**28.5**	**76.430**	3.084	1.903	34.085	17.878	34.085	17.878	8.272	5.055	54.175	31.960	54.175	31.960
P4.2 Q+M	1000	**4.45**	**3.21**	**8.180**	0.721		1.670		1.670		1.838		9.745		9.745	
P5.1 Q+M	1000	**15.93**	**14.45**	**31.350**	0.907	0.814	4.218	2.939	4.218	2.939	1.968	1.765	10.641	9.243	10.641	9.243
P5.2 Q+M	1000	**21.12**	**15.22**	**33.010**	0.721		1.660		1.660		1.563		7.844		7.844	
P6.1 Q+M	1000	**21.36**	**127.72**	**23.400**	5.979	4.278	73.797	27.124	73.797	50.460	1.096	3.796	4.616	23.268	4.616	23.268
P6.2 Q+M	1000	**14.3**	**36.85**	**92.910**	2.577		27.124		27.124		6.497		41.921		41.921	

Sample	ml	Q8(AUC)	Q9(AUC)	Q10(AUC)	AUC Q9/8	AVE.	X	AVE. X	µg/ml	AVE.	AUC Q10/8	AVE.	X	AVE. X	µg/ml	AVE.
P1.1 Q	1000	**26.83**	**95.45**	**50.490**	3.558	2.337	40.576	40.576	40.576	40.576	1.882	1.448	10.047	8.318	10.047	8.318
P1.2 Q	1000	**27.05**	**30.21**	**27.440**	1.117		7.095		7.095		1.014		4.056		4.056	
P2.1 Q	1000	**19.79**	**31.06**	**6.660**	1.569	1.284	13.304	13.304	13.304	13.304	0.337	3.267	-0.625	19.616	-0.625	19.616
P2.2 Q	1000	**16.68**	**16.67**	**103.390**	0.999		5.484		5.484		6.198		39.857		39.857	
P3.1 Q	1000	**7.62**	**12.64**	**10.930**	1.659	0.829	14.529	14.529	14.529	14.529	1.434	1.434	6.956	2.003	6.956	2.003
P3.2 Q	1000	**0**	**0**	**2.230**	0.000		-8.225		-8.225		0.000		-2.950		-2.950	
P4.1 Q	1000	**6.24**	**11.24**	**127.440**	1.801	2.641	16.484	39.512	16.484	39.512	20.423	23.867	138.094	161.875	138.094	167.314
P4.2 Q	1000	**3**	**10.44**	**81.930**	3.480		39.512		39.512		27.310		185.655		185.655	
P5.1 Q	1000	**13.04**	**37.9**	**23.220**	2.906	1.925	31.644	18.178	31.644	18.178	1.781	2.089	9.348	12.865	9.348	12.865
P5.2 Q	1000	**30.94**	**29.18**	**74.190**	0.943		4.712		4.712		2.398		13.610		13.610	
P6.1 Q	1000	**12.66**	**27.38**	**38.290**	2.163	1.398	21.442	21.442	21.442	21.442	3.024	2.125	17.938	13.116	17.938	13.116
P6.2 Q	1000	**5.96**	**3.78**	**7.300**	0.634		0.475		0.475		1.225		5.509		5.509	

Sample	mg	Q8(AUC)	Q9(AUC)	Q10(AUC)	AUC Q9/8	AVE.	X	AVE. X	µg/mg/WT	AVE.	AUC Q10/8	AVE.	X	AVE. X	µg/mg/WT	AVE.
	-	-	-	-	-	-	-	-	-	-	-	-	-	-	-	-
L1.1 C	251	**55.62**	**68.21**	**0**	1.2264	9.1382	8.5975	117.1278	0.0343	0.6619	0.000	0.835	-2.950	4.000	0.000	0.023
L1.2 C	175	**36.15**	**616.36**	**30.2**	17.0501		225.6580		1.2895		0.835		2.820		0.016	
L2.1 C	227	**26.16**	**363.17**	**38.52**	13.8826	18.1713	182.2091	241.0387	0.8027	0.8947	1.472	1.502	7.219	7.422	0.032	0.032
L2.2 C	234	**24.5**	**550.27**	**37.51**	22.4600		299.8683		1.2815		1.531		7.624		0.033	
L3.1 C	286	**16.61**	**673.51**	**49.78**	40.5485	31.6628	547.9954	426.1075	1.9161	0.9849	2.997	1.638	17.748	8.360	0.062	0.030
L3.2 C	340	**45.29**	**1031.58**	**12.6**	22.7772		304.2197		0.8948		0.278		-1.028		-0.003	
L4.1 C	383	**22.26**	**1062.64**	**13.9**	47.7376	29.3677	646.6124	394.6247	1.6883	1.1195	0.624	0.458	1.363	0.211	0.004	0.000
L4.2 C	259	**9.25**	**101.73**	**2.69**	10.9978		142.6370		0.5507		0.291		-0.941		-0.004	
L5.1 C	178	**12.62**	**322.94**	**18.7**	25.5895	31.5107	342.7975	424.0212	1.9258	1.9536	1.482	0.884	7.284	3.155	0.041	0.019
L5.2 C	255	**5.07**	**189.78**	**1.45**	37.4320		505.2449		1.9814		0.286		-0.974		-0.004	
L6.1 C	288	**21.37**	**278.63**	**18.19**	13.0384	13.0384	170.6279	190.5877	0.5925	0.6618	0.851	0.851	2.929	4.116	0.010	0.014
L6.2 C	302	**0**	**0**	**0**					0.0000		0.000	0.000	-2.950		-0.010	

Sample	mg	Q8(AUC)	Q9(AUC)	Q10(AUC)	AUC Q9/8	AVE.	X	AVE. X	µg/mg/WT	AVE.	AUC Q10/8	AVE.	X	AVE. X	µg/mg/WT	AVE.
L1.1 MP	222	**0**	**0**	**0.000**	0.000	2.599	-8.225	35.933	-0.037	0.147	0.000	0.120	-2.950	-1.276	0.000	-0.005
L1.2 MP	245	**54.91**	**142.72**	**6.590**	2.599		27.429		0.112		0.120		-2.121		-0.009	
L2.1 MP	416	**23.4**	**429.68**	**0.000**	18.362	31.319	243.660	421.391	0.586	0.648	0.000	2.335	-2.950	5.113	-0.007	0.020
L2.2 MP	275	**19.61**	**868.244**	**45.790**	44.276		599.122		2.179		2.335		13.176		0.048	
L3.1 MP	232	**33.42**	**354.46**	**33.220**	10.606	8.643	137.265	110.336	0.592	0.456	0.994	0.994	3.915	0.483	0.017	0.003
L3.2 MP	260	**14.53**	**97.06**	**0.000**	6.680		83.407		0.321		0.000		-2.950		-0.011	
L4.1 MP	293	**8.86**	**453.77**	**13.080**	51.216	48.247	694.321	653.599	2.370	2.063	1.476	0.973	7.246	3.771	0.025	0.013
L4.2 MP	349	**10.49**	**474.97**	**4.930**	45.278	41.146	612.877		1.756		0.470		0.296		0.001	
L5.1 MP	295	**7.74**	**286.48**	**3.870**	37.013		499.497	463.378	1.693	1.926	0.500	0.495	0.503	0.466	0.002	0.002
L5.2 MP	198	**6.91**	**219.37**	**3.380**	31.747	35.392	427.258		2.158		0.489		0.428		0.002	
L6.1 MP	260	**9.83**	**383.73**	**57.340**	39.037		527.257	394.823	2.028	1.013	5.833	4.078	37.335	25.214	0.144	0.095
L6.2 MP	286	**8.67**	**171.04**	**20.140**	19.728	9.864	262.390		0.917		2.323		13.093		0.046	

Sample	mg	Q8(AUC)	Q9(AUC)	Q10(AUC)	AUC Q9/8	AVE.	X	AVE. X	µg/mg/WT	AVE.	AUC Q10/8	AVE.	X	AVE. X	µg/mg/WT	AVE.
L1.1 Q+M	262	**48.95**	**204.29**	**3.930**	4.173	4.468	49.024	53.065	0.187	0.192	0.080	0.530	-2.395	0.711	-0.009	0.002
L1.2 Q+M	290	**51.6**	**245.75**	**50.560**	4.763		57.106		0.197		0.980		3.817		0.013	
L2.1 Q+M	244	**22.89**	**522.17**	**33.140**	22.812	26.679	304.699	357.746	1.249	1.247	1.448	3.071	7.049	18.257	0.029	0.059
L2.2 Q+M	330	**25.35**	**774.35**	**118.980**	30.546		410.792		1.245		4.693		29.464		0.089	
L3.1 Q+M	304	**17.33**	**480.18**	**34.650**	27.708	24.068	371.858	321.925	1.223	1.035	1.999	1.475	10.859	7.237	0.036	0.023
L3.2 Q+M	321	**33.45**	**683.31**	**31.800**	20.428		271.992		0.847		0.951		3.616		0.011	
L4.1 Q+M	249	**24.57**	**444.95**	**29.600**	18.109	14.904	240.190	196.225	0.965	1.067	1.205	0.890	5.370	3.199	0.022	0.013
L4.2 Q+M	257	**27.44**	**321.03**	**15.800**	11.699		152.260		0.592		0.576		1.027		0.004	
L5.1 Q+M	192	**14.99**	**159.43**	**15.360**	10.636	21.456	137.670	286.093	0.717	1.496	1.025	2.015	4.127	10.967	0.021	0.057
L5.2 Q+M	191	**3.52**	**113.611**	**10.580**	32.276		434.516		2.275		3.006		17.808		0.093	
L6.1 Q+M	290	**10.17**	**378.21**	**43.360**	37.189	29.639	501.909	398.339	1.731	1.467	4.264	3.103	26.495	18.479	0.091	0.067
L6.2 Q+M	245	**7.25**	**160.14**	**14.080**	22.088		294.769		1.203		1.942		10.462		0.043	

Sample	mg	Q8(AUC)	Q9(AUC)	Q10(AUC)	AUC Q9/8	AVE.	X	AVE. X	µg/mg/WT	AVE.	AUC Q10/8	AVE.	X	AVE. X	µg/mg/WT	AVE.
L1.1 Q	271	**52.66**	**267.17**	**13.710**	5.073	6.914	61.370	86.612	0.226	0.313	0.260	0.543	-1.152	0.800	-0.004	0.003
L1.2 Q	280	**39.52**	**345.95**	**32.620**	8.754		111.855		0.399		0.825		2.751		0.010	
L2.1 Q	278	**28.91**	**569.98**	**46.600**	19.716	32.215	262.223	433.679	0.943	2.639	1.612	1.543	8.182	7.703	0.029	0.029
L2.2 Q	250	**8.39**	**375.15**	**12.360**	44.714		605.135		2.421		1.473		7.224		0.029	
L3.1 Q	364	**26.33**	**614.81**	**63.340**	23.350	23.126	312.079	309.004	0.857	0.829	2.406	2.670	13.664	15.486	0.038	0.041
L3.2 Q	382	**30.95**	**708.81**	**90.790**	22.902		305.928		0.801		2.933		17.309		0.045	
L4.1 Q	330	**30.76**	**655.42**	**73.150**	21.308	16.977	284.060	224.656	0.861	0.683	2.378	1.548	13.474	7.744	0.041	0.023
L4.2 Q	327	**6.79**	**85.87**	**4.880**	12.647		165.253		0.505		0.719		2.014		0.006	
L5.1 Q	278	**10.69**	**158.13**	**19.910**	14.792	14.460	194.688	190.132	0.700	0.659	1.862	1.395	9.913	6.685	0.036	0.024
L5.2 Q	300	**11.63**	**164.31**	**10.790**	14.128		185.576		0.619		0.928		3.458		0.012	
L6.1 Q	270	**23.23**	**436.67**	**46.120**	18.798	26.828	249.631	359.781	0.925	1.713	1.985	2.639	10.761	15.279	0.040	0.053
L6.2 Q	300	**16.93**	**590.14**	**55.760**	34.858		469.932		1.566		3.294		19.796		0.066	

Sample	mg	Q8(AUC)	Q9(AUC)	Q10(AUC)	AUC Q9/8	AVE.	X	AVE. X	µg/mg/WT	AVE.	AUC Q10/8	AVE.	X	AVE. X	µg/mg/WT	AVE.
	-	-	-	-		-					-	-	-	-	-	-
B1.1 C	424	**21.69**	**743.51**	**139.07**	34.279	43.184	461.994	584.151	1.090	1.482	6.412	8.733	41.330	57.360	0.097	0.146
B1.2 C	377	**23.23**	**1210.04**	**256.78**	52.090		706.309		1.873		11.054		73.389		0.195	
B2.1 C	379	**44.47**	**928.21**	**167.69**	20.873	23.666	278.095	316.409	0.734	0.808	3.771	4.493	23.092	28.079	0.061	0.072
B2.2 C	402	**13.12**	**347.14**	**68.42**	26.459		354.722		0.882		5.215		33.065		0.082	
B3.1 C	354	**64.86**	**1590.05**	**258.44**	24.515	28.458	328.059	382.139	0.927	1.043	3.985	5.710	24.568	36.486	0.069	0.099
B3.2 C	376	**48.25**	**1563.3**	**358.78**	32.400		436.219		1.160		7.436		48.403		0.129	
B4.1 C	365	**42.64**	**706.67**	**93.39**	16.573	22.883	219.113	305.666	0.600	0.789	2.190	2.918	12.176	17.205	0.033	0.044
B4.2 C	401	**10.81**	**315.57**	**39.42**	29.192		392.220		0.978		3.647		22.234		0.055	
B5.1 C	370	**63.25**	**1837.38**	**309.2**	29.049	33.203	390.259	447.231	1.055	1.282	4.889	6.046	30.811	38.804	0.083	0.112
B5.2 C	334	**38.46**	**1436.71**	**277.04**	37.356		504.202		1.510		7.203		46.797		0.140	
B6.1 C	417	**52.76**	**2039.1**	**335.19**	38.649	37.686	521.934	508.728	1.252	1.238	6.353	7.264	40.925	47.216	0.098	0.115
B6.2 C	405	**21.17**	**777.43**	**173.06**	36.723		495.523		1.224		8.175		53.506		0.132	

Sample	mg	Q8(AUC)	Q9(AUC)	Q10(AUC)	AUC Q9/8	AVE.	X	AVE. X	µg/mg/WT	AVE.	AUC Q10/8	AVE.	X	AVE. X	µg/mg/WT	AVE.
B1.1 MP	420	**9.64**	**842.72**	**168.73**	87.419	84.745	1190.939	1154.262	2.836	1.100	17.503	18.116	117.928	122.161	0.281	0.110
B1.2 MP	357	**19.43**	**1594.65**	**363.9**	82.072		1117.585		3.130		18.729		126.393		0.354	
B2.1 MP	426	**82.23**	**2279.53**	**463.58**	27.721	32.016	372.041	430.947	0.873	1.037	5.638	6.229	35.984	40.069	0.084	0.096
B2.2 MP	408	**32.92**	**1195.32**	**224.53**	36.310		489.852		1.201		6.820		44.153		0.108	
B3.1 MP	383	**44.14**	**1246.12**	**241.17**	28.231	32.623	379.033	439.273	0.990	1.068	5.464	7.022	34.784	45.545	0.091	0.110
B3.2 MP	436	**54.33**	**2010.98**	**466.16**	37.014		499.514		1.146		8.580		56.306		0.129	
B4.1 MP	373	**46.19**	**1170.65**	**177.2**	25.344	23.883	339.433	319.387	0.910	0.884	3.836	3.624	23.544	22.075	0.063	0.061
B4.2 MP	349	**25**	**560.54**	**85.27**	22.422		299.342		0.858		3.411		20.606		0.059	
B5.1 MP	410	**4.78**	**81.24**	**10.12**	16.996	26.811	224.914	359.547	0.549	0.881	2.117	3.880	11.672	23.846	0.028	0.058
B5.2 MP	407	**21.81**	**798.8**	**123.07**	36.625		494.181		1.214		5.643		36.020		0.089	
B6.1 MP	411	**51.13**	**2211.98**	**424.61**	43.262	35.971	585.216	485.206	1.424	1.155	8.305	7.211	54.402	46.850	0.132	0.111
B6.2 MP	435	**32.53**	**932.97**	**199**	28.680		385.195		0.886		6.117		39.298		0.090	

Sample	mg	Q8(AUC)	Q9(AUC)	Q10(AUC)	AUC Q9/8	AVE.	X	AVE. X	µg/mg/WT	AVE.	AUC Q10/8	AVE.	X	AVE. X	µg/mg/WT	AVE.
B1.1 Q+M	415	**13.05**	**990.77**	**229.960**	75.921	37.961	1033.216	512.496	2.490	1.235	17.621	8.811	118.746	57.898	0.286	0.140
B1.2 Q+M	414	**0**	**0**	**0.000**	0.000		-8.225		-0.020		0.000		-2.950		-0.007	
B2.1 Q+M	370	**38.18**	**1847.9**	**347.700**	48.400	43.069	655.694	582.572	1.772	1.523	9.107	8.157	59.943	53.382	0.162	0.140
B2.2 Q+M	400	**6.77**	**255.49**	**48.790**	37.739		509.451		1.274		7.207		46.821		0.117	
B3.1 Q+M	388	**86.25**	**2441.63**	**497.800**	28.309	24.621	380.098	329.517	0.980	0.938	5.772	5.302	36.909	33.666	0.095	0.096
B3.2 Q+M	311	**29.98**	**627.6**	**144.870**	20.934		278.935		0.897		4.832		30.422		0.098	
B4.1 Q+M	410	**39.28**	**1697.98**	**265.620**	43.228	40.739	584.746	550.603	1.426	1.404	6.762	6.228	43.751	40.063	0.107	0.102
B4.2 Q+M	374	**16.19**	**619.26**	**92.190**	38.250		516.460		1.381		5.694		36.375		0.097	
B5.1 Q+M	440	**16.32**	**296.27**	**39.510**	18.154	37.705	240.798	508.985	0.547	1.245	2.421	6.275	13.770	40.386	0.031	0.099
B5.2 Q+M	400	**16.13**	**923.53**	**163.380**	57.255		777.172		1.943		10.129		67.002		0.168	
B6.1 Q+M	290	**80.4**	**2206.1**	**416.760**	27.439	26.597	368.168	356.615	1.270	1.339	5.184	5.325	32.849	33.826	0.113	0.128
B6.2 Q+M	245	**39.7**	**1022.46**	**217.020**	25.755		345.063		1.408		5.466		34.802		0.142	

Sample	mg	Q8(AUC)	Q9(AUC)	Q10(AUC)	AUC Q9/8	AVE.	X	AVE. X	µg/mg/WT	AVE.	AUC Q10/8	AVE.	X	AVE. X	µg/mg/WT	AVE.
B1.1 Q	425	**26.43**	**1079**	**213.19**	40.825	46.874	551.786	634.769	1.298	1.520	8.066	9.273	52.756	61.090	0.124	0.146
B1.2 Q	412	**15.59**	**825.08**	**163.38**	52.924		717.751		1.742		10.480		69.425		0.169	
B2.1 Q	369	**12.18**	**331.29**	**70.59**	27.200	36.671	364.882	494.807	0.989	1.226	5.796	8.260	37.075	54.092	0.100	0.134
B2.2 Q	427	**29.52**	**1362.13**	**316.56**	46.143		624.733		1.463		10.724		71.108		0.167	
B3.1 Q	410	**69.7**	**1674.68**	**369.89**	24.027	30.559	321.363	410.963	0.784	1.044	5.307	6.320	33.700	40.697	0.082	0.103
B3.2 Q	384	**58.15**	**2156.82**	**426.42**	37.091		500.563		1.304		7.333		47.693		0.124	
B4.1 Q	423	**15.29**	**505.05**	**88.94**	33.031	27.759	444.881	372.562	1.052	0.882	5.817	4.423	37.222	27.598	0.088	0.065
B4.2 Q	422	**30.18**	**678.67**	**91.44**	22.487		300.244		0.711		3.030		17.975		0.043	
B5.1 Q	397	**13.01**	**778.87**	**157.22**	59.867	36.127	812.996	487.338	2.048	2.228	12.085	7.505	80.507	48.879	0.203	0.219
B5.2 Q	436	**32.25**	**399.45**	**94.33**	12.386		161.680		0.371		2.925		17.250		0.040	
B6.1 Q	416	**60.4**	**1428.31**	**279.36**	23.648	30.753	316.158	413.629	0.760	1.071	4.625	6.526	28.992	42.120	0.070	0.110
B6.2 Q	370	**40.65**	**1538.96**	**342.56**	37.859		511.100		1.381		8.427		55.248		0.149	

Sample	mg	Q8(AUC)	Q9(AUC)	Q10(AUC)	AUC Q9/8	AVE.	X	AVE. X	µg/mg/WT	AVE.	AUC Q10/8	AVE.	X	AVE. X	µg/mg/WT	AVE.
	-	-	-	-	-	-	-	-	-	-	-	-	-	-	-	-
H1.1 C	185	**16.68**	**139.95**	**5.580**	8.390	6.221	106.868	77.109	0.578	0.475	0.335	0.291	-0.639	-0.939	-0.003	0.002
H1.2 C	127	**35.98**	**145.77**	**8.910**	4.051		47.350		0.373		0.248		-1.239		-0.010	
H2.1 C	169	**21.89**	**284.19**	**11.800**	12.983	14.277	169.863	187.614	1.005	1.003	0.539	0.550	0.773	0.848	0.005	0.005
H2.2 C	205	**97.96**	**1525.3**	**54.920**	15.571		205.364		1.002		0.561		0.922		0.004	
H3.1 C	184	**56.47**	**454.09**	**16.690**	8.041	6.945	102.080	87.046	0.555	0.443	0.296	0.352	-0.908	-0.516	-0.005	-0.003
H3.2 C	217	**67.76**	**396.34**	**27.730**	5.849		72.011		0.332		0.409		-0.123		-0.001	
H4.1 C	129	**86.91**	**1809.66**	**125.490**	20.822	17.951	277.402	238.017	2.150	1.688	1.444	1.263	7.022	5.776	0.054	0.041
H4.2 C	162	**72.58**	**1094.5**	**78.600**	15.080		198.633		1.226		1.083		4.529		0.028	
H5.1 C	159	**91.77**	**1722.57**	**77.410**	18.771	13.903	249.258	182.485	1.568	1.095	0.844	0.700	2.876	1.882	0.018	0.011
H5.2 C	186	**52.9**	**477.95**	**29.400**	9.035		115.712		0.622		0.556		0.889		0.005	
H6.1 C	171	**60.77**	**767.7**	**40.020**	12.633	9.434	165.066	121.191	0.965	0.732	0.659	0.476	1.598	0.340	0.009	0.002
H6.2 C	155	**45.77**	**285.42**	**13.460**	6.236		77.316		0.499		0.294		-0.919		-0.006	

Sample	mg	Q8(AUC)	Q9(AUC)	Q10(AUC)	AUC Q9/8	AVE.	X	AVE. X	µg/mg/WT	AVE.	AUC Q10/8	AVE.	X	AVE. X	µg/mg/WT	AVE.
H1.1 MP	172	**42.19**	**259.49**	**10.170**	6.151	7.563	76.144	95.525	0.443	0.632	0.241	0.373	-1.285	-0.375	-0.007	-0.002
H1.2 MP	140	**59.31**	**532.38**	**29.930**	8.976		114.906		0.821		0.505		0.535		0.004	
H2.1 MP	138	**83.57**	**712.38**	**41.860**	8.524	9.460	108.707	121.543	0.788	0.816	0.501	0.580	0.510	1.054	0.004	0.007
H2.2 MP	159	**83.73**	**870.44**	**55.140**	10.396		134.379		0.845		0.659		1.598		0.010	
H3.1 MP	136	**61.75**	**703.59**	**34.610**	11.394	12.196	148.074	159.074	1.089	1.050	0.560	0.681	0.921	1.755	0.007	0.011
H3.2 MP	181	**71.07**	**923.77**	**56.990**	12.998		170.074		0.940		0.802		2.588		0.014	
H4.1 MP	133	**51.5**	**733.35**	**50.830**	14.240	16.461	187.108	217.582	1.407	1.346	0.987	1.763	3.867	9.225	0.029	0.038
H4.2 MP	193	**25.41**	**474.73**	**64.510**	18.683		248.055		1.285		2.539		14.583		0.076	
H5.1 MP	158	**68.5**	**1086.24**	**37.410**	15.858	12.852	209.299	168.068	1.325	1.027	0.546	0.567	0.822	0.964	0.005	0.006
H5.2 MP	174	**36.75**	**361.84**	**21.580**	9.846		126.837		0.729		0.587		1.106		0.006	
H6.1 MP	179	**46.36**	**306.68**	**19.680**	6.615	10.006	82.518	129.027	0.461	0.747	0.425	0.727	-0.018	2.069	0.000	0.005
H6.2 MP	170	**51.77**	**693.52**	**53.270**	13.396		175.536		1.033		1.029		4.157		0.024	

Sample	mg	Q8(AUC)	Q9(AUC)	Q10(AUC)	AUC Q9/8	AVE.	X	AVE. X	µg/mg/WT	AVE.	AUC Q10/8	AVE.	X	AVE. X	µg/mg/WT	AVE.
H1.1 Q+M	170	**39.9**	**314**	**18.25**	7.869674	8.6848	99.7267	110.909	0.586627	0.7143	0.457	0.426	0.209	-0.006	0.001	0.000
H1.2 Q+M	145	**58.06**	**551.57**	**22.93**	9.5		122.091		0.842004		0.395		-0.222		-0.002	
H2.1 Q+M	169	**135.08**	**1860.8**	**84.37**	13.77554	12.243	180.74	159.714	1.069467	1.1924	0.625	0.628	1.364	1.389	0.008	0.008
H2.2 Q+M	195	**75.15**	**804.85**	**47.48**	10.70991		138.687		0.711218		0.632		1.414		0.007	
H3.1 Q+M	174	**56.68**	**555.96**	**26.09**	9.808751	12.244	126.326	159.725	0.72601	1.6036	0.460	0.693	0.229	1.839	0.001	0.035
H3.2 Q+M	134	**72.36**	**1062.13**	**67.04**	14.67841		193.125		1.441231		0.926		3.449		0.026	
H4.1 Q+M	170	**52.94**	**587.65**	**33.42**	11.1003	11.096	144.043	143.983	0.847309	0.7985	0.631	0.576	1.410	1.032	0.008	0.015
H4.2 Q+M	192	**50.53**	**560.46**	**26.36**	11.09163		143.924		0.749602		0.522		0.653		0.003	
H5.1 Q+M	182	**59.44**	**624.76**	**31.56**	10.51077	8.4528	135.956	107.726	0.747009	0.8414	0.531	0.414	0.717	-0.087	0.004	0.010
H5.2 Q+M	158	**44.73**	**286.04**	**13.33**	6.394813		79.4954		0.503135		0.298		-0.892		-0.006	
H6.1 Q+M	174	**54.44**	**566.17**	**32.73**	10.39989	8.0923	134.435	102.78	0.772613	0.8707	0.601	0.528	1.202	0.693	0.007	0.013
H6.2 Q+M	210	**40.59**	**234.8**	**18.42**	5.784676		71.1259		0.338695		0.454		0.184		0.001	

Sample	mg	Q8(AUC)	Q9(AUC)	Q10(AUC)	AUC Q9/8	AVE.	X	AVE. X	µg/mg/WT	AVE.	AUC Q10/8	AVE.	X	AVE. X	µg/mg/WT	AVE.
H1.1 Q	171	**50.61**	**411.12**	**26.060**	8.123	6.695	103.206	83.616	0.604	0.497	0.515	0.397	0.606	-0.211	0.004	-0.001
H1.2 Q	164	**21.75**	**114.56**	**6.050**	5.267		64.026		0.390		0.278		-1.029		-0.006	
H2.1 Q	142	**85.63**	**746.33**	**35.950**	8.716	12.955	111.333	169.489	0.784	1.727	0.420	0.719	-0.050	2.013	0.000	0.037
H2.2 Q	146	**101.64**	**1747.69**	**103.400**	17.195		227.645		1.559		1.017		4.076		0.028	
H3.1 Q	147	**48.27**	**253.81**	**11.280**	5.258	7.711	63.903	97.545	0.435	0.491	0.234	0.317	-1.336	-0.758	-0.009	-0.005
H3.2 Q	240	**60.82**	**618.12**	**24.380**	10.163		131.187		0.547		0.401		-0.181		-0.001	
H4.1 Q	173	**57.91**	**577.24**	**37.970**	9.968	13.982	128.509	183.570	0.743	1.483	0.656	1.013	1.579	4.045	0.009	0.023
H4.2 Q	178	**75.39**	**1356.71**	**103.280**	17.996		238.632		1.341		1.370		6.511		0.037	
H5.1 Q	169	**52.88**	**316.1**	**18.600**	5.978	10.248	73.773	132.350	0.437	1.174	0.352	0.473	-0.520	0.315	-0.003	0.002
H5.2 Q	181	**69.58**	**1010.17**	**41.300**	14.518		190.926		1.055		0.594		1.150		0.006	
H6.1 Q	182	**53.53**	**642.96**	**43.630**	12.011	8.391	156.538	106.875	0.860	0.964	0.815	0.520	2.679	0.639	0.015	0.021
H6.2 Q	140	**44.33**	**211.47**	**9.940**	4.770		57.212		0.409		0.224		-1.401		-0.010	

APPENDIX B.2: RAW DATA FOR SCGE

Table 2.1 Mouse 15µl blood cells control for day 1.

	Average Distance out of 10 comets in µm	Average Distance out of 10 comets in µm	Average Distance out of 10 comets in µm	Average Distance out of 10 comets in µm	Average Distance out of 10 comets in µm	Final Average
Total Length	95.3	96.3	90.0	87.3	81.9	90.2
Head Length	18.1	14.7	21.8	21.7	16.7	18.6
Tail Length	77.3	81.6	68.2	65.6	65.2	71.6
Tail Intensity	60.7	57.3	60.3	52.5	54.2	57.0

Table 2.2 Mouse 10µl brain cells control for day 1.

	Average Distance out of 10 comets in µm	Average Distance out of 10 comets in µm	Average Distance out of 10 comets in µm	Average Distance out of 10 comets in µm	Average Distance out of 10 comets in µm	Final Average
Total Length	91.0	90.9	88.6	90.6	84.3	89.1
Head Length	22.4	14.3	16.8	19.1	17.6	18.0
Tail Length	68.6	76.6	71.8	71.4	66.7	71.0
Tail Intensity	73.8	84.2	65.7	70.7	52.6	69.4

Table 2.3 Mouse 10µl heart cells control for day 1.

	Average Distance out of 10 comets in µm	Average Distance out of 10 comets in µm	Average Distance out of 10 comets in µm	Average Distance out of 10 comets in µm	Average Distance out of 10 comets in µm	Final Average
Total Length	106.0	105.4	106.7	105.4	107.4	106.2
Head Length	20.4	16.1	17.4	20.1	22.1	19.2
Tail Length	85.6	89.3	89.3	85.3	85.3	87.0
Tail Intensity	46.0	49.7	43.5	31.9	33.9	41.0

APPENDIX B.1: RAW DATA FOR SCGE

CONTROL GROUPS

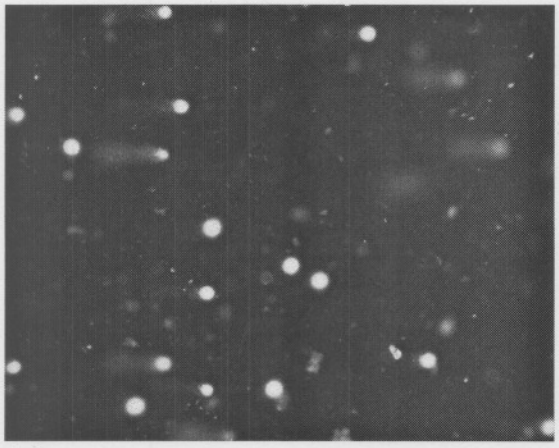

Figure 1.1. Control blood cells 10×

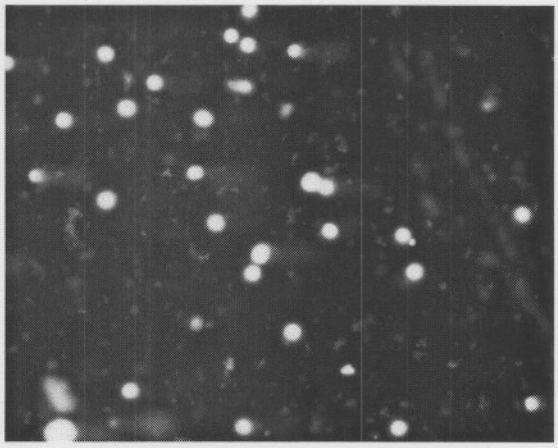

Figure 1.2. Control brain cells 10×

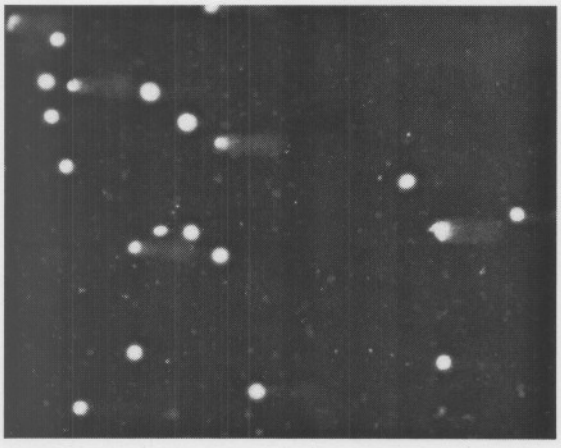

Figure 1.3. Control heart cells10×

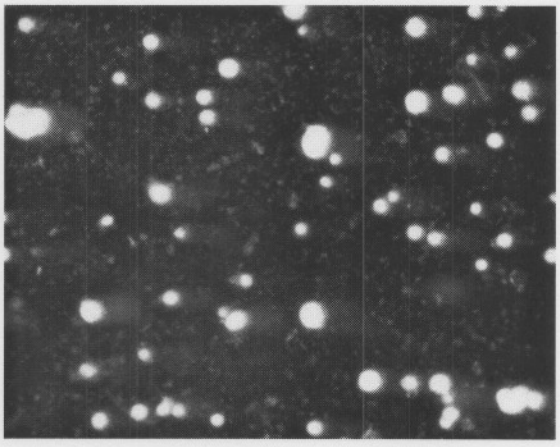

Figure 1.4. Control liver cells 10×

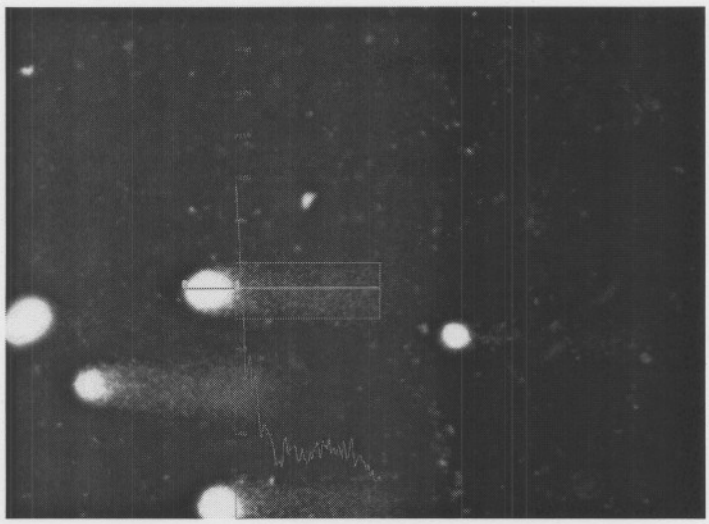

Figure 1.5. Control heart profile of the total length, head, tail and intensity 20×.*cL*=(comet length)

Q_{10} GROUPS

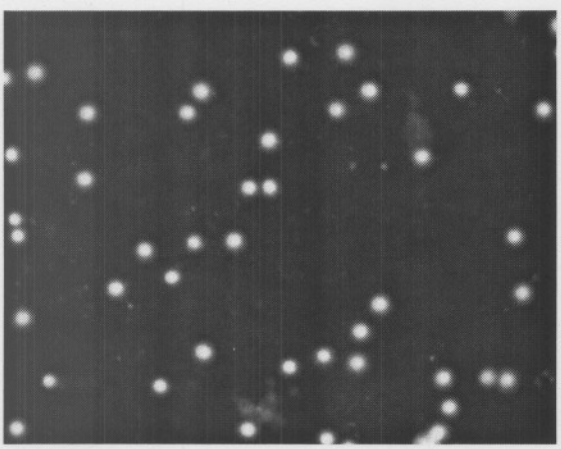

Figure 1.6. Q_{10} blood cells 10×

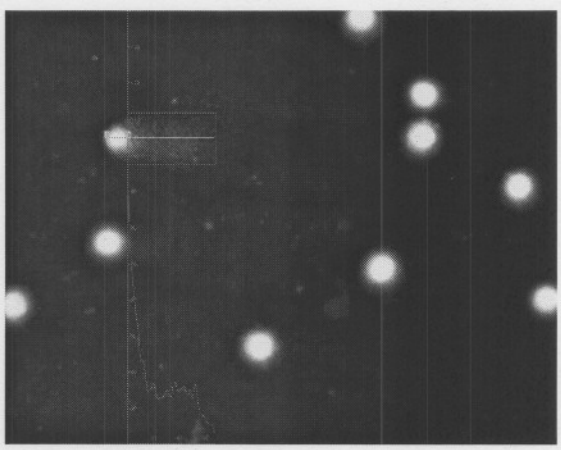

Figure 1.7. Q_{10} blood *cL* profile 20×

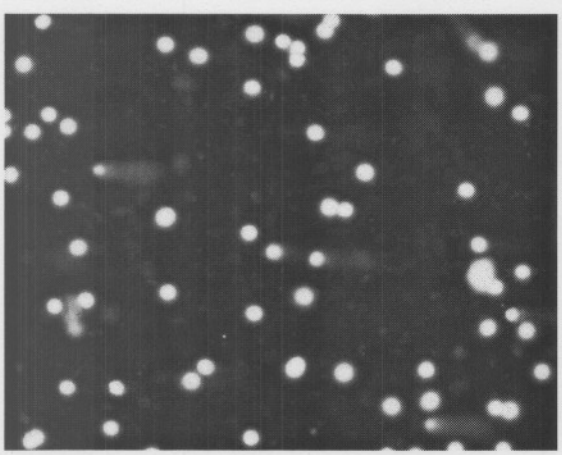

Figure 1.8. Q_{10} brain cells 10×

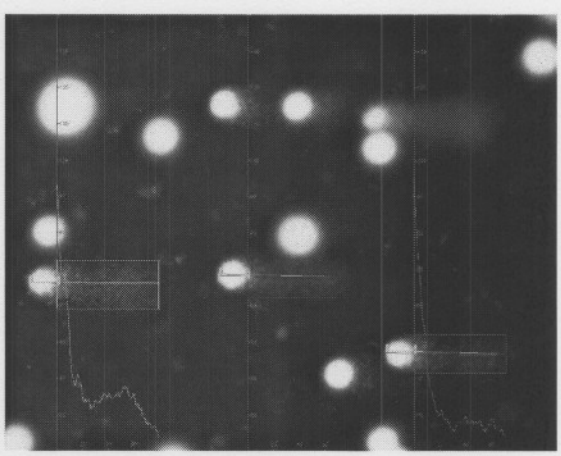

Figure 1.9. Q_{10} brain *cL* profile 20×

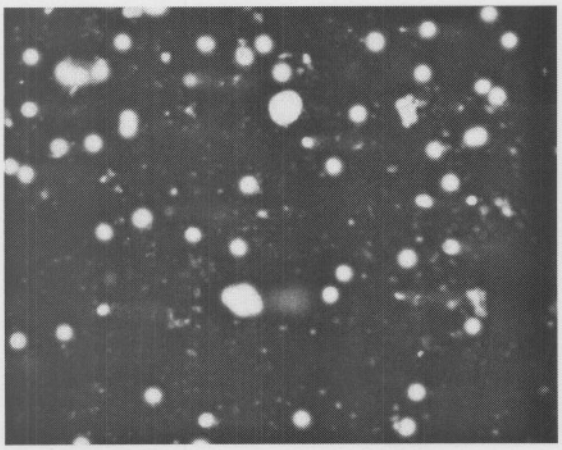

Figure 1.10. Q_{10} heart cells 10×

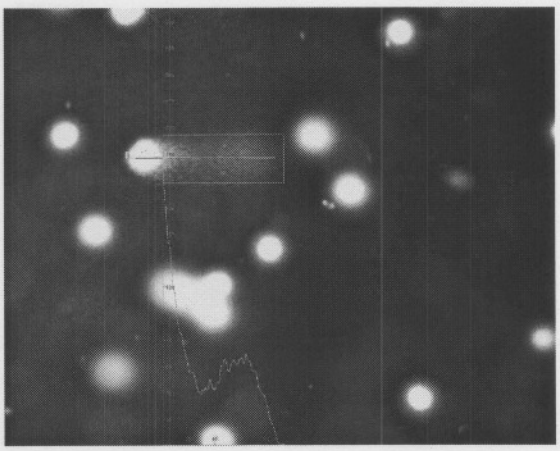

Figure 1.11. Q_{10} heart *cL* profile 20x

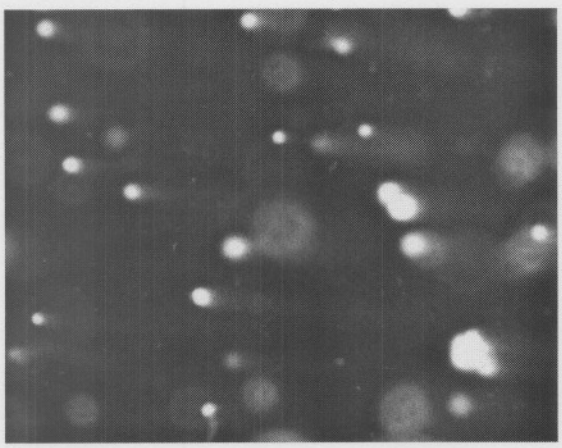

Figure 1.12. Q_{10} liver cells 10×

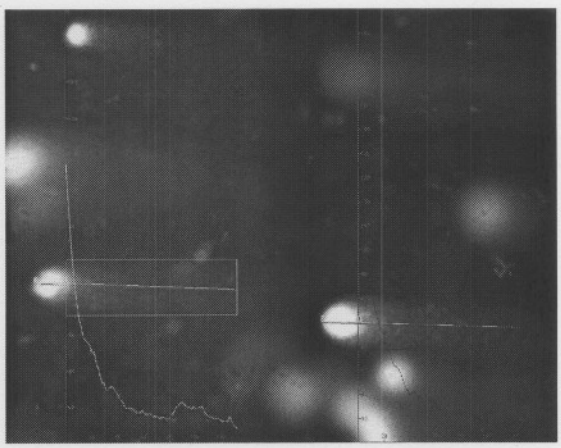

Figure 1.13. Q_{10} Liver *cL* profile 20×

Q_{10}/MPTP GROUPS

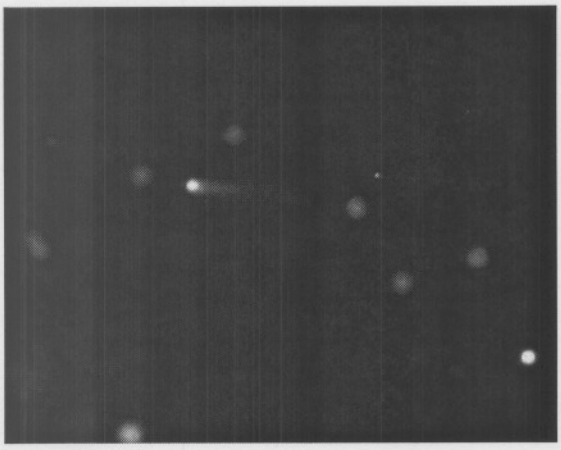

Figure 1.14. Q_{10}/MPTP blood cells 10×

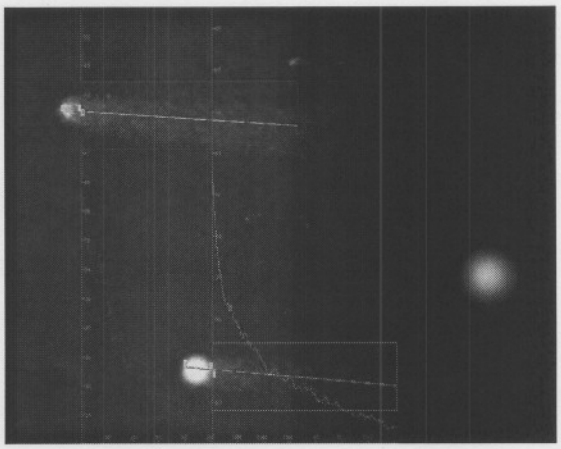

Figure 1.15. Q_{10}/MPTP blood *cL* profile 20×

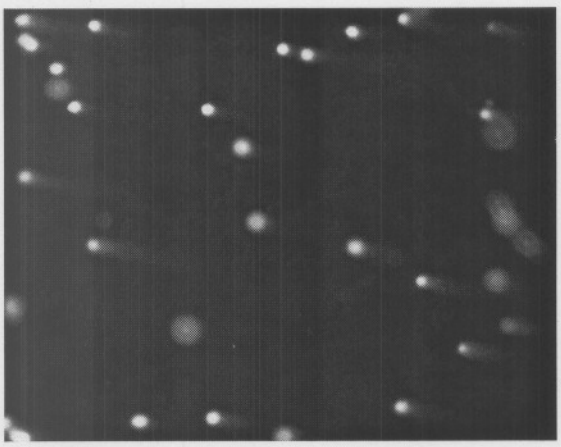

Figure 1.16. Q_{10}/MPTP brain cells 10x

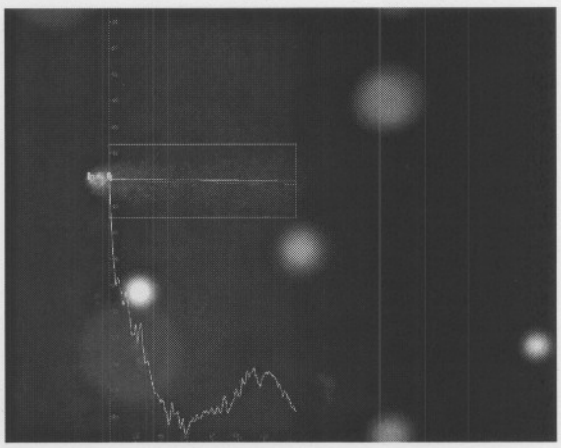

Figure 1.17. Q_{10}/MPTP brain *cL* 10× profile 20×

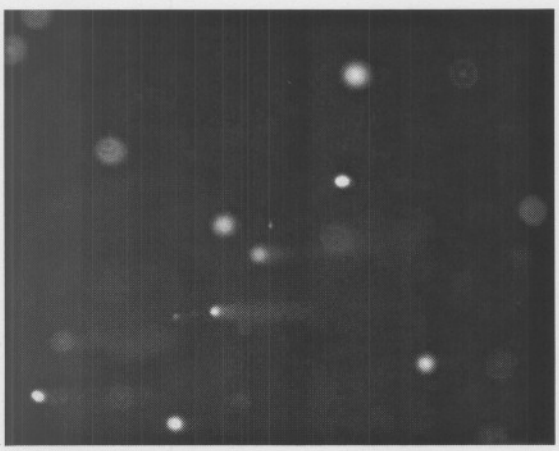

Figure 1.18. Q_{10}/MPTP heart cells 10×

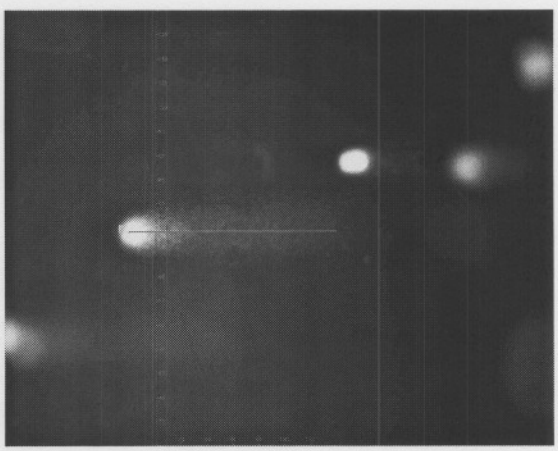

Figure 1.19. Q_{10}/MPTP heart *cL* profile 20×

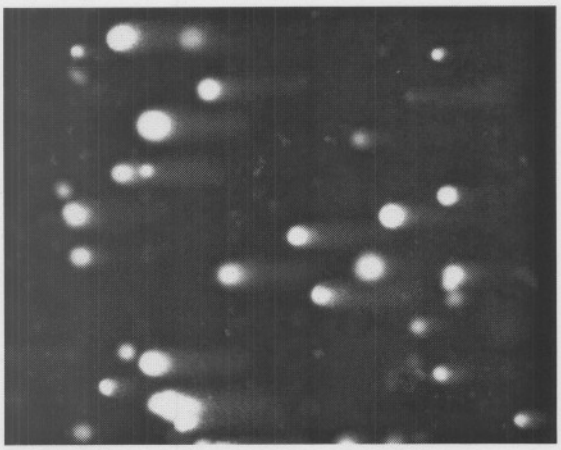

Figure 1.20. Q_{10}/MPTP liver cells 10×

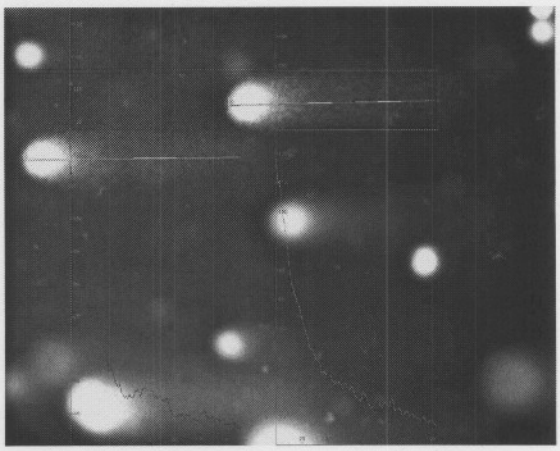

Figure 1.21. Q_{10}/MPTP liver *cL* profile 20×

MPTP GROUPS

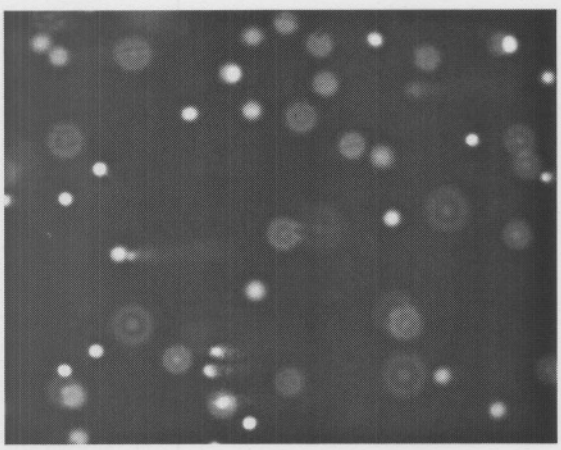

Figure 1.22. MPTP brain cells 10×

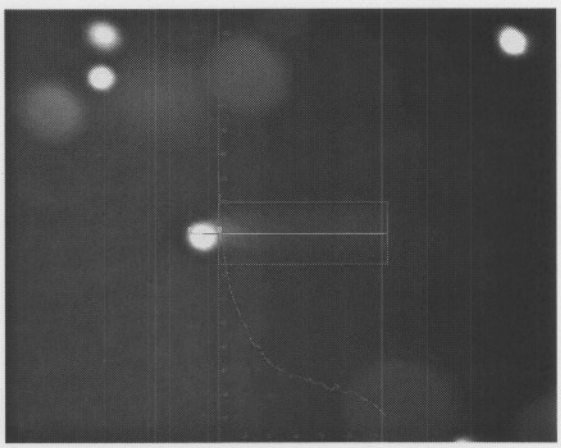

Figure 1.23. MPTP brain *cL* profile 20×

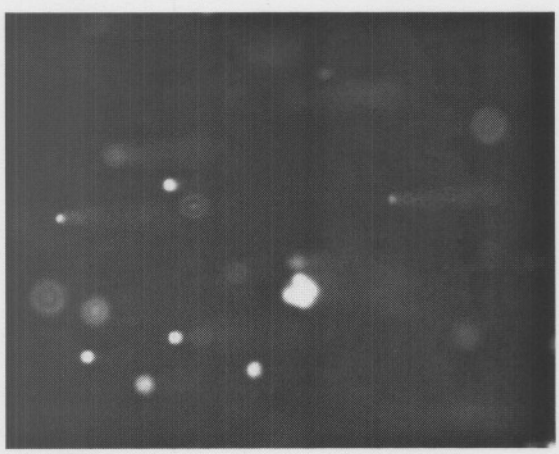

Figure 1.24. MPTP heart cells 10×

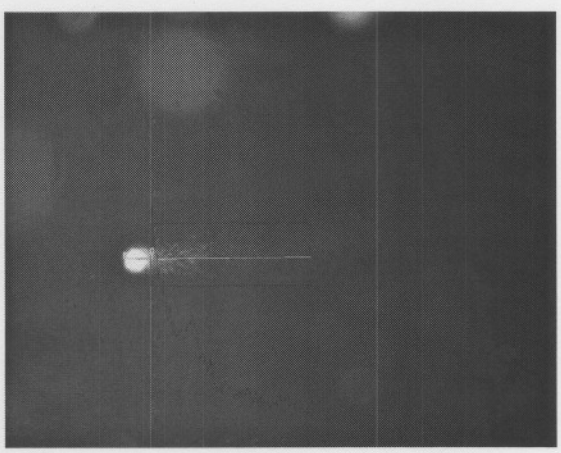

Figure 1.23. MPTP heart *cL* profile 20×

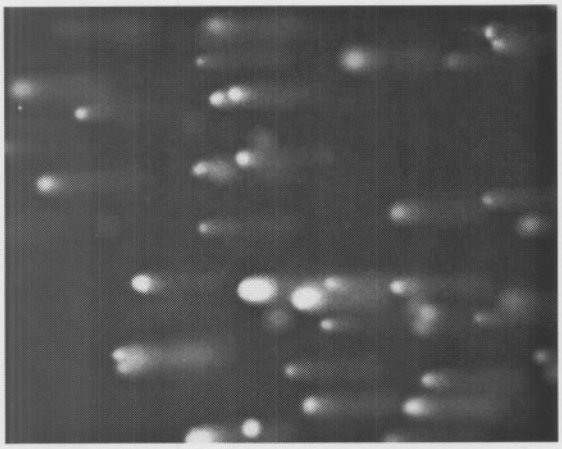

Figure 1.26. MPTP liver cells 10×

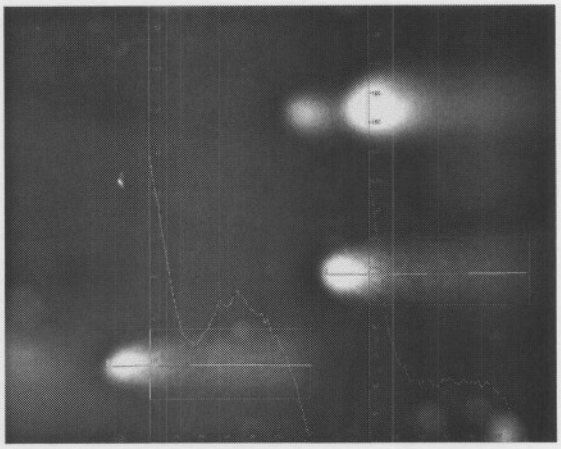

Figure 1.27. MPTP liver *cL* profile 20×

Table 2.4 Mouse 5µl liver cells control for day 1.

	Average Distance out of 10 comets in µm	Average Distance out of 10 comets in µm	Average Distance out of 10 comets in µm	Average Distance out of 10 comets in µm	Average Distance out of 10 comets in µm	Final Average
Total Length	150.3	147.3	154.2	157.5	148.0	151.4
Head Length	35.8	24.1	29.3	24.3	27.5	28.2
Tail Length	114.4	123.2	125.0	133.2	120.5	123.3
Tail Intensity	47.6	55.3	44.2	46.2	47.9	48.2

Table 2.5 Mouse 15µl blood cells Q_{10} exposure for day 1.

	Average Distance out of 10 comets in µm	Average Distance out of 10 comets in µm	Average Distance out of 10 comets in µm	Average Distance out of 10 comets in µm	Average Distance out of 10 comets in µm	Final Average
Total Length	75.6	64.2	111.8	92.5	102.1	89.3
Head Length	19.1	21.7	24.9	21.1	26.1	22.6
Tail Length	56.5	42.5	86.9	71.4	76.0	66.7
Tail Intensity	33.0	49.3	46.1	54.9	36.2	43.9

Table 2.6 Mouse 10µl brain cells Q_{10} exposure for day 1.

	Average Distance out of 10 comets in µm	Average Distance out of 10 comets in µm	Average Distance out of 10 comets in µm	Average Distance out of 10 comets in µm	Average Distance out of 10 comets in µm	Final Average
Total Length	96.0	96.7	102.7	95.0	88.0	95.7
Head Length	20.7	26.1	21.1	23.8	21.8	22.7
Tail Length	75.3	70.6	81.6	71.2	66.2	73.0
Tail Intensity	45.6	52.2	55.1	35.2	33.6	44.3

Table 2.7 Mouse 10µl heart cells Q_{10} exposure for day 1.

	Average Distance out of 10 comets in µm	Average Distance out of 10 comets in µm	Average Distance out of 10 comets in µm	Average Distance out of 10 comets in µm	Average Distance out of 10 comets in µm	Final Average
Total Length	107.8	110.4	85.7	98.1	96.1	99.6
Head Length	24.1	29.1	14.1	16.7	19.1	20.6
Tail Length	83.7	81.3	71.6	81.4	76.9	79.0
Tail Intensity	37.3	67.7	34.5	46.7	30.4	43.3

Table 2.8 Mouse 5µl liver cells Q_{10} exposure for day 1.

	Average Distance out of 10 comets in µm	Average Distance out of 10 comets in µm	Average Distance out of 10 comets in µm	Average Distance out of 10 comets in µm	Average Distance out of 10 comets in µm	Final Average
Total Length	140.2	135.8	162.6	172.3	151.4	152.4
Head Length	39.5	36.2	34.8	38.5	22.4	34.3
Tail Length	100.7	99.7	127.8	133.8	128.9	118.2
Tail Intensity	47.8	57.2	39.5	40.7	43.3	45.7

Table 2.9 Mouse 15µl blood cells Q_{10}/MPTP exposure for day 1.

	Average Distance out of 10 comets in µm	Average Distance out of 10 comets in µm	Average Distance out of 10 comets in µm	Average Distance out of 10 comets in µm	Average Distance out of 10 comets in µm	Final Average
Total Length	176.9	118.6	118.4	189.7	145.7	149.9
Head Length	17.7	19.1	23.5	16.4	18.1	19.0
Tail Length	159.1	99.5	94.9	173.3	127.6	130.9
Tail Intensity	38.4	26.4	24.8	28.9	24.5	28.6

Table 2.10 Mouse 10µl brain cells Q_{10}/MPTP exposure for day 1.

	Average Distance out of 10 comets in µm	Average Distance out of 10 comets in µm	Average Distance out of 10 comets in µm	Average Distance out of 10 comets in µm	Average Distance out of 10 comets in µm	Final Average
Total Length	153.8	145.4	144.5	106.4	159.2	141.8
Head Length	15.8	17.7	16.7	15.4	15.4	16.2
Tail Length	137.9	127.7	127.7	91.0	143.8	125.6
Tail Intensity	33.7	23.6	29.6	26.8	26.8	28.1

Table 2.11 Mouse 10µl heart cells Q_{10}/MPTP exposure for day 1.

	Average Distance out of 10 comets in µm	Average Distance out of 10 comets in µm	Average Distance out of 10 comets in µm	Average Distance out of 10 comets in µm	Average Distance out of 10 comets in µm	Final Average
Total Length	151.6	150.2	152.8	150.5	168.6	154.7
Head Length	17.7	13.4	16.1	14.7	28.4	18.1
Tail Length	133.8	136.8	136.8	135.8	140.1	136.7
Tail Intensity	20.3	20.5	28.7	38.4	47.2	31.0

Table 2.12 Mouse 5µl liver cells Q_{10}/MPTP exposure for day 1.

	Average Distance out of 10 comets in µm	Average Distance out of 10 comets in µm	Average Distance out of 10 comets in µm	Average Distance out of 10 comets in µm	Average Distance out of 10 comets in µm	Final Average
Total Length	151.5	138.2	153.2	160.6	169.2	154.5
Head Length	38.1	32.8	32.1	35.1	34.8	34.6
Tail Length	113.4	105.4	121.1	125.5	134.5	119.9
Tail Intensity	46.2	40.8	55.3	50.2	45.3	47.6

Table 2.13 Mouse 15µl blood cells MPTP exposure for day 1.

	Average Distance out of 10 comets in µm	Average Distance out of 10 comets in µm	Average Distance out of 10 comets in µm	Average Distance out of 10 comets in µm	Average Distance out of 10 comets in µm	Final Average
Total Length	176.9	156.3	118.4	189.7	145.7	157.4
Head Length	17.7	19.1	23.5	17.3	18.1	19.1
Tail Length	159.1	137.2	94.9	172.4	127.6	138.3
Tail Intensity	38.4	26.4	24.8	27.3	24.5	28.3

Table 2.14 Mouse 10µl brain cells MPTP exposure for day 1.

	Average Distance out of 10 comets in µm	Average Distance out of 10 comets in µm	Average Distance out of 10 comets in µm	Average Distance out of 10 comets in µm	Average Distance out of 10 comets in µm	Final Average
Total Length	154.2	133.1	151.9	142.5	135.1	143.4
Head Length	23.1	16.7	17.4	15.4	14.7	17.5
Tail Length	131.1	116.4	134.5	127.1	120.4	125.9
Tail Intensity	41.3	44.8	38.3	44.8	47.0	43.2

Table 2.15 Mouse 10µl heart cells MPTP exposure for day 1.

	Average Distance out of 10 comets in µm	Average Distance out of 10 comets in µm	Average Distance out of 10 comets in µm	Average Distance out of 10 comets in µm	Average Distance out of 10 comets in µm	Final Average
Total Length	146.8	174.3	167.9	160.5	167.3	163.4
Head Length	20.4	18.1	16.7	21.7	14.1	18.2
Tail Length	126.4	156.2	151.2	138.8	153.2	145.2
Tail Intensity	61.1	43.2	60.9	49.0	38.0	50.4

Table 2.16 Mouse 5µl liver cells MPTP exposure for day 1.

	Average Distance out of 10 comets in µm	Average Distance out of 10 comets in µm	Average Distance out of 10 comets in µm	Average Distance out of 10 comets in µm	Average Distance out of 10 comets in µm	Final Average
Total Length	156.2	143.5	152.9	146.2	157.9	151.3
Head Length	35.5	25.8	29.1	26.1	33.4	30.0
Tail Length	120.7	117.8	123.8	120.1	124.4	121.3
Tail Intensity	73.8	79.7	98.4	79.3	64.8	79.2

Table 2.17 Mouse 15µl blood cells control for day 2.

	Average Distance out of 10 comets in µm	Average Distance out of 10 comets in µm	Average Distance out of 10 comets in µm	Average Distance out of 10 comets in µm	Average Distance out of 10 comets in µm	Final Average
Total Length	80.3	77.4	88.4	86.4	82.9	83.1
Head Length	20.9	21.5	19.1	20.4	21.1	20.6
Tail Length	59.4	55.9	69.3	66.0	61.9	62.5
Tail Intensity	61.1	66.1	74.6	64.9	65.8	66.5

Table 2.18 Mouse 10µl brain cells control for day 2.

	Average Distance out of 10 comets in µm	Average Distance out of 10 comets in µm	Average Distance out of 10 comets in µm	Average Distance out of 10 comets in µm	Average Distance out of 10 comets in µm	Final Average
Total Length	80.6	103.5	80.4	77.6	81.3	84.7
Head Length	20.4	16.1	17.2	16.6	19.3	17.9
Tail Length	60.2	87.4	63.1	61.0	62.0	66.8
Tail Intensity	56.4	79.9	64.5	69.3	70.3	68.1

Table 2.19 Mouse 10µl heart cells control for day 2.

	Average Distance out of 10 comets in µm	Average Distance out of 10 comets in µm	Average Distance out of 10 comets in µm	Average Distance out of 10 comets in µm	Average Distance out of 10 comets in µm	Final Average
Total Length	105.4	104.4	125.1	116.5	122.1	114.7
Head Length	20.1	23.1	29.1	21.1	29.1	24.5
Tail Length	85.3	81.3	96.0	95.4	93.0	90.2
Tail Intensity	40.7	24.8	38.4	46.1	68.6	43.7

Table 2.20 Mouse 5µl liver cells control for day 2.

	Average Distance out of 10 comets in µm	Average Distance out of 10 comets in µm	Average Distance out of 10 comets in µm	Average Distance out of 10 comets in µm	Average Distance out of 10 comets in µm	Final Average
Total Length	150.2	155.3	157.2	161.1	163.3	157.4
Head Length	31.1	26.8	32.1	25.8	34.3	30.0
Tail Length	119.1	128.5	125.1	135.3	129.0	127.4
Tail Intensity	45.3	40.3	38.6	37.9	45.9	41.6

Table 2.21 Mouse 15µl blood cells Q_{10} exposure for day 2.

	Average Distance out of 10 comets in µm	Average Distance out of 10 comets in µm	Average Distance out of 10 comets in µm	Average Distance out of 10 comets in µm	Average Distance out of 10 comets in µm	Final Average
Total Length	97.0	85.2	90.0	89.1	100.3	92.3
Head Length	25.0	27.5	26.8	22.5	21.8	24.7
Tail Length	72.0	57.7	63.2	66.6	78.6	67.6
Tail Intensity	45.9	37.3	36.9	40.7	46.1	41.4

Table 2.22 Mouse 10µl brain cells Q_{10} exposure for day 2.

	Average Distance out of 10 comets in µm	Average Distance out of 10 comets in µm	Average Distance out of 10 comets in µm	Average Distance out of 10 comets in µm	Average Distance out of 10 comets in µm	Final Average
Total Length	90.0	108.0	99.3	108.4	100.7	101.3
Head Length	21.1	33.1	21.7	22.1	24.1	24.4
Tail Length	68.9	74.9	77.6	86.3	76.6	76.9
Tail Intensity	27.5	40.3	31.1	44.8	35.0	35.7

Table 2.23 Mouse 10µl heart cells Q_{10} exposure for day 2.

	Average Distance out of 10 comets in µm	Average Distance out of 10 comets in µm	Average Distance out of 10 comets in µm	Average Distance out of 10 comets in µm	Average Distance out of 10 comets in µm	Final Average
Total Length	74.3	95.3	74.3	85.0	98.0	85.4
Head Length	15.7	18.1	15.4	16.1	18.1	16.7
Tail Length	58.5	77.3	58.9	68.9	79.9	68.7
Tail Intensity	31.6	32.9	49.2	37.8	33.6	37.0

Table 2.24 Mouse 5µl liver cells Q_{10} exposure for day 2.

	Average Distance out of 10 comets in µm	Average Distance out of 10 comets in µm	Average Distance out of 10 comets in µm	Average Distance out of 10 comets in µm	Average Distance out of 10 comets in µm	Final Average
Total Length	135.9	134.1	132.7	183.6	164.2	150.1
Head Length	29.8	17.4	19.8	37.1	18.9	24.6
Tail Length	106.1	116.7	112.9	146.4	145.3	125.5
Tail Intensity	41.3	32.4	30.8	51.3	41.5	39.4

Table 2.25 Mouse 15µl blood cells Q_{10}/MPTP exposure for day 2.

	Average Distance out of 10 comets in µm	Average Distance out of 10 comets in µm	Average Distance out of 10 comets in µm	Average Distance out of 10 comets in µm	Average Distance out of 10 comets in µm	Final Average
Total Length	181.1	162.0	176.7	155.5	160.5	167.2
Head Length	17.7	20.7	21.1	19.3	21.2	20.0
Tail Length	163.4	141.2	155.6	136.2	139.3	147.2
Tail Intensity	24.7	25.4	26.4	25.5	27.8	25.9

Table 2.26 Mouse 10µl brain cells Q_{10}/MPTP exposure for day 2.

	Average Distance out of 10 comets in µm	Average Distance out of 10 comets in µm	Average Distance out of 10 comets in µm	Average Distance out of 10 comets in µm	Average Distance out of 10 comets in µm	Final Average
Total Length	181.1	162.0	176.7	155.5	160.5	167.2
Head Length	17.7	20.7	21.1	19.3	21.2	20.0
Tail Length	163.4	141.2	155.6	136.2	139.3	147.2
Tail Intensity	24.7	25.4	26.4	25.5	27.8	25.9

Table 2.27 Mouse 10µl heart cells Q_{10}/MPTP exposure for day 2.

	Average Distance out of 10 comets in µm	Average Distance out of 10 comets in µm	Average Distance out of 10 comets in µm	Average Distance out of 10 comets in µm	Average Distance out of 10 comets in µm	Final Average
Total Length	157.9	160.9	162.4	159.7	167.2	161.6
Head Length	20.4	17.7	18.3	14.3	18.3	17.8
Tail Length	138.1	141.8	144.1	145.4	149.0	143.7
Tail Intensity	22.8	30.8	32.2	35.9	27.2	29.8

Table 2.28 Mouse 5µl liver cells Q_{10}/MPTP exposure for day 2.

	Average Distance out of 10 comets in µm	Average Distance out of 10 comets in µm	Average Distance out of 10 comets in µm	Average Distance out of 10 comets in µm	Average Distance out of 10 comets in µm	Final Average
Total Length	188.3	188.3	181.3	169.6	190.0	183.5
Head Length	54.5	37.1	38.8	38.5	36.5	41.1
Tail Length	133.8	151.2	142.5	131.2	153.5	142.4
Tail Intensity	58.9	64.2	55.4	45.1	71.9	59.1

Table 2.29 Mouse 15µl blood cells MPTP exposure for day 2.

	Average Distance out of 10 comets in µm	Average Distance out of 10 comets in µm	Average Distance out of 10 comets in µm	Average Distance out of 10 comets in µm	Average Distance out of 10 comets in µm	Final Average
Total Length	181.1	162.0	176.7	155.5	160.5	167.2
Head Length	17.7	20.7	21.1	19.3	21.2	20.0
Tail Length	163.4	141.2	155.6	136.2	139.3	147.2
Tail Intensity	24.7	25.4	26.4	25.5	27.8	25.9

Table 2.30 Mouse 10µl brain cells MPTP exposure for day 2.

	Average Distance out of 10 comets in µm	Average Distance out of 10 comets in µm	Average Distance out of 10 comets in µm	Average Distance out of 10 comets in µm	Average Distance out of 10 comets in µm	Final Average
Total Length	147.3	152.4	135.8	137.2	155.3	145.6
Head Length	15.3	13.3	19.3	14.3	18.2	16.1
Tail Length	132.0	139.1	116.5	123.0	137.0	129.5
Tail Intensity	43.3	48.0	36.9	44.8	45.3	43.6

Table 2.31 Mouse 10µl heart cells MPTP exposure for day 2

	Average Distance out of 10 comets in µm	Average Distance out of 10 comets in µm	Average Distance out of 10 comets in µm	Average Distance out of 10 comets in µm	Average Distance out of 10 comets in µm	Final Average
Total Length	155.2	156.3	165.2	168.3	167.3	162.4
Head Length	17.3	18.2	14.3	19.2	20.1	17.8
Tail Length	138.0	138.0	151.0	149.0	147.1	144.6
Tail Intensity	44.2	48.6	62.5	53.9	39.6	49.8

Table 2.32 Mouse 5µl liver cells MPTP exposure for day 2.

	Average Distance out of 10 comets in µm	Average Distance out of 10 comets in µm	Average Distance out of 10 comets in µm	Average Distance out of 10 comets in µm	Average Distance out of 10 comets in µm	Final Average
Total Length	159.2	159.2	158.6	146.8	143.2	153.4
Head Length	32.1	26.8	20.1	24.7	26.4	26.0
Tail Length	127.1	132.4	138.5	122.1	116.8	127.4
Tail Intensity	80.1	61.0	57.6	71.9	73.2	68.8

Table 2.33 Mouse 15µl blood cells control for day 3.

	Average Distance out of 10 comets in µm	Average Distance out of 10 comets in µm	Average Distance out of 10 comets in µm	Average Distance out of 10 comets in µm	Average Distance out of 10 comets in µm	Final Average
Total Length	83.7	80.1	85.3	79.1	82.5	82.1
Head Length	16.3	15.2	15.9	19.2	20.5	17.4
Tail Length	67.4	64.9	69.4	59.9	62.0	64.7
Tail Intensity	62.5	63.5	67.3	59.4	60.2	62.6

Table 2.34 Mouse 10µl brain cells control for day 3.

	Average Distance out of 10 comets in µm	Average Distance out of 10 comets in µm	Average Distance out of 10 comets in µm	Average Distance out of 10 comets in µm	Average Distance out of 10 comets in µm	Final Average
Total Length	79.6	87.6	85.2	86.2	80.9	83.9
Head Length	19.6	17.5	18.2	19.4	20.1	19.0
Tail Length	60.0	70.1	67.0	66.8	60.8	64.9
Tail Intensity	55.1	68.2	64.8	66.3	66.1	64.1

Table 2.35 Mouse 10µl heart cells control for day 3.

	Average Distance out of 10 comets in µm	Average Distance out of 10 comets in µm	Average Distance out of 10 comets in µm	Average Distance out of 10 comets in µm	Average Distance out of 10 comets in µm	Final Average
Total Length	104.3	100.3	119.4	119.5	120.6	112.8
Head Length	19.4	22.1	25.2	20.9	25.1	22.5
Tail Length	84.9	78.2	94.2	98.6	95.5	90.3
Tail Intensity	40.9	30.5	34.9	40.9	49.5	39.3

Table 2.36 Mouse 5µl liver cells control for day 3.

	Average Distance out of 10 comets in µm	Average Distance out of 10 comets in µm	Average Distance out of 10 comets in µm	Average Distance out of 10 comets in µm	Average Distance out of 10 comets in µm	Final Average
Total Length	151.3	156.2	154.2	155.7	158.5	155.2
Head Length	25.9	24.5	38.5	20.6	29.5	27.8
Tail Length	125.4	131.7	115.7	135.1	129.0	127.4
Tail Intensity	44.6	48.0	30.3	42.4	39.2	40.9

Table 2.37 Mouse 15µl blood cells Q_{10} exposure for day 3.

	Average Distance out of 10 comets in µm	Average Distance out of 10 comets in µm	Average Distance out of 10 comets in µm	Average Distance out of 10 comets in µm	Average Distance out of 10 comets in µm	Final Average
Total Length	89.5	88.4	91.3	86.3	95.1	90.1
Head Length	21.7	23.7	21.1	20.9	24.8	22.4
Tail Length	67.8	64.7	70.2	65.4	70.3	67.7
Tail Intensity	46.2	40.9	40.8	42.1	42.6	42.5

Table 2.38 Mouse 10µl brain cells Q_{10} exposure for day 3.

	Average Distance out of 10 comets in µm	Average Distance out of 10 comets in µm	Average Distance out of 10 comets in µm	Average Distance out of 10 comets in µm	Average Distance out of 10 comets in µm	Final Average
Total Length	95.3	100.6	102.9	105.8	99.4	100.8
Head Length	22.4	25.4	24.9	19.7	23.7	23.2
Tail Length	72.9	75.2	78.0	86.1	75.7	77.6
Tail Intensity	35.7	42.6	35.1	40.9	36.2	38.1

Table 2.39 Mouse 10µl heart cells Q_{10} exposure for day 3.

	Average Distance out of 10 comets in µm	Average Distance out of 10 comets in µm	Average Distance out of 10 comets in µm	Average Distance out of 10 comets in µm	Average Distance out of 10 comets in µm	Final Average
Total Length	90.5	93.1	80.2	81.4	91.4	87.3
Head Length	16.4	17.9	15.0	19.4	20.4	17.8
Tail Length	74.1	75.2	65.2	62.0	71.0	69.5
Tail Intensity	35.4	33.1	40.9	36.7	38.9	37.0

Table 2.40 Mouse 5µl liver cells Q_{10} exposure for day 3.

	Average Distance out of 10 comets in µm	Average Distance out of 10 comets in µm	Average Distance out of 10 comets in µm	Average Distance out of 10 comets in µm	Average Distance out of 10 comets in µm	Final Average
Total Length	145.8	140.9	139.7	151.7	159.7	147.6
Head Length	21.9	22.4	23.3	25.7	22.4	23.1
Tail Length	123.9	118.5	116.4	126.0	137.3	124.4
Tail Intensity	39.3	36.1	37.7	44.7	31.8	37.9

Table 2.41 Mouse 15µl blood cells Q_{10}/MPTP exposure for day 3.

	Average Distance out of 10 comets in µm	Average Distance out of 10 comets in µm	Average Distance out of 10 comets in µm	Average Distance out of 10 comets in µm	Average Distance out of 10 comets in µm	Final Average
Total Length	167.8	165.2	170.6	160.5	173.8	167.6
Head Length	19.6	21.8	23.3	21.1	22.7	21.7
Tail Length	148.2	143.4	147.3	139.4	151.1	145.9
Tail Intensity	23.4	24.9	21.4	26.7	28.1	24.9

Table 2.42 Mouse 10µl brain cells Q_{10}/MPTP exposure for day 3.

	Average Distance out of 10 comets in µm	Average Distance out of 10 comets in µm	Average Distance out of 10 comets in µm	Average Distance out of 10 comets in µm	Average Distance out of 10 comets in µm	Final Average
Total Length	153.6	167.8	165.4	166.6	170.0	164.7
Head Length	21.1	19.7	21.8	16.8	19.9	19.9
Tail Length	132.5	148.1	143.6	149.8	150.1	144.8
Tail Intensity	30.1	30.8	25.7	26.1	29.4	28.4

Table 2.43 Mouse 10µl heart cells Q_{10}/MPTP exposure for day 3.

	Average Distance out of 10 comets in µm	Average Distance out of 10 comets in µm	Average Distance out of 10 comets in µm	Average Distance out of 10 comets in µm	Average Distance out of 10 comets in µm	Final Average
Total Length	159.6	161.8	166.6	160.3	161.8	162.0
Head Length	21.4	20.4	19.4	20.9	21.8	20.8
Tail Length	138.1	141.8	147.2	139.4	140.0	141.3
Tail Intensity	25.4	29.7	34.9	30.7	36.7	31.5

Table 2.44 Mouse 5µl liver cells Q_{10}/MPTP exposure for day 3.

	Average Distance out of 10 comets in µm	Average Distance out of 10 comets in µm	Average Distance out of 10 comets in µm	Average Distance out of 10 comets in µm	Average Distance out of 10 comets in µm	Final Average
Total Length	190.7	192.4	185.4	175.4	162.3	181.2
Head Length	44.7	41.8	40.3	39.4	49.1	43.1
Tail Length	146.0	150.6	145.1	136.0	113.2	138.2
Tail Intensity	49.6	55.1	53.1	52.7	66.1	55.3

Table 2.45 Mouse 15µl blood cells MPTP exposure for day 3.

	Average Distance out of 10 comets in µm	Average Distance out of 10 comets in µm	Average Distance out of 10 comets in µm	Average Distance out of 10 comets in µm	Average Distance out of 10 comets in µm	Final Average
Total Length	179.5	172.3	180.9	159.4	160.5	170.5
Head Length	20.6	22.8	18.4	17.9	21.3	20.2
Tail Length	158.9	149.5	162.5	141.5	139.2	150.3
Tail Intensity	25.7	20.9	27.6	20.5	29.7	24.9

Table 2.46 Mouse 10µl brain cells MPTP exposure for day 3.

	Average Distance out of 10 comets in µm	Average Distance out of 10 comets in µm	Average Distance out of 10 comets in µm	Average Distance out of 10 comets in µm	Average Distance out of 10 comets in µm	Final Average
Total Length	141.3	155.6	142.1	140.9	160.9	148.2
Head Length	20.6	18.9	20.3	22.4	16.1	19.7
Tail Length	120.7	136.7	121.8	118.5	144.8	128.5
Tail Intensity	46.8	50.3	32.7	55.6	47.2	46.5

Table 2.47 Mouse 10µl heart cells MPTP exposure for day 3.

	Average Distance out of 10 comets in µm	Average Distance out of 10 comets in µm	Average Distance out of 10 comets in µm	Average Distance out of 10 comets in µm	Average Distance out of 10 comets in µm	Final Average
Total Length	154.9	155.3	159.4	160.9	160.3	158.2
Head Length	20.6	19.1	16.4	18.7	20.3	19.0
Tail Length	134.3	136.2	143.0	142.2	140.0	139.1
Tail Intensity	43.9	44.1	46.7	49.2	49.7	46.7

Table 2.48 Mouse 5µl liver cells MPTP exposure for day 3.

	Average Distance out of 10 comets in µm	Average Distance out of 10 comets in µm	Average Distance out of 10 comets in µm	Average Distance out of 10 comets in µm	Average Distance out of 10 comets in µm	Final Average
Total Length	158.3	155.6	157.4	150.1	153.4	155.0
Head Length	33.4	30.1	25.8	27.4	22.4	27.8
Tail Length	124.9	125.5	131.6	122.7	131.0	127.1
Tail Intensity	70.1	69.7	69.3	66.1	68.4	68.7

Table 2.49 Mouse 15µl blood cells control for day 4.

	Average Distance out of 10 comets in µm	Average Distance out of 10 comets in µm	Average Distance out of 10 comets in µm	Average Distance out of 10 comets in µm	Average Distance out of 10 comets in µm	Final Average
Total Length	80.2	79.3	86.9	81.2	78.3	81.2
Head Length	17.6	19.5	18.2	20.7	14.3	18.1
Tail Length	62.6	59.8	68.7	60.6	64.0	63.1
Tail Intensity	64.8	66.8	59.7	50.8	69.5	62.3

Table 2.50 Mouse 10µl brain cells control for day 4.

	Average Distance out of 10 comets in µm	Average Distance out of 10 comets in µm	Average Distance out of 10 comets in µm	Average Distance out of 10 comets in µm	Average Distance out of 10 comets in µm	Final Average
Total Length	81.6	79.5	79.6	80.6	75.8	79.4
Head Length	20.6	19.7	15.8	22.5	21.1	19.9
Tail Length	61.0	59.8	63.8	58.1	54.7	59.5
Tail Intensity	54.6	67.9	70.3	60.8	69.1	64.5

Table 2.51 Mouse 10µl heart cells control for day 4.

	Average Distance out of 10 comets in µm	Average Distance out of 10 comets in µm	Average Distance out of 10 comets in µm	Average Distance out of 10 comets in µm	Average Distance out of 10 comets in µm	Final Average
Total Length	100.3	95.6	111.3	115.2	122.8	109.0
Head Length	25.6	19.4	27.4	18.3	24.6	23.1
Tail Length	74.7	76.2	83.9	96.9	98.2	86.0
Tail Intensity	39.5	32.7	30.5	42.8	45.9	38.3

Table 2.52 Mouse 5µl liver cells control for day 4.

	Average Distance out of 10 comets in µm	Average Distance out of 10 comets in µm	Average Distance out of 10 comets in µm	Average Distance out of 10 comets in µm	Average Distance out of 10 comets in µm	Final Average
Total Length	149.4	144.3	150.9	160.7	155.2	152.1
Head Length	20.6	20.7	35.7	30.6	35.1	28.5
Tail Length	128.7	123.6	115.2	130.1	120.1	123.5
Tail Intensity	44.9	42.7	43.2	48.9	40.2	44.0

Table 2.53 Mouse 15µl blood cells Q_{10} exposure for day 4.

	Average Distance out of 10 comets in µm	Average Distance out of 10 comets in µm	Average Distance out of 10 comets in µm	Average Distance out of 10 comets in µm	Average Distance out of 10 comets in µm	Final Average
Total Length	92.4	91.6	65.7	88.6	90.6	85.8
Head Length	20.3	21.8	20.1	22.9	25.9	22.2
Tail Length	72.1	69.8	45.6	65.7	64.7	63.6
Tail Intensity	47.6	42.2	45.7	43.3	41.8	44.1

Table 2.54 Mouse 10µl brain cells Q_{10} exposure for day 4.

	Average Distance out of 10 comets in µm	Average Distance out of 10 comets in µm	Average Distance out of 10 comets in µm	Average Distance out of 10 comets in µm	Average Distance out of 10 comets in µm	Final Average
Total Length	102.6	105.3	101.7	104.8	106.4	104.2
Head Length	20.4	20.9	22.2	20.1	28.7	22.5
Tail Length	82.2	84.4	79.5	84.7	77.7	81.7
Tail Intensity	38.4	39.7	30.4	35.7	39.1	36.7

Table 2.55 Mouse 10µl heart cells Q_{10} exposure for day 4.

	Average Distance out of 10 comets in µm	Average Distance out of 10 comets in µm	Average Distance out of 10 comets in µm	Average Distance out of 10 comets in µm	Average Distance out of 10 comets in µm	Final Average
Total Length	94.8	93.4	91.4	89.7	80.4	89.9
Head Length	19.4	20.7	18.7	19.7	19.7	19.6
Tail Length	75.4	72.7	72.7	70.0	60.7	70.3
Tail Intensity	33.7	30.8	39.4	33.3	40.8	35.6

Table 2.56 Mouse 5µl liver cells Q_{10} exposure for day 4.

	Average Distance out of 10 comets in µm	Average Distance out of 10 comets in µm	Average Distance out of 10 comets in µm	Average Distance out of 10 comets in µm	Average Distance out of 10 comets in µm	Final Average
Total Length	144.7	139.4	146.7	149.3	149.9	146.0
Head Length	25.7	19.7	17.3	20.9	22.8	21.3
Tail Length	119.0	119.7	129.4	128.4	127.1	124.7
Tail Intensity	42.1	37.9	37.4	43.7	33.9	39.0

Table 2.57 Mouse 15µl blood cells Q_{10}/MPTP exposure for day 4.

	Average Distance out of 10 comets in µm	Average Distance out of 10 comets in µm	Average Distance out of 10 comets in µm	Average Distance out of 10 comets in µm	Average Distance out of 10 comets in µm	Final Average
Total Length	170.6	169.9	177.7	159.4	153.7	166.3
Head Length	22.6	23.3	21.7	20.7	19.4	21.5
Tail Length	148.0	146.6	156.0	138.7	134.3	144.7
Tail Intensity	25.7	27.9	21.7	23.4	25.5	24.8

Table 2.58 Mouse 10µl brain cells Q_{10}/MPTP exposure for day 4.

	Average Distance out of 10 comets in µm	Average Distance out of 10 comets in µm	Average Distance out of 10 comets in µm	Average Distance out of 10 comets in µm	Average Distance out of 10 comets in µm	Final Average
Total Length	155.1	155.6	161.1	159.9	156.4	157.6
Head Length	20.1	17.8	23.1	20.2	23.6	21.0
Tail Length	135.0	137.8	138.0	139.7	132.8	136.7
Tail Intensity	28.7	28.9	27.7	26.6	23.3	27.0

Table 2.59 Mouse 10µl heart cells Q_{10}/MPTP exposure for day 4.

	Average Distance out of 10 comets in µm	Average Distance out of 10 comets in µm	Average Distance out of 10 comets in µm	Average Distance out of 10 comets in µm	Average Distance out of 10 comets in µm	Final Average
Total Length	157.4	160.7	159.7	161.1	163.3	160.4
Head Length	22.7	19.4	22.2	29.9	20.8	23.0
Tail Length	138.1	141.8	137.5	131.2	142.5	138.2
Tail Intensity	31.7	30.7	31.1	35.7	32.7	32.4

Table 2.60 Mouse 5µl liver cells Q_{10}/MPTP exposure for day 4.

	Average Distance out of 10 comets in µm	Average Distance out of 10 comets in µm	Average Distance out of 10 comets in µm	Average Distance out of 10 comets in µm	Average Distance out of 10 comets in µm	Final Average
Total Length	185.6	193.4	190.6	189.4	175.4	186.9
Head Length	52.1	55.4	38.4	46.7	51.1	48.7
Tail Length	133.5	138.0	152.2	142.7	124.3	138.1
Tail Intensity	50.1	50.1	54.7	49.7	51.7	51.3

Table 2.61 Mouse 15µl blood cells MPTP exposure for day 4.

	Average Distance out of 10 comets in µm	Average Distance out of 10 comets in µm	Average Distance out of 10 comets in µm	Average Distance out of 10 comets in µm	Average Distance out of 10 comets in µm	Final Average
Total Length	182.6	175.3	188.8	160.9	155.3	172.6
Head Length	22.5	20.8	23.3	15.3	29.7	22.3
Tail Length	160.1	154.5	165.5	145.6	125.6	150.3
Tail Intensity	20.6	25.9	22.2	27.9	25.3	24.4

Table 2.62 Mouse 10µl brain cells MPTP exposure for day 4.

	Average Distance out of 10 comets in µm	Average Distance out of 10 comets in µm	Average Distance out of 10 comets in µm	Average Distance out of 10 comets in µm	Average Distance out of 10 comets in µm	Final Average
Total Length	139.3	147.8	160.6	139.9	161.2	149.8
Head Length	22.6	20.3	25.9	24.8	23.1	23.3
Tail Length	116.7	127.5	134.7	115.1	138.1	126.4
Tail Intensity	47.1	49.7	40.3	39.7	44.2	44.2

Table 2.63 Mouse 10µl heart cells MPTP exposure for day 4.

	Average Distance out of 10 comets in µm	Average Distance out of 10 comets in µm	Average Distance out of 10 comets in µm	Average Distance out of 10 comets in µm	Average Distance out of 10 comets in µm	Final Average
Total Length	155.6	160.1	150.9	166.4	149.7	156.5
Head Length	21.6	22.2	19.7	26.4	24.4	22.9
Tail Length	134.0	137.9	131.2	140.0	125.3	133.7
Tail Intensity	40.9	49.7	41.9	43.7	44.1	44.1

Table 2.64 Mouse 5µl liver cells MPTP exposure for day 4.

	Average Distance out of 10 comets in µm	Average Distance out of 10 comets in µm	Average Distance out of 10 comets in µm	Average Distance out of 10 comets in µm	Average Distance out of 10 comets in µm	Final Average
Total Length	157.8	159.7	151.2	159.4	155.2	156.7
Head Length	29.7	31.8	29.7	22.4	21.9	27.1
Tail Length	128.1	127.9	121.5	137.0	133.3	129.6
Tail Intensity	69.7	66.4	65.1	66.1	63.1	66.1

Table 2.65 Mouse 15µl blood cells control for day 5.

	Average Distance out of 10 comets in µm	Average Distance out of 10 comets in µm	Average Distance out of 10 comets in µm	Average Distance out of 10 comets in µm	Average Distance out of 10 comets in µm	Final Average
Total Length	86.2	87.2	70.2	69.3	84.3	79.4
Head Length	19.3	15.9	20.8	22.7	16.8	19.1
Tail Length	66.9	71.3	49.4	46.6	67.5	60.3
Tail Intensity	60.5	70.6	63.2	59.3	65.2	63.8

Table 2.66 Mouse 10µl brain cells control for day 5.

	Average Distance out of 10 comets in µm	Average Distance out of 10 comets in µm	Average Distance out of 10 comets in µm	Average Distance out of 10 comets in µm	Average Distance out of 10 comets in µm	Final Average
Total Length	77.6	86.5	84.9	77.4	83.4	82.0
Head Length	19.4	26.4	14.8	18.7	20.2	19.9
Tail Length	58.2	60.1	70.1	58.7	63.2	62.1
Tail Intensity	63.9	70.1	60.5	60.7	73.9	65.8

Table 2.67 Mouse 10µl heart cells control for day 5.

	Average Distance out of 10 comets in µm	Average Distance out of 10 comets in µm	Average Distance out of 10 comets in µm	Average Distance out of 10 comets in µm	Average Distance out of 10 comets in µm	Final Average
Total Length	99.5	102.7	100.9	135.4	114.8	110.7
Head Length	20.9	25.7	18.5	20.2	25.0	22.1
Tail Length	78.6	77.0	82.4	115.2	89.8	88.6
Tail Intensity	42.8	29.7	38.7	40.0	31.8	36.6

Table 2.68 Mouse 5µl liver cells control for day 5.

	Average Distance out of 10 comets in µm	Average Distance out of 10 comets in µm	Average Distance out of 10 comets in µm	Average Distance out of 10 comets in µm	Average Distance out of 10 comets in µm	Final Average
Total Length	150.6	159.7	144.7	138.9	150.1	148.8
Head Length	25.1	22.4	30.6	29.1	32.2	27.9
Tail Length	125.5	137.3	114.1	109.8	117.9	120.9
Tail Intensity	50.1	59.7	45.8	40.7	44.6	48.2

Table 2.69 Mouse 15µl blood cells Q_{10} exposure for day 5.

	Average Distance out of 10 comets in µm	Average Distance out of 10 comets in µm	Average Distance out of 10 comets in µm	Average Distance out of 10 comets in µm	Average Distance out of 10 comets in µm	Final Average
Total Length	89.6	95.7	97.7	90.6	91.4	93.0
Head Length	19.7	22.3	24.9	25.1	20.1	22.4
Tail Length	69.9	73.4	72.8	65.5	71.3	70.6
Tail Intensity	40.9	41.3	42.8	45.7	39.7	42.1

Table 2.70 Mouse 10µl brain cells Q_{10} exposure for day 5.

	Average Distance out of 10 comets in µm	Average Distance out of 10 comets in µm	Average Distance out of 10 comets in µm	Average Distance out of 10 comets in µm	Average Distance out of 10 comets in µm	Final Average
Total Length	100.6	106.7	103.5	101.8	100.9	102.7
Head Length	21.1	22.9	24.7	25.0	23.3	23.4
Tail Length	79.5	83.8	78.8	76.8	77.6	79.3
Tail Intensity	35.7	40.6	31.7	39.7	42.5	38.0

Table 2.71 Mouse 10µl heart cells Q_{10} exposure for day 5.

	Average Distance out of 10 comets in µm	Average Distance out of 10 comets in µm	Average Distance out of 10 comets in µm	Average Distance out of 10 comets in µm	Average Distance out of 10 comets in µm	Final Average
Total Length	93.7	89.4	90.8	92.4	90.7	91.4
Head Length	20.9	22.7	19.4	22.7	23.7	21.9
Tail Length	72.8	66.7	71.4	69.7	67.0	69.5
Tail Intensity	30.7	31.8	35.4	32.2	35.8	33.2

Table 2.72 Mouse 5µl liver cells Q_{10} exposure for day 5.

	Average Distance out of 10 comets in µm	Average Distance out of 10 comets in µm	Average Distance out of 10 comets in µm	Average Distance out of 10 comets in µm	Average Distance out of 10 comets in µm	Final Average
Total Length	137.7	143.1	142.7	152.2	160.7	147.3
Head Length	16.7	22.7	25.4	19.7	25.7	22.0
Tail Length	121.0	120.4	117.3	132.5	135.0	125.2
Tail Intensity	39.4	33.8	34.9	39.7	35.5	36.7

Table 2.73 Mouse 15µl blood cells Q_{10}/MPTP exposure for day 5.

	Average Distance out of 10 comets in µm	Average Distance out of 10 comets in µm	Average Distance out of 10 comets in µm	Average Distance out of 10 comets in µm	Average Distance out of 10 comets in µm	Final Average
Total Length	177.6	172.3	179.4	169.9	159.6	171.8
Head Length	23.7	22.1	27.7	29.9	20.3	24.7
Tail Length	153.9	150.2	151.7	140.0	139.3	147.0
Tail Intensity	26.8	23.3	22.8	24.6	27.1	24.9

Table 2.74 Mouse 10µl brain cells Q_{10}/MPTP exposure for day 5.

	Average Distance out of 10 comets in µm	Average Distance out of 10 comets in µm	Average Distance out of 10 comets in µm	Average Distance out of 10 comets in µm	Average Distance out of 10 comets in µm	Final Average
Total Length	162.5	160.4	163.4	164.7	159.4	162.1
Head Length	26.4	20.9	23.3	26.1	26.8	24.7
Tail Length	136.1	139.5	140.1	138.6	132.6	137.4
Tail Intensity	27.7	28.8	25.5	21.5	23.7	25.4

Table 2.75 Mouse 10µl heart cells Q_{10}/MPTP exposure for day 5.

	Average Distance out of 10 comets in µm	Average Distance out of 10 comets in µm	Average Distance out of 10 comets in µm	Average Distance out of 10 comets in µm	Average Distance out of 10 comets in µm	Final Average
Total Length	158.4	159.7	161.2	169.7	149.7	159.7
Head Length	19.7	18.3	23.3	25.8	23.4	22.1
Tail Length	138.1	141.8	137.9	143.9	126.3	137.6
Tail Intensity	31.7	33.4	35.7	26.6	23.1	30.1

Table 2.76 Mouse 5µl liver cells Q_{10}/MPTP exposure for day 5.

	Average Distance out of 10 comets in µm	Average Distance out of 10 comets in µm	Average Distance out of 10 comets in µm	Average Distance out of 10 comets in µm	Average Distance out of 10 comets in µm	Final Average
Total Length	192.1	196.4	189.4	193.1	197.4	193.7
Head Length	55.1	53.7	59.4	49.7	51.9	54.0
Tail Length	137.0	142.7	130.0	143.4	145.5	139.7
Tail Intensity	49.7	44.9	42.7	44.7	46.8	45.8

Table 2.77 Mouse 15µl blood cells MPTP exposure for day 5.

	Average Distance out of 10 comets in µm	Average Distance out of 10 comets in µm	Average Distance out of 10 comets in µm	Average Distance out of 10 comets in µm	Average Distance out of 10 comets in µm	Final Average
Total Length	180.6	177.9	173.3	169.4	164.4	173.1
Head Length	20.6	22.1	28.4	23.3	21.1	23.1
Tail Length	160.0	155.8	144.9	146.1	143.3	150.0
Tail Intensity	21.1	30.9	27.9	22.1	28.1	26.0

Table 2.78 Mouse 10µl brain cells MPTP exposure for day 5.

	Average Distance out of 10 comets in µm	Average Distance out of 10 comets in µm	Average Distance out of 10 comets in µm	Average Distance out of 10 comets in µm	Average Distance out of 10 comets in µm	Final Average
Total Length	138.7	146.8	144.3	140.3	152.1	144.4
Head Length	21.6	21.8	20.6	23.4	19.7	21.4
Tail Length	117.1	125.0	123.7	116.9	132.4	123.0
Tail Intensity	44.6	43.1	42.1	40.9	44.7	43.1

Table 2.79 Mouse 10µl heart cells MPTP exposure for day 5.

	Average Distance out of 10 comets in µm	Average Distance out of 10 comets in µm	Average Distance out of 10 comets in µm	Average Distance out of 10 comets in µm	Average Distance out of 10 comets in µm	Final Average
Total Length	153.7	159.7	161.1	153.4	157.9	157.2
Head Length	22.3	20.9	20.4	23.1	22.2	21.8
Tail Length	131.4	138.8	140.7	130.3	135.7	135.4
Tail Intensity	39.7	41.1	47.3	40.9	44.9	42.8

Table 2.80 Mouse 5µl liver cells MPTP exposure for day 5.

	Average Distance out of 10 comets in µm	Average Distance out of 10 comets in µm	Average Distance out of 10 comets in µm	Average Distance out of 10 comets in µm	Average Distance out of 10 comets in µm	Final Average
Total Length	152.3	159.3	156.4	155.5	151.7	155.0
Head Length	30.9	30.7	25.7	29.4	21.1	27.6
Tail Length	121.4	128.6	130.7	126.1	130.6	127.5
Tail Intensity	64.7	67.9	61.3	70.1	69.8	66.8

Table 2.81 Mouse 15µl blood cells control for day 6.

	Average Distance out of 10 comets in µm	Average Distance out of 10 comets in µm	Average Distance out of 10 comets in µm	Average Distance out of 10 comets in µm	Average Distance out of 10 comets in µm	Final Average
Total Length	79.5	82.4	86.5	79.6	90.8	83.8
Head Length	14.8	20.6	18.4	20.9	24.0	19.7
Tail Length	64.7	61.8	68.1	58.7	66.8	64.0
Tail Intensity	59.4	61.8	70.9	66.7	60.8	63.9

Table 2.82 Mouse 10µl brain cells control for day 6

	Average Distance out of 10 comets in µm	Average Distance out of 10 comets in µm	Average Distance out of 10 comets in µm	Average Distance out of 10 comets in µm	Average Distance out of 10 comets in µm	Final Average
Total Length	80.5	80.9	79.4	83.4	89.4	82.7
Head Length	20.6	14.9	19.4	13.8	24.9	18.7
Tail Length	59.9	66.0	60.0	69.6	64.5	64.0
Tail Intensity	60.3	66.7	60.9	67.8	59.4	63.0

Table 2.83 Mouse 10µl heart cells control for day 6.

	Average Distance out of 10 comets in µm	Average Distance out of 10 comets in µm	Average Distance out of 10 comets in µm	Average Distance out of 10 comets in µm	Average Distance out of 10 comets in µm	Final Average
Total Length	110.6	100.8	94.7	126.8	122.6	111.1
Head Length	25.9	18.3	20.0	21.3	20.9	21.3
Tail Length	84.7	82.5	74.7	105.6	101.7	89.8
Tail Intensity	44.1	25.8	25.4	49.8	30.9	35.2

Table 2.84 Mouse 5µl liver cells control for day 6.

	Average Distance out of 10 comets in µm	Average Distance out of 10 comets in µm	Average Distance out of 10 comets in µm	Average Distance out of 10 comets in µm	Average Distance out of 10 comets in µm	Final Average
Total Length	147.6	155.9	163.4	155.4	157.9	156.0
Head Length	30.7	18.4	37.2	25.4	30.6	28.5
Tail Length	116.9	137.5	126.2	130.0	127.3	127.6
Tail Intensity	44.8	51.2	56.7	39.8	49.7	48.4

Table 2.85 Mouse 15µl blood cells Q_{10} exposure for day 6.

	Average Distance out of 10 comets in µm	Average Distance out of 10 comets in µm	Average Distance out of 10 comets in µm	Average Distance out of 10 comets in µm	Average Distance out of 10 comets in µm	Final Average
Total Length	93.3	94.7	90.1	99.4	89.4	93.4
Head Length	24.6	21.8	23.3	20.9	22.8	22.7
Tail Length	68.7	72.9	66.8	78.5	66.6	70.7
Tail Intensity	41.9	39.7	40.7	44.4	40.0	41.3

Table 2.86 Mouse 10µl brain cells Q_{10} exposure for day 6.

	Average Distance out of 10 comets in µm	Average Distance out of 10 comets in µm	Average Distance out of 10 comets in µm	Average Distance out of 10 comets in µm	Average Distance out of 10 comets in µm	Final Average
Total Length	99.7	110.6	105.4	102.3	109.7	105.5
Head Length	17.4	23.4	20.7	25.6	22.9	22.0
Tail Length	82.3	87.2	84.7	76.7	86.8	83.5
Tail Intensity	31.7	38.8	33.9	35.4	34.1	34.8

Table 2.87 Mouse 10µl heart cells Q_{10} exposure for day 6.

	Average Distance out of 10 comets In µm	Average Distance out of 10 comets in µm	Average Distance out of 10 comets in µm	Average Distance out of 10 comets in µm	Average Distance out of 10 comets in µm	Final Average
Total Length	99.7	95.1	93.8	97.7	91.1	95.5
Head Length	19.4	18.4	25.4	18.3	29.6	22.2
Tail Length	80.3	76.7	68.4	79.4	61.5	73.3
Tail Intensity	33.8	35.5	33.7	36.1	39.0	35.6

Table 2.88 Mouse 5µl liver cells Q_{10} exposure for day 6.

	Average Distance out of 10 comets in µm	Average Distance out of 10 comets in µm	Average Distance out of 10 comets in µm	Average Distance out of 10 comets in µm	Average Distance out of 10 comets in µm	Final Average
Total Length	144.4	153.3	161.8	155.9	129.4	149.0
Head Length	20.9	24.5	23.8	31.8	20.9	24.4
Tail Length	123.5	128.8	138.0	124.1	108.5	124.6
Tail Intensity	40.9	45.5	41.1	42.4	39.4	41.9

Table 2.89 Mouse 15µl blood cells Q_{10}/MPTP exposure for day 6.

	Average Distance out of 10 comets in µm	Average Distance out of 10 comets in µm	Average Distance out of 10 comets in µm	Average Distance out of 10 comets in µm	Average Distance out of 10 comets in µm	Final Average
Total Length	180.5	185.7	170.3	165.8	170.9	174.6
Head Length	20.4	19.7	21.4	25.1	22.0	21.7
Tail Length	160.1	166.0	148.9	140.7	148.9	152.9
Tail Intensity	22.1	20.9	23.3	25.5	26.7	23.7

Table 2.90 Mouse 10µl brain cells Q_{10}/MPTP exposure for day 6.

	Average Distance out of 10 comets in µm	Average Distance out of 10 comets in µm	Average Distance out of 10 comets in µm	Average Distance out of 10 comets in µm	Average Distance out of 10 comets in µm	Final Average
Total Length	155.9	159.4	170.4	166.1	153.4	161.0
Head Length	23.7	20.9	19.4	17.8	16.7	19.7
Tail Length	132.2	138.5	151.0	148.3	136.7	141.3
Tail Intensity	29.7	29.1	30.7	20.8	20.7	26.2

Table 2.91 Mouse 10µl heart cells Q_{10}/MPTP exposure for day 6.

	Average Distance out of 10 comets in µm	Average Distance out of 10 comets in µm	Average Distance out of 10 comets in µm	Average Distance out of 10 comets in µm	Average Distance out of 10 comets in µm	Final Average
Total Length	160.4	162.4	159.4	163.4	157.7	160.7
Head Length	23.3	25.4	26.7	24.9	21.3	24.3
Tail Length	138.1	141.8	132.7	138.5	136.4	137.5
Tail Intensity	30.7	29.4	25.4	27.9	26.1	27.9

Table 2.92 Mouse 5µl liver cells Q_{10}/MPTP exposure for day 6.

	Average Distance out of 10 comets in µm	Average Distance out of 10 comets in µm	Average Distance out of 10 comets in µm	Average Distance out of 10 comets in µm	Average Distance out of 10 comets in µm	Final Average
Total Length	191.3	184.6	193.7	199.1	190.2	191.8
Head Length	51.2	51.3	53.8	54.7	51.9	52.6
Tail Length	140.1	133.3	139.9	144.4	138.3	139.2
Tail Intensity	48.7	44.9	41.9	43.8	46.8	45.2

Table 2.93 Mouse 15µl blood cells MPTP exposure for day 6.

	Average Distance out of 10 comets in µm	Average Distance out of 10 comets in µm	Average Distance out of 10 comets in µm	Average Distance out of 10 comets in µm	Average Distance out of 10 comets in µm	Final Average
Total Length	188.7	190.3	169.3	187.7	159.3	179.1
Head Length	14.3	25.6	20.0	16.4	13.8	18.0
Tail Length	174.4	164.7	149.3	171.3	145.5	161.0
Tail Intensity	17.3	22.1	21.1	25.9	20.3	21.3

Table 2.94 Mouse 10µl brain cells MPTP exposure for day 6.

	Average Distance out of 10 comets in µm	Average Distance out of 10 comets in µm	Average Distance out of 10 comets in µm	Average Distance out of 10 comets in µm	Average Distance out of 10 comets in µm	Final Average
Total Length	140.6	140.2	150.1	134.6	142.9	141.7
Head Length	22.6	23.7	22.7	28.9	22.1	24.0
Tail Length	118.0	116.5	127.4	105.7	120.8	117.7
Tail Intensity	43.9	39.7	40.9	39.7	41.9	41.2

Table 2.95 Mouse 10µl heart cells MPTP exposure for day 6.

	Average Distance out of 10 comets in µm	Average Distance out of 10 comets in µm	Average Distance out of 10 comets in µm	Average Distance out of 10 comets in µm	Average Distance out of 10 comets in µm	Final Average
Total Length	155.4	160.3	149.7	150.3	156.9	154.5
Head Length	20.1	22.9	19.7	22.2	23.7	21.7
Tail Length	135.3	137.4	130.0	128.1	133.2	132.8
Tail Intensity	42.1	40.3	41.1	43.9	47.9	43.1

Table 2.96 Mouse 5µl liver cells MPTP exposure for day 6.

	Average Distance out of 10 comets in µm	Average Distance out of 10 comets in µm	Average Distance out of 10 comets in µm	Average Distance out of 10 comets in µm	Average Distance out of 10 comets in µm	Final Average
Total Length	153.4	151.3	157.7	153.5	156.6	154.5
Head Length	29.4	28.1	29.6	22.1	25.8	27.0
Tail Length	124.0	123.2	128.1	131.4	130.8	127.5
Tail Intensity	62.1	60.4	65.7	63.3	62.4	62.8

APPENDIX B.3: TAIL MOMENT DATA FOR SCGE

The following results were obtained after analyses were completed using the SCGE technique.

LYMPHOCYTES (BLOOD)

Table 3.1. Day 1

41102	Control blood	Coenzyme Q10 Blood	Coenzyme Q10/MPTP Blood	MPTP Blood
Total Comet Length (µm)	90.17	89.29	149.87	157.39
Head Length (µm)	18.60	22.58	18.98	19.19
Tail Length (µm)	71.57	66.68	130.89	138.26
Intensity (DNA Migration)	56.97	43.88	28.59	28.26
Tail Moment = (TL)(Int) (µm)	4077.53	2925.70	3742.20	3907.50

Table 3.2. Day 2

06\11\02	Control blood	Coenzyme Q10 Blood	Coenzyme Q10/MPTP Blood	MPTP Blood
Total Comet Length (µm)	83.84	92.33	167.16	167.16
Head Length (µm)	20.59	24.72	20.01	20.01
Tail Length (µm)	62.50	67.62	147.15	147.15
Intensity (DNA Migration)	66.51	41.37	25.95	25.95
Tail Moment = (TL)(Int) (µm)	4156.95	2797.41	3817.98	3817.98

Table 3.3. Day 3

08\11\02	Control blood	Coenzyme Q10 Blood	Coenzyme Q10/MPTP Blood	MPTP Blood
Total Comet Length (µm)	82.133	90.13	167.58	170.53
Head Length (µm)	17.41	22.44	21.70	20.20
Tail Length (µm)	64.72	67.69	145.88	150.33
Intensity (DNA Migration)	62.56	42.52	24.90	24.88
Tail Moment = (TL)(Int) (µm)	4048.68	2878.09	3632.41	3740.16

Table 3.4. Day 4

10\11\02	Control blood	Coenzyme Q10 Blood	Coenzyme Q10/MPTP Blood	MPTP Blood
Total Comet Length (µm)	81.17	85.78	166.26	172.58
Head Length (µm)	18.06	22.21	21.54	22.32
Tail Length (µm)	63.12	63.57	144.72	150.26
Intensity (DNA Migration)	62.32	44.12	24.84	24.38
Tail Moment = (TL)(Int) (µm)	3933.14	2804.88	3594.84	3663.34

Table 3.5. Day 5

12\11\02	Control blood	Coenzyme Q10 Blood	Coenzyme Q10/MPTP Blood	MPTP Blood
Total Comet Length (µm)	79.44	93.00	171.76	173.12
Head Length (µm)	19.10	22.42	24.74	23.10
Tail Length (µm)	60.35	70.58	147.02	150.02
Intensity (DNA Migration)	63.76	42.08	24.92	26.02
Tail Moment = (TL)(Int) (µm)	3847.91	2970.01	3663.74	3904.12

Table 3.6. Day 6

14\11\02	Control blood	Coenzyme Q10 Blood	Coenzyme Q10/MPTP Blood	MPTP Blood
Total Comet Length (µm)	83.76	93.38	174.64	179.06
Head Length (µm)	19.74	22.68	21.72	18.02
Tail Length (µm)	64.02	70.70	152.92	161.04
Intensity (DNA Migration)	63.92	41.34	23.70	21.33
Tail Moment = (TL)(Int) (µm)	4092.41	2922.74	3624.20	3435.71

BRAIN

Table 3.7. Day 1

04\11\02	Control Brain	Coenzyme Q10 Brain	Coenzyme Q10/MPTP Brain	MPTP Brain
Total Comet Length (μm)	89.07	95.67	141.84	143.36
Head Length (μm)	18.04	22.69	16.20	17.46
Tail Length (μm)	71.03	72.98	125.60	125.90
Intensity (DNA Migration)	69.40	44.34	28.10	43.21
Tail Moment = (TL)(Int) (μm)	4929.62	3235.80	3528.89	5439.89

Table 3.8. Day 2

06/11\02	Control Brain	Coenzyme Q10 Brain	Coenzyme Q10/MPTP Brain	MPTP Brain
Total Comet Length (μm)	84.66	101.28	158.05	145.57
Head Length (μm)	17.91	24.42	17.27	16.05
Tail Length (μm)	66.76	76.86	140.78	129.52
Intensity (DNA Migration)	68.07	35.73	28.81	43.65
Tail Moment = (TL)(Int) (μm)	4544.15	2746.25	4055.81	5652.94

Table 3.9. Day 3

08/11/02	Control Brain	Coenzyme Q10 Brain	Coenzyme Q10/MPTP Brain	MPTP Brain
Total Comet Length (μm)	83.90	100.79	164.68	148.16
Head Length (μm)	18.96	23.22	19.86	19.66
Tail Length (μm)	64.94	77.57	144.82	128.50
Intensity (DNA Migration)	64.10	38.10	28.42	46.51
Tail Moment = (TL)(Int) (μm)	4162.65	2955.57	4115.78	5976.54

Table 3.10. Day 4

10/11/02	Control Brain	Coenzyme Q10 Brain	Coenzyme Q10/MPTP Brain	MPTP Brain
Total Comet Length (μm)	79.42	104.16	157.62	149.76
Head Length (μm)	19.94	22.46	20.96	23.34
Tail Length (μm)	59.48	81.70	136.66	126.42
Intensity (DNA Migration)	64.54	36.66	27.04	44.20
Tail Moment = (TL)(Int) (μm)	3838.84	2995.12	3695.23	5587.76

Table 3.11. Day 5

12/11/02	Control Brain	Coenzyme Q10 Brain	Coenzyme Q10/MPTP Brain	MPTP Brain
Total Comet Length (μm)	81.95	102.70	162.08	144.44
Head Length (μm)	19.90	23.40	24.71	21.42
Tail Length (μm)	62.05	79.30	137.37	123.02
Intensity (DNA Migration)	65.81	38.04	25.44	43.08
Tail Moment = (TL)(Int) (μm)	4083.57	3016.57	3494.79	5299.70

Table 3.12. Day 6

14/11/02	Control Brain	Coenzyme Q10 Brain	Coenzyme Q10/MPTP Brain	MPTP Brain
Total Comet Length (μm)	82.72	105.54	161.04	141.68
Head Length (μm)	18.71	22.00	19.70	24.00
Tail Length (μm)	64.01	83.54	141.34	117.68
Intensity (DNA Migration)	63.01	34.78	26.20	41.22
Tail Moment = (TL)(Int) (μm)	4033.02	2905.52	3703.11	4850.77

HEART

Table 3.13. Day 1

04\11\02	Control Heart	Coenzyme Q10 Heart	Coenzyme Q10/MPTP Heart	MPTP Heart
Total Comet Length (μm)	106.16	99.60	154.73	163.36
Head Length (μm)	19.20	20.62	18.07	18.20
Tail Length (μm)	86.96	78.98	136.66	145.17
Intensity (DNA Migration)	41.02	43.34	31.01	50.43
Tail Moment = (TL)(Int) (μm)	3566.59	3422.55	4237.73	7320.92

Table 3.14. Day 2

06\11\02	Control Heart	Coenzyme Q10 Heart	Coenzyme Q10/MPTP Heart	MPTP Heart
Total Comet Length (μm)	114.69	85.36	161.60	162.45
Head Length (μm)	24.49	16.66	17.78	17.83
Tail Length (μm)	90.19	68.70	143.68	144.62
Intensity (DNA Migration)	43.73	37.01	29.76	49.75
Tail Moment = (TL)(Int) (μm)	3943.92	2542.40	4276.55	7195.23

Table 3.15. Day 3

08\11\02	Control Heart	Coenzyme Q10 Heart	Coenzyme Q10/MPTP Heart	MPTP Heart
Total Comet Length (μm)	112.81	87.31	162.02	158.16
Head Length (μm)	22.53	17.81	20.77	19.02
Tail Length (μm)	90.28	69.50	141.31	139.14
Intensity (DNA Migration)	39.34	37.00	31.48	46.72
Tail Moment = (TL)(Int) (μm)	3551.54	2571.50	4448.56	6500.62

Table 3.16. Day 4

10\11\02	Control Heart	Coenzyme Q10 Heart	Coenzyme Q10/MPTP Heart	MPTP Heart
Total Comet Length (μm)	109.05	89.94	160.44	156.54
Head Length (μm)	23.06	19.64	23.00	22.86
Tail Length (μm)	85.99	70.30	138.23	133.68
Intensity (DNA Migration)	38.28	35.60	32.38	44.06
Tail Moment = (TL)(Int) (μm)	3291.51	2502.68	4475.82	5889.94

Table 3.17. Day 5

12\11\02	Control Heart	Coenzyme Q10 Heart	Coenzyme Q10/MPTP Heart	MPTP Heart
Total Comet Length (μm)	110.66	91.40	159.74	157.16
Head Length (μm)	22.06	21.87	22.10	21.78
Tail Length (μm)	88.60	69.52	137.61	135.38
Intensity (DNA Migration)	36.60	33.18	30.10	42.77
Tail Moment = (TL)(Int) (μm)	3242.76	2306.81	4142.00	5790.74

Table 3.18. Day 6

14\11\02	Control Heart	Coenzyme Q10 Heart	Coenzyme Q10/MPTP Heart	MPTP Heart
Total Comet Length (μm)	111.10	95.48	160.66	154.52
Head Length (μm)	21.27	22.21	24.32	21.72
Tail Length (μm)	89.83	73.27	137.51	132.80
Intensity (DNA Migration)	35.20	35.62	27.90	43.06
Tail Moment = (TL)(Int) (μm)	3162.02	2609.66	3836.47	5718.37

Table 3.23. Day 5

12\11\02	Control Liver	Coenzyme Q10 Liver	Coenzyme Q10/MPTP Liver	MPTP Liver
Total Comet Length (µm)	148.80	147.28	193.68	155.04
Head Length (µm)	27.88	22.04	53.96	27.56
Tail Length (µm)	120.92	125.24	139.72	127.48
Intensity (DNA Migration)	48.18	36.66	45.76	66.76
Tail Moment = (TL)(Int) (µm)	5825.93	4591.30	6393.59	8510.56

Table 3.24. Day 6

14\11\02	Control Liver	Coenzyme Q10 Liver	Coenzyme Q10/MPTP Liver	MPTP Liver
Total Comet Length (µm)	156.04	148.96	191.79	154.50
Head Length (µm)	28.46	24.38	52.57	27.00
Tail Length (µm)	127.58	124.58	139.21	127.50
Intensity (DNA Migration)	48.44	41.85	45.22	62.78
Tail Moment = (TL)(Int) (µm)	6179.98	5213.92	6295.26	8004.45